Persistent Hole Burning of Zinc Porphyrin with Energy and Electron Transfer Mechanisms

(エネルギーおよび電子移動機構による亜鉛ポルフィリンの永続的ホールバーニング)

Shinjiro Machida

町田真二郎

Persistent Hole Burning of Zinc Porphyrin with Energy and Electron Transfer Mechanisms

Persistent Hole Burning of Zinc Porphyrin with Energy and Electron Transfer Mechanisms

Thesis submitted to The University of Tokyo
for the Degree of Doctor of Engineering

1994

Shinjiro Machida

Acknowledgements

I wish to express my sincere gratitude to Professor Kazuyuki Horie for giving me his constant guidance and encouragement in all phases of this work. I also wish to express my gratitude to Professor emeritus Itaru Mita for providing me the interesting and challenging theme and guiding me in the early stage of this work.

I wish my thanks to Professor Akira Fujishima, Professor Sei-ichiro Koda, Professor Kenjiro Miyano, and Professor Naoki Toshima for their helpful comments and discussions.

I would like to express my thanks to Dr. Takashi Yamashita for his invaluable guidance and discussions. I also would like to thank Dr. Akira Furusawa, Dr. Norio Murase, and Dr. Taro Suzuki for their helpful discussions and comments.

I am grateful to Dr. Toshinori Torii, Mr. Makoto Ikemoto, Miss Ryoko Matsuno, Mr. Osamu Kyono and all my collaborations for their useful discussions and their friendship.

I am also grateful to Professor Akira Iwama and Mr. Satoru Honmura for giving glicydil azide polymer to me and helping the preparation of the samples.

Finally, I am greatly indebted to my parents, family and all my friends who have constantly supported and encouraged me to make the study possible and fruitful.

Contents

1. General Introduction

2. Guest Chromophore, Apparatus, and Measurements for PHB

3. Two-Color PHB in Polymers Containing Carboxylic Acid

3.1 Introduction

3.3 Results and Discussion

4. Photon-Gated PHB by Donor-Acceptor Electron Transfer: ZnTTBP in Poly[(chloromethyl)styrene] (PCMS)

4.1 Introduction

4.3 Results and Discussion

5. Photon-Gated PHB via Two-Color Sensitization of Photoreactive Matrix Polymer: ZnTTBP in Glicydil Azide Polymer (GAP)

5.1 Introduction

5.3 Results and Discussion

6. PHB for Organic Dye Doped in Semiconductor System: ZnTTBP in Titanium Dioxide (TiO_2)

6.1 Introduction

6.2 Sample Preparation

6.3 Results and Discussion

CHAPTER 1

General Introduction

In this chapter, the principle of persistent hole burning (PHB) is introduced, and the hole burning mechanisms of the reported materials are reviewed. The possible applications and the scientific interests concerned with PHB are also reviewed. The concept of photon-gated PHB and the purpose of this thesis study are introduced. In the end of this chapter, the synopsis of the thesis is outlined.

1.1 Principle of Persistent Hole Burning (PHB)

Persistent hole burning (PHB) (or persistent spectral hole burning, PSHB) is a general term of phenomena that a dip or a hole is created in the absorption spectrum of a chromophore by site-selective excitation, and persists for a longer time than the excited lifetime of the chromophore1). Fig.1.1 illustrates the principle of PHB. The site-selecitve excitation is possible in the situation that the absorption line width of each chromophore (this is called "homogeneous width") is smaller than the width of the whole absorption band profile (called "inhomogeneous width"). In such a case, the whole absorption line is called "inhomogeneous band". This situation is often realized at low temperatures because the optical linewidth of each chromophore decreases dramatically as temperature becomes lower. The production of a spectral hole occurs when the excited chromophore changes their resonant frequencies after the relaxation from the excited states. Thus, the most essential process for PHB is how the resonant frequency of the chromophore is changed. In the next section, the mechanisms of the hole production process is surveyed.

1.2 Hole Burning Mechanisms

Since the first ovservation of the PHB phenomena[2,3], many (probably more than 100) materials have been proved to show PHB. However, the number of hole burning mechanisms reported so far is not so large compared to the number of the materials. Among the hole burning mechansims, there are two styles of the change in the resonant frequencies. In the first style, the selectively-excited chromophore becomes to a different chemical species during the PHB process. In this case the resonant frequency of the chromophore moves out from the initial inhomogeneous band as shown in Fig.1.1. The second style is that the chemical structure (or the electronic sturucture) of the chromophore itself is not changed in the hole production. In this case, the guest-host interaction between the chromophore and matrix is changed by the excitation and the subsequent process. So the resonant frequency of the hole burning product still remains at some place in the inhomogeneous band and the homogeneous linewidth is hardly changed in the second case.

Table 1.1 shows the reported PHB mechanisms and the representative materials with the mechanisms. The PHB of the first style, in which the resonant frequency of the burning product is in a different region from the initial inhomogeneous band, can proceed only when the chromophore undergoes chemical reaction. Wherever holes are created by photochemical processes PHB is called "photohemical hole burning". (Notice that not all the photochemical systems belong to the first style.) The reaction types of photochemicstry reported in the first style PHB systems are ionization[4,5], decomposition[6,7], donor-acceptor electron transfer[8,9] and isomerization[10]. Fig.1.2 shows an example of PHB mechanism by decomposition reaction of dimethyl s-tetrazine[7].

The second style PHB systems, in which the photoproduct remains in the burnig band, involve both photochemical and nonphotochemical mechanisms. The proton tautomerization of free-base porphyrins and phthalocyanines[11-13] and hydrogen-bond rearrangement of quinizarine from intra- to inter-molecular bonding[14] are the mechanisms of this style and usually classified as photochemical processes. (However, the latter seems to be a nonphotochemical process.) Fig.1.3 and 1.4 show the reaction schemes leading to PHB for the case of free-base porphyrin and quinizarine, respectively. If the hole production is caused by nonphotochemical processes such as a conformational change in the matrix, PHB is called "nonphotochemical hole burning (NPHB)"[15]. As a matter of course, all NPHB systems belong to this class. If the matrix around the excited chromophore undergoes chemical reaction but the chromophore itself does not, the second style PHB occurs. The material of this type is first observed in this thesis study and described in chapt. 5.

1.3. Possible Applications and Scientific Interests

PHB has been taken interests both for pure science and applications. The first proposed and the most well-known application of the PHB phenomenon is the frequency-domain optical memory[1]. The recording density of the present optical memory systems is limited by the diffraction-limit of the laser spot. If the PHB phenomenon is applied to an optical memory system, the frequency-domain can be used for data storage by using the presence or absence of a hole for 1 bit of digital data (Fig.1.5). Then, the recording density should increase to more than 10^3 times because in many systems the ratio of the inhomogeneous width to the homogeneous width is more than 10^3 at liquid helium temperature.

In addition to an optical digital memory system, the possible applications of PHB materials have grown to cover a variety of optical devices. By using holographic technique, PHB material can be applied to a high-density hologram media[16]. The photon-echo phenomenon and electric field effects provide us possibilities of using PHB materials as a time-domain[17] or an electric-field-domain[18] optical memory and as an image-processing device[19] or optical operating[20] devices.

However, PHB materials have many problems to be solved for the realization of such attractive applications. For any type of applications, the working temperature is preferably to be high. The holes can hardly be observed above liquid nitrogen temperature in most of PHB systems. But some materials show the high performance of high-temperature hole reservation and hole observation. In table 1.2, typical high-temperature PHB materials and the highest temperatures of hole reservation and hole observation (or formation) acieved for these materials are listed. Among them, Sm^{2+}-doped systems[21-23] are remarkable because they are the only materials which show the room-temperature PHB. Fig.1.6 shows an example of room-temperature PHB of Sm^{2+}/ $SrFCl_{0.5}Br_{0.5}$ system[21].

As for the application to a memory system, the high speed writing needs highly efficient materials and the high speed readout needs the materials with low degree of the laser-induced hole filling[24]. The non-destructive readout is also required for PHB memory systems. This problem is considered to be solved by using photon-gated PHB materials[1]. The idea of the photon-gated PHB is introduced in the next section.

PHB is quite attractive not only as a means of new optical devices but also as a spectroscopic method of low-temperature solid-state photophysics and photochemistry. Table 1.3 lists some of the phenomena which can be probed by the PHB spectroscopy and the PHB properties affecting these phenomena. By the PHB spectroscopy we can obtain the homogeneous width of a chromophore which offers the informations about excited-state lifetime[25] or pure dephasing lifetime[26]. The phonon side hole and pseudo-phonon side hole, which are produced by the electron-phonon coupling, inform us of the low-energy excitation modes of amorphous matrices[27]. By the measurement of hole shapes at various temperatures we can also get the informations about thermal relaxation process of the matrices[28] and the temperature dependence of Debye-Waller factor[29]. The measurement of frequency dependence of growth rates of the resonant and satellite holes make it possible the analysis of the vibronic components of the inhomogeneous band[30,31].

PHB spectroscopy is a very sensitive detection method of photoinduced processes because the change of the exremely small number of the chromophore can be detected by the PHB method compared to a conventional absorption spectroscopy. Thus, we can observe the initial stage of the solid-state photoreactions which have the inhomogeneous distribution of the reaction rates[32] with the PHB method.

1.4. Concept of Photon-Gated PHB

As is described in the previous section, the concept of photon-gated PHB has its origin for the non-destructive readout of the PHB memory. Fig.1.7 illustrates the scheme of photon-gated PHB. In the photon-gated materials, the persistent holes are formed efficiently only when the gating light (λ_2) of another wavelength from the burning light (λ_1) is irradiated simultaneously with the burning light[1]. In other words, the photoreaction leading to PHB proceeds only from a highly excited states in the photon-gated systems. The readout of the memory is possible by scanning the λ_1 only, so the non-destructive readout is achieved. Thus, the ratio of the hole growth rate in the presence of λ_2 to that without λ_2 is desirable to be high. Table 1.4 lists the mechanisms for photon-gated PHB, and the reported materials and their properties. Fig.1.8 illustrates the energy diagram of photon-gated PHB by ionization reaction for carbazole/boric acid glass system[5]. Fig.1.9 shows the scheme of photon-gated PHB by donor-acceptor electron transfer for zinc porphyrin with chloroform in polymer system[8] .

The photon-gated PHB materials is attractive also for pure sience. At first, the photon-gated systems allow us to measure the holes without changing the hole shape by the scanning light. In addition, if we measure the burning efficiencies with and without the gating light, the photoreaction from the highly excited states can be easily detected and distinguished from the phororeaction from the lowest excited state. The most photochemical and photophysical processes undergo from the lowest excited state, namely, the S_1 or T_1 state. The photochemical reactions from the highly excited states are one of the recent topics in photochemistry[33] . Thus, the photon-gated PHB systems are the good examples of the nonlinear (multi photon) photochemistry and photophysics.

1.5. Synopsis of The Thesis

The main purpose of this thesis study is the investigation of new PHB materials with new type mechanisms and new type matrices. This is significant because as the variation of the PHB materials becomes larger, the possibility of the applications and the scientific importance should become greater.

This thesis study also aims to clarify various aspects of low-temperature solid-state photophysics and photochemistry.

In particular, I turned much attention to the photoinduced processes from the highly excited states such as electron and energy transfer in this study. The photoreactions via highly excited states are one of the important fields but not so much studied. The photon-gated PHB is a very good method for studying this field.

In Chapter 2, the PHB chromophore, the experimental apparatus, and the measurement procedure which are commonly used for this thesis study are described. The synthesis and purification procedure of the PHB chromophore (a zinc porphyrin derivative) are described. The apparatus used for the PHB measurement is outlined. Typical measuring or estimation procedure of the quantum efficiency for hole formation, the gating ratio, and the cycle annealing and intensity dependence experiments are introduced.

Chapter 3, "Two-Color PHB in Polymers Containing Carboxylic Acid", reports the first observation of photon-gated PHB by nonphotochemical process. The contribution of the carboxylic acid and carboxyl proton to the gating effect is measured. The thermal stability of the holes by the one-color and two-color mechanism are measured and discussed. The TLS properties in carboxylic acid-containing polymers are illustrated according to the obtained results. A mechanism of the two-color PHB in the presence of carboxylic acid is proposed.

Chapter 4, "Photon-Gated PHB by Donor-Acceptor Electron Transfer: ZnTTBP in Poly[(Chloromethyl)styrene] (PCMS)", provides a photon-gated PHB system by electron transfer reaction in which the matrix polymer has the electron acceptor in the monomer unit. The burning efficiency and the gating ratio are measured for ZnTTBP/PCMS and other similar systems, and the burning mechanism for the case of one-color excitation is clarified. The important factors for PHB systems by electron transfer are considered.

Chapter 5, "Photon-Gated PHB via Two-Color Sensitization of Photoreactive Matrix Polymer: ZnTTBP in Glycidyl Azide Polymer (GAP)", presents a new type mechanism of photon-gated PHB: sensitization via triplet-triplet energy transfer. The concept of the new mechanism is introduced. The photon-gating enhancement, the intensity dependence, and the annealing and burning temperature dependence are measured for the ZnTTBP/GAP system and discussed on the basis of the hole burning mechanism.

In Chapter 6, "PHB for Organic Dye Doped in Semiconductor System: ZnTTBP in Titanium Dioxide (TiO_2)", the first type guest-host combination of a PHB material is provided. The preparation and characterization of the ZnTTBP/TiO_2 samples are described. The PHB properties are measured and the PHB mechanism is discussed. The high-temperature PHB is demonstrated and the temperature dependence of Debye-Waller

References

1) W. E. Moerner ed., "Persistent Spectral Hole Burning: Science and Applications". Springer, Berlin (1988).

2) A. A. Gorokhovskii, R. K. Kaarli, L. A. Rebane; JETP Lett., 20, 216 (1974).

3) B. M. Kharlamov, R. I. Personov, L. A. Bykovskaya; Opt. Commun., 12, 191 (1974).

4) A. Winnacker, R. M. Shelby, and R. M. Macfarlane; J. de Phys C 7, 543 (1985).

5) H. W. Lee, M. Gehrtz, E. E. Marinero, and W. E. Moerner; Chem. Phys. Lett., 118, 611 (1985).

6) M. Iannone, G. W. Scott, D. Brinza, and D. R. Coulter; J. Chem. Phys., 85, 4863 (1986).

7) R. M. Hochstrasser and D. S. King; J. Am. Chem. Soc., 97, 4760 (1975).

8) T. P. Carter, C. Bräuchle, V. Y. Lee, M. Manavi, and W. E. Moerner; J. Phys. Chem., 91, 3998 (1987).

9) V. G. Maslov; Opt. Spectrosk., 43, 388 (1977).

10) G. Adamson, G. Gradl, and B. E. Köhler; J. Chem. Phys., 90, 3038 (1989).

11) A. A. Gorokhovski, R. K. Kaarli, and L. A. Rebane; JETP Lett., 20, 216 (1974).

12) S. Völker amd J. H. van der Waals; Molec. Phys. 32, 1703 (1976).

13) A. Furusawa, K. Horie, K. Kuroki, and I. Mita; J. Appl.

References

1) W. E. Moerner ed., "Persistent Spectral Hole Burning: Science and Applications". Springer, Berlin (1988).

2) A. A. Gorokhovskii, R. K. Kaarli, L. A. Rebane; JETP Lett., 20, 216 (1974).

3) B. M. Kharlamov, R. I. Personov, L. A. Bykovskaya; Opt. Commun., 12, 191 (1974).

4) A. Winnacker, R. M. Shelby, and R. M. Macfarlane; J. de Phys C 7, 543 (1985).

5) H. W. Lee, M. Gehrtz, E. E. Marinero, and W. E. Moerner; Chem. Phys. Lett., 118, 611 (1985).

6) M. Iannone, G. W. Scott, D. Brinza, and D. R. Coulter; J. Chem. Phys., 85, 4863 (1986).

7) R. M. Hochstrasser and D. S. King; J. Am. Chem. Soc., 97, 4760 (1975).

8) T. P. Carter, C. Bräuchle, V. Y. Lee, M. Manavi, and W. E. Moerner; J. Phys. Chem., 91, 3998 (1987).

9) V. G. Maslov; Opt. Spectrosk., 43, 388 (1977).

10) G. Adamson, G. Gradl, and B. E. Köhler; J. Chem. Phys., 90, 3038 (1989).

11) A. A. Gorokhovski, R. K. Kaarli, and L. A. Rebane; JETP Lett., 20, 216 (1974).

12) S. Völker amd J. H. van der Waals; Molec. Phys. 32, 1703 (1976).

13) A. Furusawa, K. Horie, K. Kuroki, and I. Mita; J. Appl.

Phys., 66, 6041 (1989).

14) W. Breinl, J. Friedlich, and D. Haarer; Phys. Rev., B 34, 7271 (1986).

15) R. Jankowiak and G. J. Small; Science, 237, 618 (1987).

16) A. Renn, A. J. Meixner, U. P. Wild and F. A. Burkhalter; Chem. Phys., 93, 157 (1985).

17) T. W. Mossberg; Opt. Lett., 7, 77 (1982).

18) U. P. Wild, S. E. Bucher and F. A. Burkhalter; Appl. Opt. 24, 1526 (1985).

19) M. K. Kim and R. Kachru; J. Opt. Soc. Am., B 4, 305 (1987).

20) U. P. Wild, C. D. Caro, S. Bernet, M. Traber and A. Renn; J. Lumin., 48 & 49, 335 (1991).

21) R. Jaaniso, H. Bill; Europhys. Lett., 16, 569 (1991).

22) J. Zhang, S. Huang, J. Yu; 発光学報, 12, 181 (1991).

23) K. Hirao, T. Todoroki, and N. Soga., J. Lumin., 55, 217 (1992).

24) N. Murase and K. Horie; Chem. Phys. Lett., 209, 42 (1993).

25) M. Vácha, F. Adamec, M. Ambroz, J. Dian, J. Psencík, and J. Hála; J. Mol. Str., 294, 131 (1993).

26) L. A. Rabane, A. A. Gprokhovski, and J. V. Kikas; Appl. Phys., B 29, 235 (1982).

27) A. Furusawa, K. Horie, and I. Mita; Chem. Phys. Lett., 161, 227 (1989).

28) W. Köhler and J. Friedrich; Phys. Rev. Lett., 59, 2199 (1987).

29) A. Furusawa and K. Horie; J. Chem. Phys., 94, 80 (1991).

30) K. Horie, M. Ikemoto, T. Suzuki, S. Machida, T. Yamashita, and N. Murase; Chem. Phys. Lett., 195, 563 (1992).

31) N. Murase, M. Ikemoto, and K. Horie; J. Chem. Phys., 99, 6313 (1993).

32) K. Horie and I. Mita; Adv. Polym. Sci., 88, 77 (1989).

33) Y. Nishimura, Y. Kaneko, T. Arai, H. Sakuragi, K. Tokumaru, M. Kiten, S. Yamamura, and D. Matsunaga; Chem. Lett., 1935 (1990).

Table 1.1. PHB mechanisms and representative materials

Mechanism I : 1st style II : 2nd style (see text)		Guest Molecule or Color Center	Matrix
I	Ionization	Sm^{2+}	CaF_2, BaClF, $BaFCl_{0.5}Br_{0.5}$ $SrFCl_{0.5}Br_{0.5}$, $Sr_{0.5}Mg_{0.5}FCl_{0.5}Br_{0.5}$, Fluorohafnate glasses
		Co^{2+}	$LiGa_5O_8$
		Ti^{3+}	$Y_3Al_5O_{12}$
		Cr^{3+}	$SrTiO_3$
		F_2 color center	Neutron-irradiated sapphire
		Carbazole	Boric acid glass
	Decomposition	Antracene-tetracene photoeduct	PMMA
		s-tetrazine derivatives	Benzene, Terphenyl
		5,10-dihydrophenazine	Fluorene
	Donor-Acceptor Electron Transfer	Zn (or Mg) tetrabenzoporphine derivatives	Organic halogenated compounds -PMMA Organic cyanide compounds -PMMA
		Zn porphyrin	Pyridine dimer anion-Ether
		Tetraphenylporphine	p-Benzoquinone-PMMA
		Zn porphyrin	Sulfonium salt-EDTA-PVA
	Isomerization	1,3,5,7-octatetraene	n-hexane
II	Hydrogen Tautomerization	Free-base porphyrins and Free-base phthalocyanines	n-Alkanes, Polymers, and Organic and inorganic glasses etc.
	Inter- to Intra-Hydrogen-bond rearrangement	Quinizarine and Hydroxynaphtoquinone	Polymers and Inorganic glasses
	Sensitization	Zn tetratolyltetrabenzoporphyrin (ZnTTBP)	Glycidyl azide polymer Acyloxyimino polymers Norbornadiene-PMMA
	Nonphotochemical processes	Porphyrins, Ionic dyes, Ions, and many photostable molecules	Polymers and Glasses

Table 1.2. High-temperature PHB materials

Materials	Highest Reservation Temperatures	Highest Burning (Observation) Temperatures
Tetraphenylporphine sulfonate/Poly (vinyl alcohol)	150	120
Tetraphenylporphine (TPP)/Phenoxy resin	120	100
TPP/Epoxy resin		80
Octaethylporphine/γ-Al_2O_3 (adsorbed)		90
Quinizarine/SiO_2	65	
Quinizarine/γ-Al_2O_3 (adsorbed)		77
ZnTTBP-$CHCl_3$/PMMA		90
ZnTTBP/Glycidyl azide polymer	> 80	80
ZnTTBP/TiO_2		140
5,10-Dihydrophenazine/Fluorene	320	
Neutron-irradiated sapphire	520	
Sm^{2+}/BaClF	300	
Sm^{2+}/$SrFCl_{0.5}Br_{0.5}$		296
Sm^{2+}/$Sr_{0.5}Mg_{0.5}FCl_{0.5}Br_{0.5}$		R.T.
Sm^{2+}/$BaFCl_{0.5}Br_{0.5}$		R.T.
Sm^{2+}/Fluorohafnate glasses		R.T.
Neutron-irradiated diamond		R.T.

Table 1.3. Phenomena probed by PHB spectroscopy

PHB property		Phenomena probed
Hole width	Energy dependence	Homogeneous width (pure dephasing lifetime and excited state lifetime)
	Temperature dependence	Dephasing mechanism (electron-phonon coupling, energy transfer etc.)
	Cycle temperature dependence	Thermally induced spectral diffusion (Structural relaxation, Intrinsic TLS)
	Time dependence	Spectral diffusion (Intrinsic TLS, structural relaxation)
Hole area	Energy dependence	Quantum efficiencies
	Intensity dependence	Bottleneck lifetimes
	Temperature dependence	(Temperature depedence of) Debye-Waller factors (DWF)
	Cycle temperature dependence	Thermally induced hole filling (barrier heights to reverse reaction, Structural relaxation which induces site redistribution)
	Time dependence	Spontaneous hole filling (barrier heights to reverse reaction)
Energy difference from zero-phonon hole to pseudo-phonon side hole or phonon-side hole		Low-energy excitation modes of host matrices
Satellite hole	Positions	Vibronic and other excited state splittings
	Growth rate	Vibronic overlaps of inhomogeneous band (Real values of photoreaction, Absorption cross sections and DWF for vibronic transition)
Antihole positions		Nature and number of product states, ground state splittings
Laser-induced hole filling		Laser-induced back reaction, Non-site-selective excitation
External field effects	E-field	Stark effect, site symmetry
	H-field	Zeeman effect, degeneracy of transition
	Strain field	Stress coupling coefficients, symmetry
Gating light effects		Photoreactions from highly excited state (electron transfer, energy transfer, etc.)

Table 1.4. Photon-gated PHB mechanisms and materials

Mechanism	Material	λ_1 (nm)	λ_2 (nm)	Gating ratio
Ionization	$Sm^{2+}/BaClF$	688	454-630	10^6
	$Sm^{2+}/SrClF$	691	350	
	Sm^{2+}/CaF_2	696	515	
	$Co^{2+}/LiGa_5O_8$	660	680	20
	$Cr^{3+}/SrTiO_3$	794	780-1060	
	Carbazole/Boric acid glass	335	407-515	400
	Perylene/Boric acid glass	440	440	
Electron transfer	$ZnTTBP-CHCl_3/PMMA$	630	350-500	10^2-10^4
	ZnTTBP-ArCN/PMMA	630	488-515	10
	ZnTPBP-p-hydroxybenzaldehyde	630	488-515	
	TPP/ArX	643	515	
	ZnTSPP-Sulfonium salt-EDTA/PVA	600	488	8
Decomposition	Antracene-tetracene educt/PMMA	327	442	~2
	s-tetrazine derivetives/Benzene	580	580	
	5,10-dihydrophenazine/Fluorene	360	500	
	Carbazole/PMMA	337	488	
Sensitization	ZnTTBP/Glycidyl azide polymer	630	488-515	2500
	ZnTTBP/Acyloxyimino polymer	630	488-515	90
	ZnTTBP-norbornadiene/PMMA	630	488-515	36
Nonphotochemical process	ZnTTBP/Poly(vinyl hydrogenphthalate	630	488-515	3

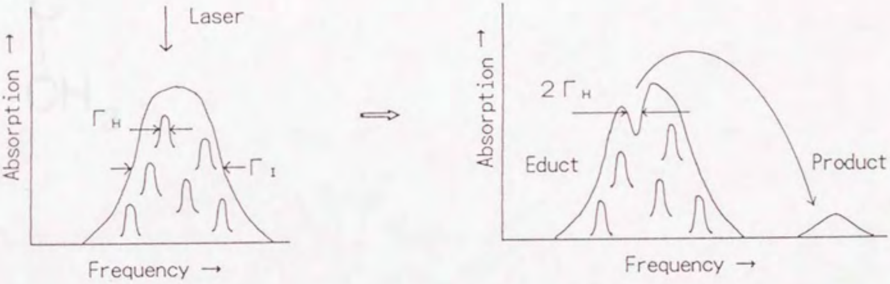

Fig.1.1. Principle of PHB.

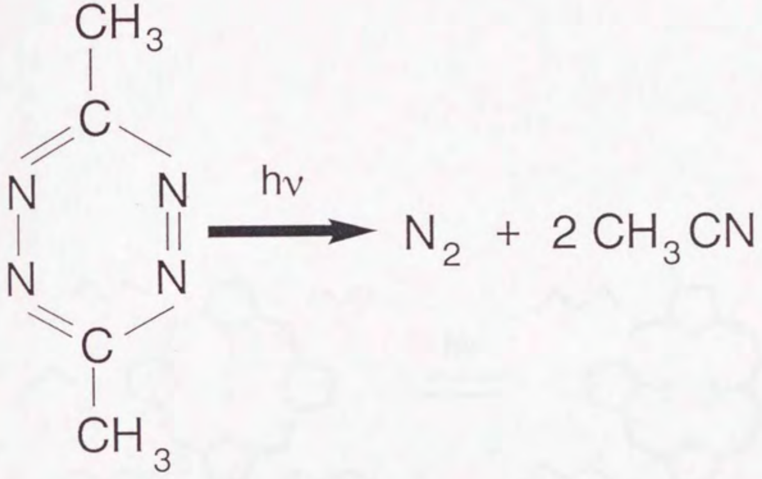

Fig.1.2. Reaction scheme of PHB for dimethyl s-tetrazine.

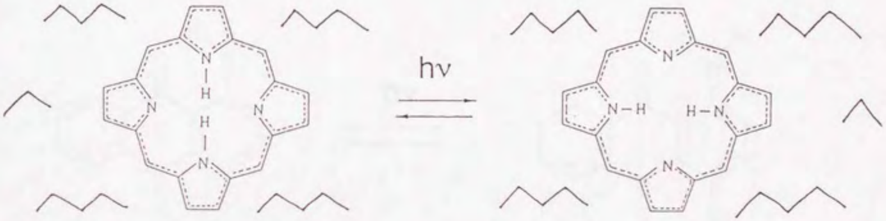

Fig.1.3. Tautomerization mechanism of PHB for free-base porphyrin.

Fig.1.4. Intra- to inter-molecule hydrogen-bond rearrangement of quinizarine.

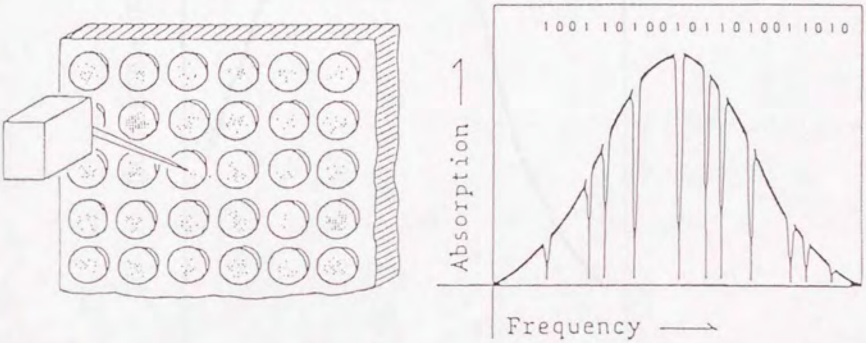

Fig.1.5. Synopsis of PHB memory.

Fig.1.6. Room temperature PHB for $Sm^{2+}/SrFCl_{0.5}Br_{0.5}$[21].

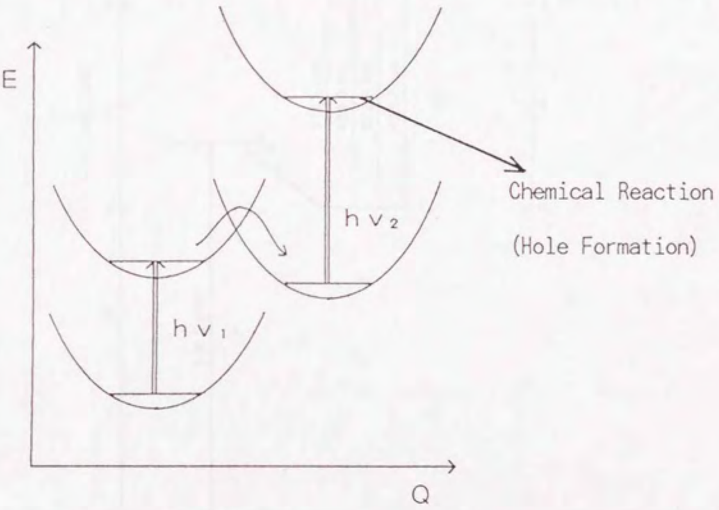

Fig.1.7. Principle of photon-gated PHB.

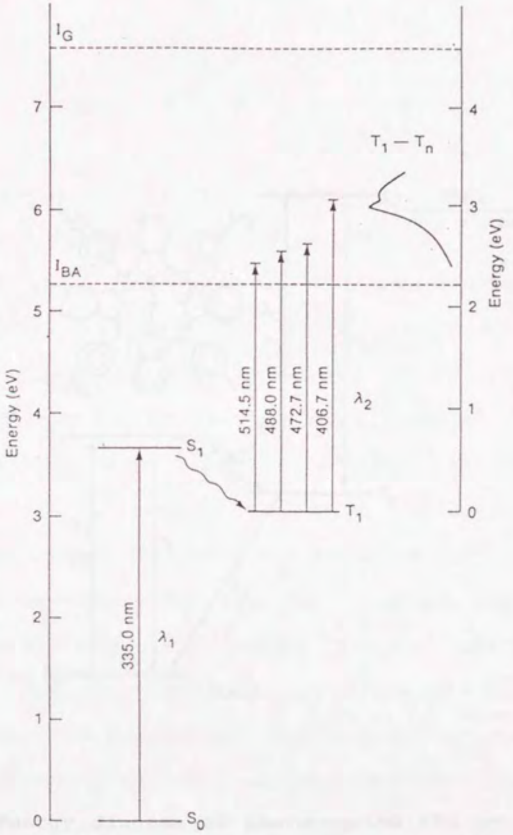

Fig.1.8. Energy diagram of photon-gated PHB by ionization for carbazole/boric acid glass system[5)].

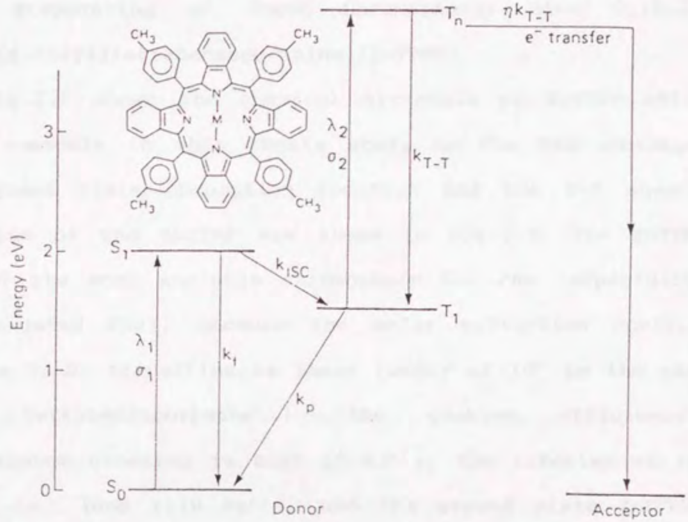

Fig.1.9. Energy diagram of photon-gated PHB by donor-acceptor electron transfer for ZnTTBP-$CHCl_3$/PMMA system[8].

CHAPTER 2

Guest Chromophore, Apparatus, and Measurements for PHB

2.1. Preparation of Guest Chromophore: Zinc 9,18,27,36-tetra(4-tolyl)tetrabenzoporphine (ZnTTBP)

Fig.2.1 shows the chemical structure of ZnTTBP which is used commonly in this thesis study as the PHB chromophore. The gound state absorption spectrum and the T-T absorption spectrum of the ZnTTBP are shown in Fig.2.2. The ZnTTBP is one of the most suitable chromophore for PHB (espetially for photon-gated PHB), because the molar extinction coefficient of the S_0-S_1 transition is large (order of 10^5 in the case of zinc tetrabenzoporphine[1]), the quantum efficiency of intersystem crossing is high (0.82[2]), the lifetime of the T_1 state is long (>10 ms[3]), and the ground state ZnTTBP has little absorption cross section around the maximum of T-T absorption band[4]. In addition, the wavelength regions of the lowest S_0-S_1 transition and the T-T transition of ZnTTBP just fit for our laser apparatus (a DCM ring dye laser and an argon ion laser).

The ZnTTBP was synthesized from potassium phthalimide (Kanto Chemicals), p-tolylacetic acid (Tokyo Chemical Industry), and zinc acetate (Kanto Chemicals) as follows[3,5]. A mixture of the 4:4:1 molar ratio of potassium phthalimide, sodium p-tolylacetate, and zinc acetate was heated under nitrogen flow at 300-350 ℃ for 2 hours. The obtained solid was ground and extracted with hot water, n-hexane, and chloroform. The chloroform extract was concentrated and purified by column chromatography on alumina with benzene and with acetone. The product was further purified by TLC with benzene. It is true that the obtained ZnTTBP was not fully purified. But we checked that the degree of purification does not affect the PHB properties.

As for the methods of sample preparation, they are described in each section of the thesis.

2.2 Apparatus for PHB Experiments

Fig.2.3 shows the experimental apparatus for PHB measurements. The samples were put vacuum grease on the surface and were sandwiched between sapphire plates in order to get enough thermal contact. Then the samples were set in a cryostat with a cryogenic refrigerator (Sumitomo, SRD204). The holes were burnt usually at 20 K by irradiating with an Ar^+-laser (Coherent, Innova 70)-pumped DCM ring dye laser (Coherent, 699-01) or with a He-Ne laser (NEC, GL55800) around 630 nm as the burning light, and with an Ar^+ laser (NEC, GLG3200) as the gating light. The burnt holes were detected through the change in transmittance with a 1 m monochromator (Jasco, CT100C) with a halogen lamp and an optical chopper, a photomultiplier (Hamamatsu, R943-02), and a lock-in amplifier(Jasco, LA126W). The spectral resolution of this apparatus is 0.01 nm and is enough for the measurements at 20 K.

The absorption spectra of the samples at room temperature were measured with a UV/VIS spectrophotometer (Jasco, UVIDEC-660). The infrared spectra of the samples (chapt. 3 and 6) were measured with an infrared spectrophotometer (Jasco, IR-700).

2.3. Typical Measurement Procedures of PHB.

Most essential parameters of PHB for the thesis study are quantum efficiencies for hole formation, Φ, and gating ratio, G. The Φ is defined as the ratio of the number of the chromophore which contributes to the hole formation to the number of the absorbed photon per unit volume. Fig.2.4 illustrates a scheme for the estimation of the Φ. The ratio of the chromophore which consists a hole to all the chromophore in the sample should equal to the ratio of the hole area to the inhomogeneous band area. Therefore, the Φ can be represented as the following equation (1)[6,7]:

$$\Phi = -\{d\underline{A}/d\underline{t}\}_{t=0}/\{10^3\,\underline{I}_0(1-10^{-A_0})\,\varepsilon\,\underline{R}\} \qquad (1)$$

wherer $\underline{A}$ is a time-varing absorbance at the burning wavelength, $\underline{A}_0$ is the absorbance at the burning wavelength before irradiation, $\underline{I}_0$ is the incident laser intensity given in einstein $cm^{-2}s^{-1}$, ε is the molar extinction coefficient for the peak absorption at room temperature, and $\underline{R}=\Gamma_i/\Gamma_{hole}$ is the reciprocal initial ratio of a hole width, Γ_{hole}, to an inhomogeneous width, Γ_i. The Φ calculated by the equation (1) should agree with a real value of quantum efficiency of photoreaction in the case that the whole observed inhomogeneous band consists only of sharp homogeneous lines. In general, phonon-side band and vibronic components are included in the observed inhomogeneous band in amorphous matrix[8,9]. So the quantum efficiency of hole burning is much lower than that of photoreaction[9].

The gating ratio, G, is defined as the ratio of Φ for the case of two-color irradiation, Φ_2, to the Φ for the one-color irradiation, Φ_1. Of course, the Φ_2 and G differ with the intensity of the gating light. In this thesis study, I estimate the Φ_2 and G from the results in which the λ_2 intensity is low enough that the width of two-color hole is same with that of one-color hole.

Tyipical hole profiles during cycle annealing experiment are shown in Fig.2.5. The scheme of cycle annealing experiment is also shown in Fig.2.5. In this experiment, a hole is burnt at low temperature (20 K in the thesis study) in the first place, and measured on the profile, and then temperature of the sample is elevated and a hole profile is measured. Next the system is cooled down to the initial hole-burning temperature, and a hole profile is measured. This temperature cycle is repeated several times with stepwise raising of the eleveted temperatures. The cycle annealing experiment provide reversible and irreversible thermally induced change in hole profiles. The reversible change in hole area informs the temperature dependence of Debye-Waller factor[10]. The irreversible decrease in hole area reflects thermally induced backreaction (this is mainly observed for NPHB system) and structural relaxation which induces site redistribution. The reversible change in hole width during cycle annealing is due to the temperature dependence of homogeneous width, and the irreversible increase in hole width is called "spectral diffusion" which is caused by thermally induced structural relaxation or tunneling between the two-level-system.

The bottleneck lifetime is obtained by λ_1-intensity dependence of hole depth. Fig.2.6 shows a diagram of the absorption saturation due to the bottleneck of T_1 state of the chromophore. When the λ_1 intensity is so large that the pumping rate is higher than the rate of deactivation processes from T_1 state, almost all of the chromophore which can absorb the λ_1 light exist in the T_1 state and the λ_1 absorption becomes saturated. The intensity of λ_1 which induces absorption saturation, $\underline{I}_s$, is estimated by the following equations, (2), (3):

$$\underline{I}_s = \underline{hc}/\,(\sigma\, \Phi_{ISC}\ \tau_{T1}\, \lambda_1) \qquad (2)$$

$$\sigma = 10^3\, \varepsilon\, \Gamma_i/(\underline{N}_A \ \log \underline{e}\ \Gamma_h) \qquad (3)$$

where σ is absorption cross section of a ZnTTBP molecule, Φ_{ISC} is quantum yield of intersystem crossing, τ_{T1} lifetime of T_1, $\underline{h}$ is Plank constant, $\underline{c}$ is velocity of light, N_A is Avogadro's number, Γ_i is inhomogeneous width, and Γ_h is homogeneous width. In the case of ZnTTBP, the values are: $\Phi_{ISC}=0.9$, $\tau_{T1}= \sim 40$ ms, $\varepsilon = \sim 10^5$, and $\Gamma_i/\Gamma_h = \sim 300$ (at 20 K). So the $\underline{I}_s$ should be about 100μ W/cm^2 at 20 K and this is consistent with the results in chapters 4 and 5. If there exists another fast deactivation pass from S_1 or T_1 states such as electron or energy transfer, the $\underline{I}_s$ should become larger. This is indicated in chapter 6.

References

1) M. Gouterman; J. Mol. Spectrosc. 6, 138 (1961).

2) A. T. Gradyushko and M. P. Tsvirko; Opt. Spectrosk., 31, 291 (1971).

3) T. P. Carter, C. Bräuchle, V. Y. Lee, M. Manavi, and W. E. Moerner; J. Phys. Chem., 91, 3998 (1987).

4) M. P. Tsvirko, V. V. Sapunov, and K. N. Solovev; Opt. Spectrosk., 34, 1094 (1973).

5) V. N. Kopranenkov, S. N. Dashkevich, and E. A. Lykyanets; Zh. Obshch. Khim., 51, 2513 (1981).

6) W. E. Moerner, M. Gehrtz, and A. L. Huston; J. Phys. Chem., 88, 6459 (1984).

7) T. Suzuki, K. Horie, and T. Yamashita; Chem. Mater., 5, 366 (1993).

8) K. Horie, M. Ikemoto, T. Suzuki, S. Machida, T. Yamashita, and N. Murase; Chem. Phys. Lett., 195, 563 (1992).

9) N. Murase, M. Ikemoto, and K. Horie; J. Chem. Phys., 99, 6313 (1993).

10) A. Furusawa and K. Horie; J. Chem. Phys., 94, 80 (1991).

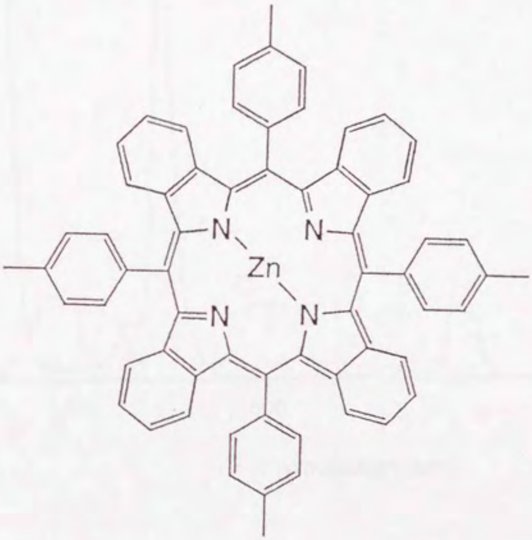

Fig.2.1. Chemical structure of ZnTTBP.

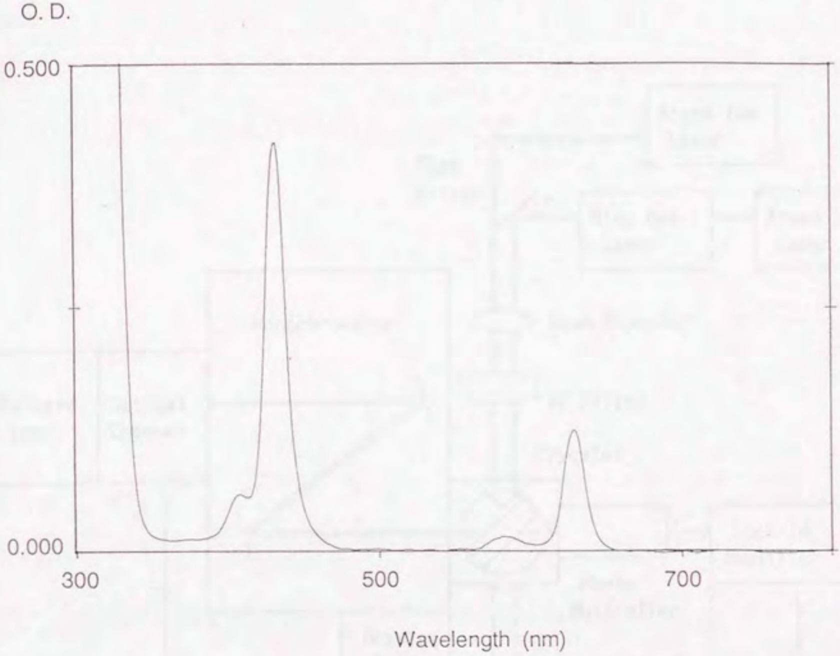

Fig.2.2. Absorption spectrum of ZnTTBP in acetone solution.

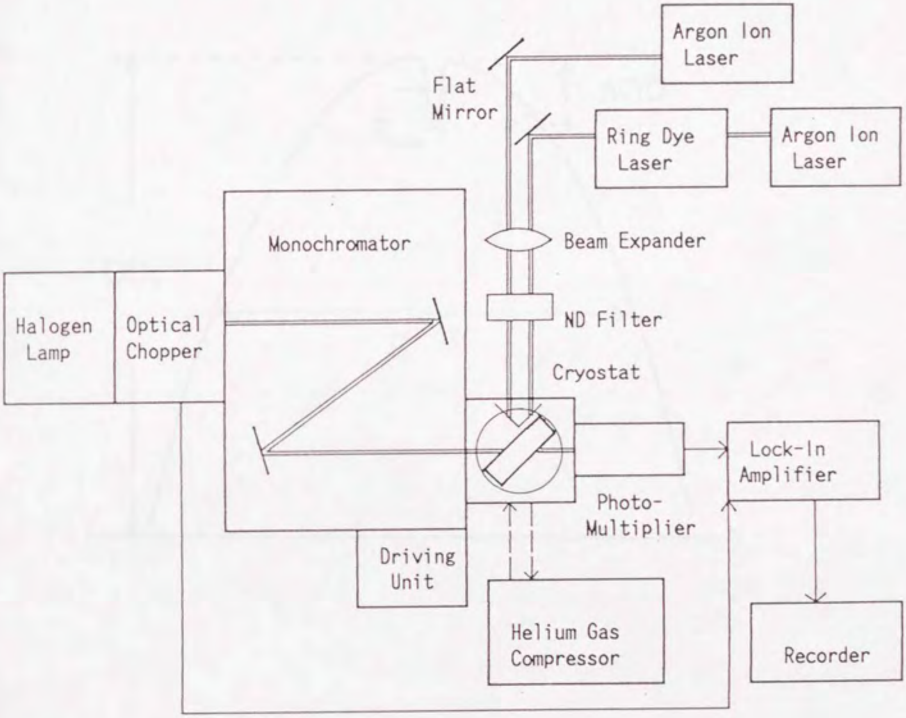

Fig.2.3. Experimental apparatus for PHB.

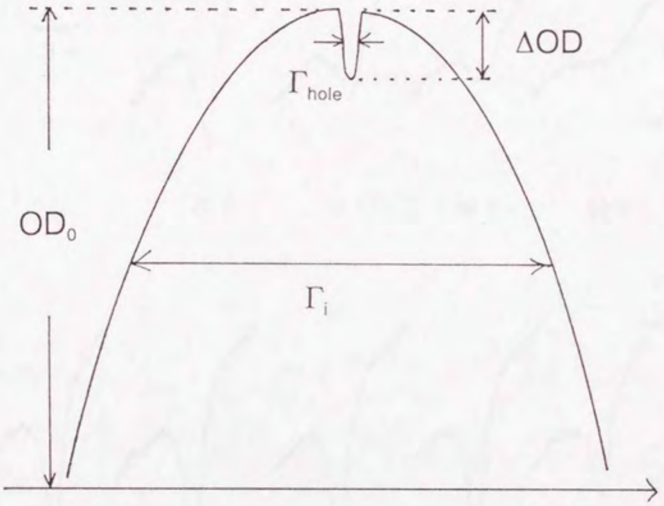

Fig.2.4. Scheme of estimation of quantum efficiency for hole formation.

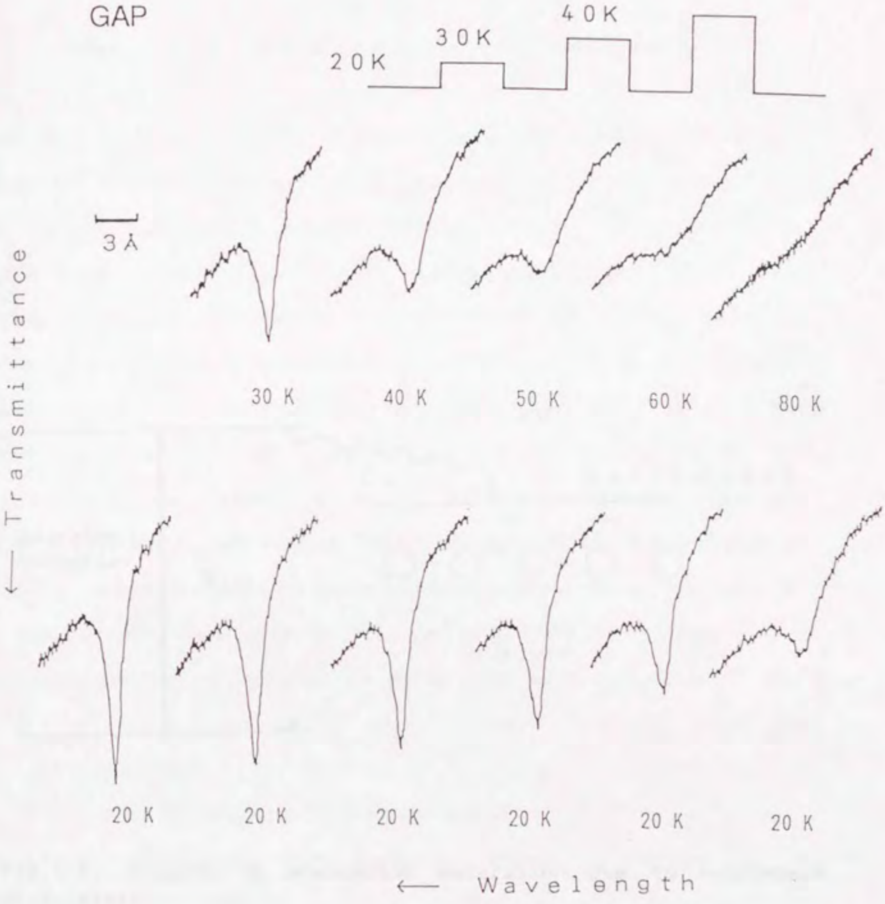

Fig.2.5. Scheme of cycle annealing experiment and typical hole profiles during cycle annealing for ZnTTBP/GAP system.

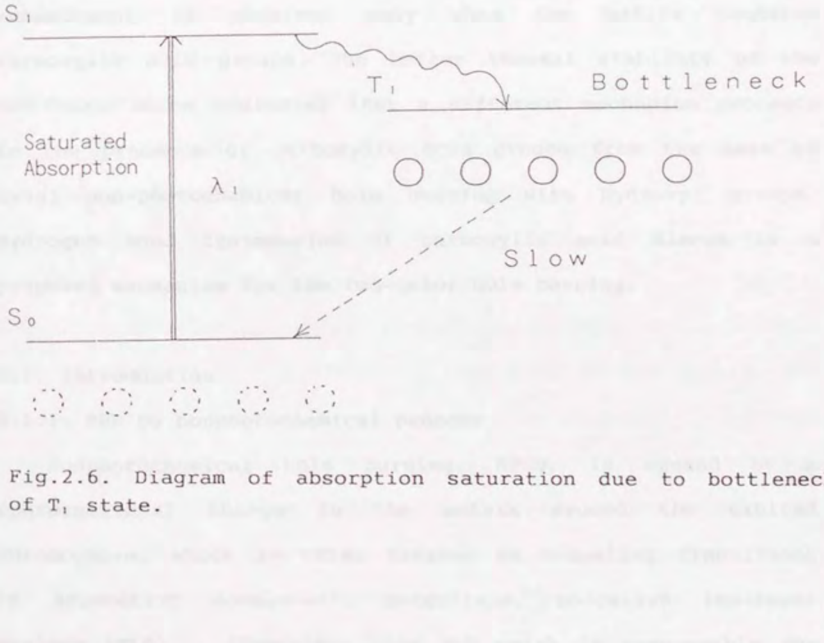

Fig.2.6. Diagram of absorption saturation due to bottleneck of T_1 state.

CHAPTER 3

Two-Color PHB in Polymers Containing Carboxylic Acid

In this chapter, it is reported that persistent holes are formed 1.3～3.0 times more efficiently when the guest molecule (ZnTTBP) are excited by two colors than by one color alone in the matrices containing carboxylic acid. The deuteration of carboxylic acid reduces the enhancement of hole formation by two-color irradiation. The two-color enhancement is observed only when the matrix contains carboxylic acid groups. The better thermal stability of the two-color holes indicates that a different mechanism proceeds in the presence of carboxylic acid groups from the case of usual non-photochemical hole burning with hydroxyl groups. Hydrogen bond tautomerism of carboxylic acid dimers is a proposed mechanism for the two-color hole burning.

3.1. Introduction

3.1.1. PHB by nonphotochemical process

Nonphotochemical hole burning, NPHB, is caused by a conformational change in the matrix around the excited chromophore, which is often treated as tunneling transitions in asymmetric double-well potentials, so-called two-level systems (TLS)[1]. (Sometimes this TLS which is responsible for the NPHB process is called "extrinsic TLS" to distinguish it from "intrinsic TLS" which exists without impurities1). The intrinsic TLS is considered to be far more spatially extended and to induce spectral diffusion1). In this chapter, the term "TLS" is used for the meaning of "extrinsic TLS".)

3.1.2. NPHB in Hydrogen-Bonding Polymers

The hole formation efficiency of NPHB systems is generally low, but efficient NPHB is observed for ionic dye doped in hydrogen-bonding polymers2,3). The hole formation mechanism in such systems is concluded to be a rearrangement of hydrogen-bonding in the vicinity of the excited chromophore, because NPHB was not observed to occur or much less efficient in non-hydrogen-bonding polymers and less efficient in hydroxyl-deuterated polymers3).

Recently, an NPHB system in which the hole formation is enhanced by two-color excitation was reported4). The system is zinc tetrabenzoporphine (ZnTBP) with crotonic acid (CA) doped in phenoxy resin (PhR). In the ZnTBP-CA/PhR system, the holes burnt by two-color excitation was superior in thermal stability to the holes by one-color excitation, which was probed by temperature cycling (annealing) experiments. The mechanism of hole formation in ZnTBP-CA/PhR is supposed to be the rearrangement of hydrogen-bond of CA, but the mechanism of photon-gating is not yet clear.

In this chapter, we report the results of one- and two-color hole burning, and cyclic annealing of burnt holes, in various hydrogen-bonding polymers and discuss the mechanism of hole burning and photon-gating. We used zinc 9,18,27,36-tetra(4-tolyl)tetrabenzoporphine (ZnTTBP) as guest molecules. As matrix polymers we used poly(vinyl hydrogenphthalate) (PVHP), carboxyl-deuterated PVHP (PVDP), 1:1 copolymer of methacrylic acid with methyl methacrylate (P(MA-MMA)), poly(acrylic acid) (PAcA), poly(amid acid) (pyromellitic acid with oxydianiline) (PAmA), phenoxy resin, and cellulose acetate (hydroxyl content: 39.8%) (CelAc). The enhancement of hole formation by two-color irradiation has been observed in the matrix polymers which have contained carboxylic acid groups (PVHP, P(MA-MMA), PAcA, and PAmA), and has not been observed in the polymers containing mere hydroxyl groups (PhR and CelAc). The gating ratio, or the degree of the enhancement, has become smaller in PVDP than in PVHP. The better thermal stability of two-color holes has been observed in the matrices containing carboxylic acid as had been observed in ZnTBP-CA/PhR4). The estimated hole area burnt by the two-color mechanism has hardly been reduced by annealing at low temperatures in each system in contrast to the area of one-color hole which has been reduced drastically by the annealing. These facts suggest that another mechanism quite different from the slight configurational change which is usulally considered as NPHB process should exists in carboxylic acid-containing polymers. The proposed two-color mechanism is a hydrogen bond tautomerism of carboxylic acid dimers. Although the exact evidence for this mechanism is not yet obtained, the mechanism explains successfully the experimental results.

3.2. Sample Preparation

The PVHP (Tokyo Kasei), CelAc (Sowa Science), PAcA (Aldrich), and PAmA (Ube) were used without further purification. The P(MA-MMA) was prepared from the 1:1 mixture of distilled methacrylic acid (Tokyo Kasei) and methyl methacrylate (Wako Pure Chemical Industries), by radical polymerization using 2,2'-azobis- (isobutyronitrile) (Tokyo Kasei) as an initiator. The P(MA-MMA) and PhR (Union Carbide Japan) were used after reprecipitation. The PVDP was prepared by reprecipitation of PVHP into D_2O. Sample films containing about 1×10^{-4} mol/kg of ZnTTBP were prepared with solvent casting by using tetrahydrofuran as a solvent.

3.3. Results and Discussion

3.3.1. Two-Color PHB for ZnTTBP/PVHP

Fig.3.1 shows the absorption spectrum of ZnTTBP/PVHP at room temperature. The spectrum is almost the same as that of ZnTTBP in solution (see chapt.1, Fig.1.3). The acidity of the carboxylic acid in PVHP does not affect the electronic structure of ZnTTBP. (In the case of free-base porphyrin, the acidic matrix causes protonation to the internal nitrogen atom and changes its absorption spectrum drasticallly$^{5)}$.)

Fig.3.2 shows typical hole profiles of ZnTTBP/PVHP burnt by two-color and one-color irradiations. Traces (a), (b), and (c) were formed by 3, 6, and 10 min irradiations, respectively, with λ_1 at 632.9 nm (38 μW/cm^2) and with λ_2 (8 mW/cm^2). Further 2 min irradiation of λ_1 at 632.9 nm (380 μW/cm^2) and λ_2 (8 mW/cm^2) on sample (c) produced trace (d). Traces (e), (f), (g), and (h) show the growth of a one-color hole at 631.4 nm burnt with the same irradiation conditions as for traces (a), (b), (c), and (d), respectively, but without λ_2. Apparently the presence of λ_2 enhances the hole formation compared to the irradiation of λ_1 only. The gating ratio, which is the ratio of the quantum efficiency for hole formation in the case of two-color irradiation, Φ_2, to that in the case of one-color irradiation, Φ_1, is about 3 in this ZnTTBP/PVHP system.

Fig.3.3 shows the absorption spectra of the lowest <u>Q</u> band of ZnTTBP/PVHP before (dashed line) and after (full line) two-color (λ_1: 56 mW/cm^2, λ_2: 45 mW/cm^2) irradiation for 90 min. A broad antihole appears on the short-wavelength side of the hole at 629 nm and the whole band area is not changed by the irradiation. This fact suggests that the hole formation mechanism for ZnTTBP/PVHP is not the chemical reaction of ZnTTBP such as decomposition or electron ejection. No change in the area of the absorption band of the guest chromophore during hole formation has been observed in ZnTTBP/GAP, in which the holes are created by the sensitized photoreaction of the matrix polymer[6,7]. But PVHP contains no photoreactive group, so the hole formation mechanism for ZnTTBP/PVHP is attributed to a non-photochemical process.

The PVHP contains carboxylic acid, which undergoes hydrogen-bonding. In hydrogen-bonding polymers, non-photochemical holes of ionic dyes are reported to be formed far more efficiently than in non-hydrogen-bonding polymers[2], and more efficiently than in hydroxyl-deuterated polymers[3]. The hole formation mechanism in such systems is believed to be the rearrangement of hydrogen-bonds near excited guest chromophores. In Fig.3.4, hole profiles of the two-color [(a), (b), (c), and (d)] and the one-color [(e), (f), (g), and (h)] holes for ZnTTBP/PVDP are shown. Traces (a), (b), (c), and (d) show the two-color hole at 630.0 nm burnt by the 1, 3, 5, and 10 min irradiations, respectively, of λ_1 (75 μW/cm^2) and λ_2 (19 mW/cm^2). The holes in traces (e), (f), (g), and (h) were produced at 631.2 nm by the same irradiation conditions as for traces (a), (b), (c), and (d), repectively, but without λ_2. In Fig.3.4, the gating enhancement is not so apparent (gating ratio: 1.2) as in PVHP. This fact is shown more clearly in Fig.3.5. Fig.3.5

shows the D_r, which is the ratio of the depth of a two-color hole to the depth of a one-color hole for equal λ_1 irradiation times and λ_1 burn intensities, as a function of the irradiated energy of λ_1 for ZnTTBP in PVHP and PVDP. In PVDP, the D_r values are much lower than the D_r in PVHP. This fact indicates that the two-color-enhanced hole burning process in PVHP includes some movement of the carboxyl proton in PVHP. The absolute values of Φ_2 and Φ_1 in PVDP are similar to those in PVHP (in the order of 10^{-5}-10^{-6}) although the carboxyl proton is deuterated in PVDP. This may be due to the existence of phenyl ring because we also observed efficient one-color NPHB in polystyrene as well as in PVHP and PVDP.

3.3.2. Two-Color PHB in Several Hydrogen-Bonding Polymers

Fig.3.6 shows the irradiation time dependences of the hole depth in several hydrogen-bonding polymers, i. e. PVHP, P(MA-MMA), CelAc, and PhR. The enhancement of hole formation by two-color excitation is also observed in P(MA-MMA) as in PVHP although D_r (~ 1.3) is lower than that in PVHP. On the other hand, in CelAc and PhR the irradiation time dependences of hole formation are unchanged irrespective to the existence of λ_2. The gated holes are not burnt in the matrices which do not have carboxylic acid even if the matrix polymers have hydrogen bonds.

The enhancement of hole formation by the simultaneous irradiation of λ_2 is observed in PAcA and PAmA as well as it is observed in PVHP and P(MA-MMA). Fig.3.7 and Fig.3.8 shows the hole profiles of one- and two-color holes for PAcA and PAmA, respectively, with the same irradiation time and irradiation intensity of λ_1. In Fig.3.7 and Fig.3.8, the λ_2 enhances hole burning (the D_r is about 2). If matrix polymer contains carboxylic acid, the gating enhancement is observed without exception. So we attribute the origin of the gating enhancement to be the rearrangement of the hydrogen-bond of the carboxylic acid groups in these polymers.

3.3.3. Thermal Stability of Holes Burnt by One-Color and Two-Color Mechanisms

The changes in the normalized hole area of ZnTTBP/PVHP after cyclic temperature annealing are shown in Fig.3.9. The holes, formed at 20 K by 10 min irradition of λ_1 (75 $\mu W/cm^2$) and λ_2 (15 mW/cm^2), or 75 $\mu W/cm^2$ of λ_1 only, were measured at 20 K after annealing at certain temperatures. The two-color hole keeps 77% of its value after annealing to 28 K, whereas the area of one-color hole becomes 57% of its initial value by cyclic annealing to 28 K. The better thermal stability of the two-color hole as compared to the one-color hole has also been observed in ZnTBP-CA/PhR[4].

Fig.3.10 shows the annealing temperature dependence of hole width for ZnTTBP/PVHP. The holes were burnt at 20 K with the same irradiation condition of Fig.3.3 and measured at annealing temperatures or at 20 K after annealing. The hole widths at certain annealing temperatures, or at 20 K after annealing are not influenced by the fact whether the holes are burnt via one-color excitation or two-color excitation. The hole width at 20 K is broader than the hole width of tetraphenylporphine in various polymers[8)] and ZnTTBP/GAP[7)] at 20 K, and it is probably due to the interaction between guest molecules caused by moderate solubility of ZnTTBP with PVHP. Although the holes are broadened at higher temperatures, the hole width measured at 20 K is unchanged by cyclic annealing up to 36 K.

There are two possible mechanisms of thermally induced hole filling, or irreversible decrease in hole area. One is the backward process of hole burning, which means that the molecules selectively excited and having changed their resonant frequencies change the resonant frequencies again to the frequencies before burning by thermal activation. This is often observed below 40 K in NPHB systems owing to the low barrier height of TLS[9)]). The other is the structural relaxation of host matrix which causes the change in local environments and resonant frequencies of the guest molecules throughout the system, and also results in spectral diffusion. But in this case of ZnTTBP/PVHP, no irreversible hole broadening occurs below 36 K. According to the previous study of our group on the thermally induced hole filling in various tetraphenylporphine-doped polymer systems[8], the structural relaxation of matrix polymers leading to hole filling hardly occurs below 80 K. In addition, if thermally induced hole filling by structural relaxation had occurred, all the holes must have been filled to the same degree irrespective to the mechanism of the hole formation. So we conclude that the hole filling below 40 K is caused by the backward process of hole burning and that the two-color hole includes a component burnt by a different mecnanism from that of one-color holes.

But of course, the hole formation process of one-color hole can also proceed under two-color irradiation. The population of S_1 and T_1 should be the same under the same excitation intensity of λ_1 irrespective of the existence of λ_2 because the gating light should not change the lifetime of S_1 and T_1, and because the lifetime of T_n is extremely short ($<10^{-14}$ s). So we can presume that the hole formation efficiency by one-color mechanism for each system are the same whether the λ_2 exists or not. Then the difference in hole area between the two-color hole and the one-color hole under the same irradiation time and irradiation intensity of λ_1 can be regarded as the area of the hole formed by the two-color mechanism. In Fig.3.11, the annealing temperature dependence of the normalized hole area by two-color mechanism which was estimated by subtracting the area of one-color hole from the area of two-color hole, and the normalized hole area of one-color hole, for PVHP and PVDP are shown. The holes were burnt by 10 min irradiation of λ_1 (75 μW/cm^2) and λ_2 (15 mW/cm^2) or of 75 μ/cm^2 λ_1 only. In contrast to the one-color area the hole area by two-color mechanism is hardly reduced by annealing below 40 K for each system. This fact indicates that the part of the hole by the two-color mechanism in these polymers does not undergo backward reaction below 40 K and has a quite different character from that of the one-color hole.

The better thermal stability of the two-color hole has also been observed in P(MA-MMA). Fig.3.12 shows the one- and two-color hole profiles for ZnTTBP/P(MA-MMA) before [(a) and (b)] and after (c) annealing to 36 K. Trace (a) shows the spectrum after 5 min irradiation of 0.38 mW/cm^2 dye laser at 629.4 nm and 8 mW/cm^2 Ar$^+$ laser. Trace (b) shows the spectrum after 5 min irradiation of λ_1 at 628.3 nm (0.38 mW/cm^2) on the sample (a). In trace (b), the two-color hole at 629.4 nm decreases in its area to 84 % by the one-color irradiation at 628.3 nm. Trace (c) shows the spectrum of the one- and two-color holes at 20 K after their annealing to 36 K. The annealing reduced the area of both holes, but the degree of filling for the two-color hole is smaller than that for the one-color hole.

Further, no decrease in hole area by two-color mechanism at the initial stage of annealing is indicated not only in PVHP and PVDP but also in P(MA-MMA) and PhR with CA4). Table 3.1 shows the degree of hole filling, which is estimated from the slope of the temperature dependence curve of the normalized hole area from 20 K to 30 K, of the one- and two-color hole, $\underline{f}_1$ and $\underline{f}_2$, respectively, and its ratio, $\underline{f}_2/\underline{f}_1$ and $\underline{f}_1/\underline{f}_2$, for ZnTTBP for PVHP, PVDP, P(MA-MMA), CelAc, and PhR with CA4) systems. If the hole formation efficiency by one-color mechanism is unchanged irrespective of the existence of λ_2 (a=b in Fig.3.13), and if the filled part of the two-color hole all consists of one-color mechanism at the beginning of annealing (p=q in Fig.3.13), the values of $\underline{f}_2/\underline{f}_1$ is the fraction of the one-color part in the area of two-color hole. In Fig.3.13, the ratio of hole area is represented by the ratio of hole depth because the hole widths are the same between the one-color and two-color holes and the hole widths are unchanged by the annealing up to 30 K. The values of $\underline{f}_1/\underline{f}_2$ mean thus the area of two-color hole divided by the one-color part, which should be equal to the ratio of hole depth, D_r, on above presumptions as shown in Fig.3.13. In table 6.1, $\underline{f}_1/\underline{f}_2$ value agrees well with the experimental value of D_r in each polymer, which ascertains the above presumptions reasonable.

3.3.4. Mechanism of Two-Color Non-Photochemical Hole Burning in Carboxylic Acid-Containing Polymers

By considering the above results and dicussion, another TLS different from the TLS which is usually considered as NPHB mechanism should exist in carboxylic acid-containing polymers. Fig.3.14 shows the schematic models of the two types of TLSs, namely, the TLS specific to the carboxylic acid-containing polymers (TLS_{COOH}) and the TLS of hydroxyl groups (TLS_{OH}). Symbols (a), (b), and (c) show the TLSs that interact with the impurities (ZnTTBP molecules) in its ground state (S_0), lowest excited state (S_1 or T_1), and highly excited state (T_n), respectively. In each TLS model here, the initial state is chosen to the low-energy (left) side. The relevant parameters for the description of TLS are the energy asymmetry Δ and the tunneling parameter λ, which is connected with the barrier height V as follows[1),

$$\lambda = \underline{d}(2\underline{m}V)^{1/2} / \underline{\hbar}$$

where $\underline{m}$ is tunneling mass and $\underline{d}$ is the displacement. The barrier height V of TLS_{COOH} is still large in its ground state (a), but becomes small in its higher excited state (c), because the holes produced by two-color mechanism are hardly formed by one-color excitation. The barrier height of TLS_{OH} is so small in its lowest excited state that the one-color holes can be observed (b), and does not become so small in its higher excited state as to enhance the hole formation (c). By the difference in thermal stability of the hole by the one- and two-color mechanisms, the barrier height of thermally induced backward process $V-\frac{1}{2}\Delta-E_0$ in TLS_{COOH} is larger than that in TLS_{OH}.

The TLS_{COOH} should involve some movement of carboxyl proton because the gating enhancement is not so apparent in PVDP as is in PVHP. But what kind of motion of proton in carboxylic acid corresponds to the TLS_{COOH} is not yet clear. Fig.3.15 shows a possible mechanism of the two-color hole burning in carboxylic acid. The proposed mechanism is the proton tautomerism of carboxylic acid dimers. The proton tautomerization of carboxylic acid should require higher activation energy than the other hydrogen-bond rearrangement of hydroxyl groups because the tautomerization requires the cleavage and production of chemical bonds and requires the large and coincident motion of the two protons. So the backward tautomerization of carboxylic acid should not occur so easily as the hydrogen-bond rearrangement of hydroxyl groups does. Olson et. al.[10] reported the NPHB in the mixed molecular crystal of pentacene in benzoic acid and attributed the hole burning and antihole formation to hydrogen bond tautomerism of benzoic acid dimers near the excited pentacene molecules. It is not so strange that the hydrogen-bond tautomerism of carboxylic acid is induced by the excitation of guest chromophore in polymer systems if it is induced in molecular crystal.

It is well-known that carboxylic acid usually exists as dimers and forms dimers even in gas phase. But in polymer systems, not all the carboxylic acid groups can form dimers because the chemical bonds in main chain restrict the motion of carboxylic acid to form dimers. The carboxylic acid dimers can be identified by infrared spectra. Fig.3.16 shows the infrared spectra of PVHP and P(MA-MMA). Both polymers show the absorption bands in 3000~2500 cm^{-1} characteristic with carboxylic acid dimers. In the case of PVHP, a rough estimation of the ratio of carboxylic acid groups which form dimers to all the carboxylic acid groups was carried out by comparing the absorbance of dimer absorptions (2650 and 2550 cm^{-1}) divided by the absorbance of the benzene ring (1500 cm^{-1}) as internal standard in the IR spectrum of PVHP, to that for monomethyl terephthalate all of which can be regarded to exist as dimers. According to this estimation, about half of the carboxylic acid groups can form dimers in PVHP. Of course it is true that this estimation is not so exact because the ratio would change by the casting condition, but it can be said that sufficient numbers of carboxylic acid groups exist as dimers nearby the ZnTTBP molecules.

The question of why the tautomerization occurs mainly via two-color excitation still remains if the two-color hole burning in PVHP and P(MA-MMA) involves the hydrogen bond tautomerism. Olson et. al.,[11] who attributed the NPHB of pentacene/benzoic acid system to the hydrogen bond tautomerism of carboxylic acid, proposed two possible causes of tautomerization around the excited chromophore for their system. One is the changes in equibrium lattice configuration which are induced by the increase in polarizability of guest chromophore in its excited state. It may be possible that the two-color-excited ZnTTBP increases its polarizability and causes the tautomerization of carboxylic acid dimers in their vicinity, and that the polarization of one-color-excited ZnTTBP is not so large as to cause the tautomerization. The other proposed cause of tautomerization of carboxylic acid dimers near guest molecules is the local lattice heating by the relaxation process of excited chromophore. The released energy by ZnTTBP of T_n in its relaxation process is two times larger than the energy of ZnTTBP of S_1, and thus, it may also be possible that only the lattice around two-color-excited ZnTTBP becomes "hot" enough to trigger the tautomerization.

The calculations by Graf et. al.[11] showed that the potential barrier of the tautomerization of formic acid dimers is lowered from 200 kJ/mol to 60 kJ/mol by the cooperative motion of the heavy atom framework. In polymer systems, the potential barrier height should have a large distribution due to the inhomogeneity of amorphous solid. So our results may suggest that the cooperative motion of heavy nuclei sufficient to cross over or tunnel through the barrier of the tautomerization can not be induced by the excitation of impurity chromophore with less than 400 kJ/mol (T_n energy of ZnTTBP) of excitation energy.

3.4. Conclusion

The one- and two-color non-photochemical hole burning has been carried out in several hydrogen-bonding polymers. The enhancement of hole formation by two-color excitation and the better thermal stability of the two-color holes has been observed in the matrix polymers containing carboxylic acid. This enhancement has markedly become reduced by the deuteration of carboxylic acid in PVHP. The estimated hole area by the two-color mechanism has hardly been filled by annealing up to 40 K in PVHP and PVDP. The ratio of the filling degree of the one-color holes at the beginning of annealing to that of the two-color holes has agreed well with the ratio of the depth of two-color hole to that of one-color hole in each polymer. These facts suggest that another TLS different from the TLS which is usually considered as NPHB process exists in polymers containing carboxylic acid. A possible mechanism of two-color hole burnig in carboxylic acid-containing polymers is proposed. The proposed two-color mechanism is hydrogen-bond tautomerism of carboxylic acid dimers near excited chromophore. Further studies including on NPHB are required to make clear the microscopic structures and local rearrangements of hydrogen bonds, especially hydrogen bonds in carboxylic acid, in amorphous polymers at low temperatures.

References

1) R. Jankowiak and G. J. Small; Science, 237, 618 (1987).

2) B. L. Fearey, T. P. Carter, and G. J. Small; J. Phys. Chem., 87, 3590 (1983).

3) B. L. Fearey, R. P. Stout, J. M. Hayes, and G. J. Small; J. Chem. Phys., 78, 7013 (1983).

4) K. Horie, Z.-L. Zhang, L.-Q. Shi, S. Machida, T. Suzuki, S.-M. Yao, and M.-H. Zhang; Polym. J., 24, 715 (1992).

5) A. Furusawa, K. Kuroki, K. Horie, and I. Mita; Polym., 32, 2167 (1991).

6) S. Machida, K. Horie, and T. Yamashita; Appl. Phys. Lett., 60, 286 (1992).

7) S. Machida, K. Horie, O. Kyono, and T. Yamashita; J. Lumin., 56, 85 (1993)

8) A. Furusawa and K. Horie; J. Chem. Phys., 94, 80 (1991).

9) W. Köhler and J. Friedrich; Phys. Rev. Lett., 59, 2199 (1987).

10) R. W. Olson, H. W. Lee, F. G. Patterson, M. D. Fayer, R. M. Shelby, D. P. Burum, and R. M. Macfarlane; J. Chem. Phys., 77, 2283 (1982).

11) E. Graf, R. Meyer, T.-K. Ha, and R. R. Ernst; J. Phys. Chem., 75, 2914 (1981).

Table 3.1. Degree of hole filling at the beginning of annealing for one- and two-color holes ($\underline{f}_1$ and $\underline{f}_2$ respectively), values of $\underline{f}_2/\underline{f}_1$ and $\underline{f}_1/\underline{f}_2$, and gating ratio, G[*], for ZnTTBP in PVHP, P(MA-MMA), and CelAc, and for ZnTBP-CA/PhR4) systems.

	$\underline{f}_1$ (%/K)	$\underline{f}_2$ (%/K)	$\underline{f}_2/\underline{f}_1$	$\underline{f}_1/\underline{f}_2$	G
PVHP	5.3	2.9	0.55	1.8	1.7
PVDP	5.0	4.1	0.82	1.2	1.2
P(MA-MMA)	5.6	4.6	0.82	1.2	1.3
CelAc	3.8	3.7	0.97	1.0	1.0
ZnTTBP-CA	5.8	3.2	0.55	1.8	2.0

[*] G values are calculated from the hole depths of one- and two-color holes which are burnt for the annealing experiments, so the G in PVHP is different from the value obtained from the depths at the initial stage of hole burning.

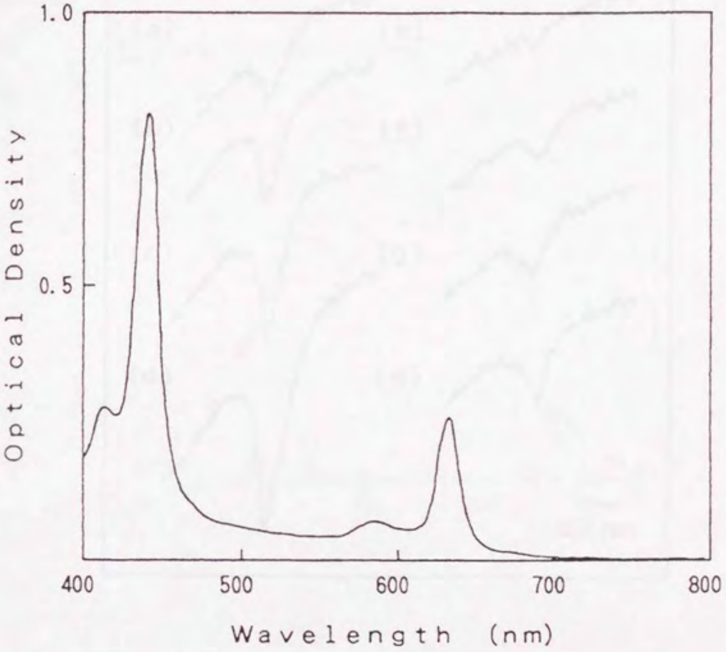

Fig.3.1. Absorption spectrum of ZnTTBP/PVHP at room temperature.

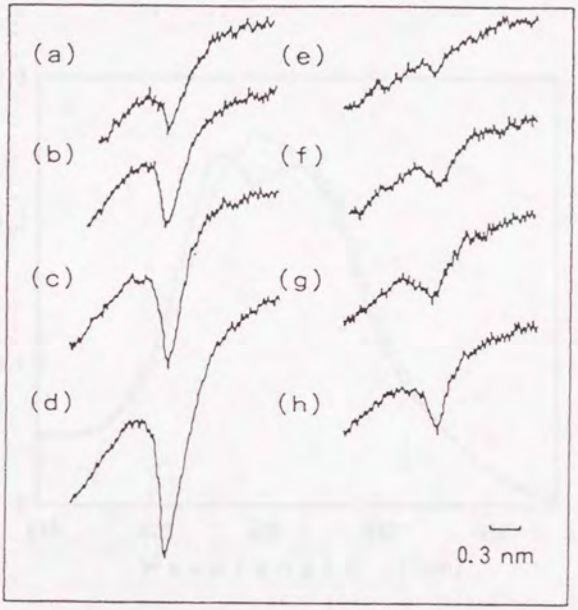

Fig.3.2. Hole profiles for ZnTTBP/PVHP burnt by two- and one-color irradiations at 20 K. Traces (a), (b), and (c) were formed by 3, 6, and 10 min, respectively, irradiations with λ_1 at 632.9 nm (38 μW/cm^2) and λ_2 (8 mW/cm^2). Further 2 min irradiation of λ_1 at 632.9 nm (380 μW/cm^2) and λ_2 (8 mW/cm^2) produced trace (d). Traces (e), (f), (g), and (h) show the growth of a one-color hole burnt at 631.4 nm by the same irradiation condition as traces (a), (b), (c), and (d), respectively, but without λ_2.

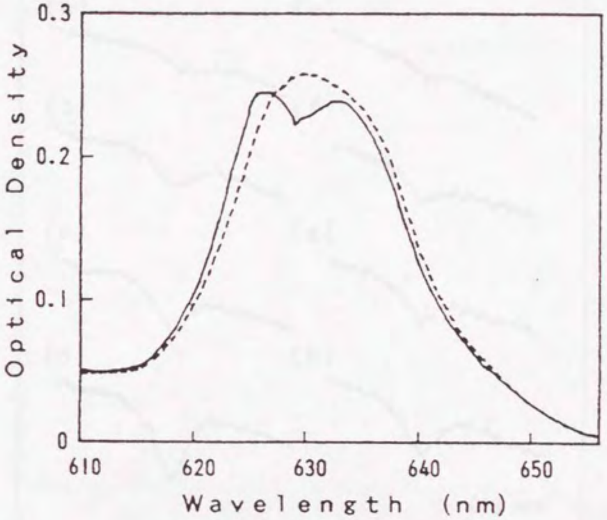

Fig.3.3. Absorption spectra of the lowest Q band of ZnTTBP before (full line) and after (dashed line) a two-color irradiation at 629 nm with 56 mW/cm² of λ_1 and 45 mW/cm² of λ_2 for 90 min.

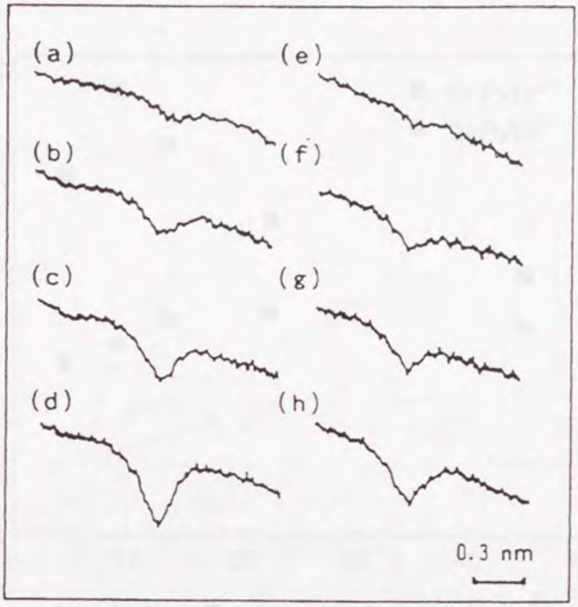

Fig.3.4. Two-color and one-color hole profiles for ZnTTBP/PVDP at 20 K. Traces (a), (b), (c), and (d) show a two-color hole at 630.0 nm burnt by 1, 3, 5, and 10 min irradiations, respectively, of λ_1 (75 μ W/cm^2) and λ_2 (15 mW/cm^2). Traces (e), (f), (g), and (h) show the growth of a one-color hole at 631.2 nm burnt by the same irradiation conditions as for traces (a), (b), (c), and (d), respectively, but without λ_2.

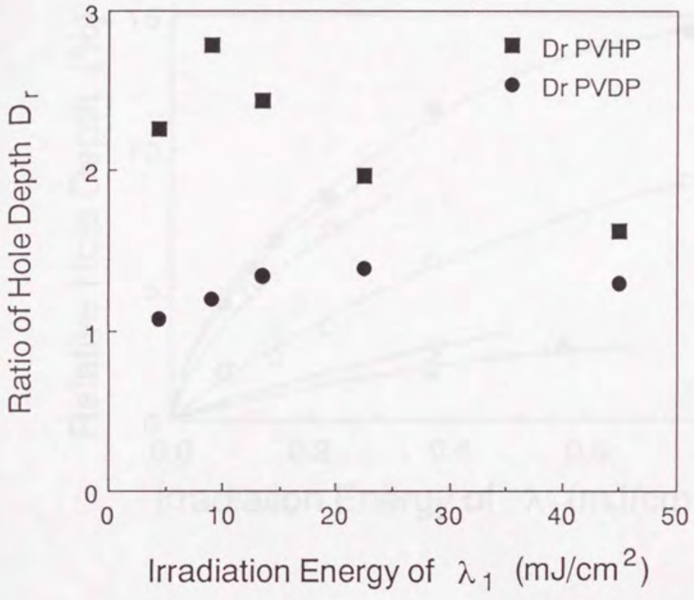

Fig.3.5. Ratio of the depth of two-color hole to the depth of a one-color hole for equal λ_1 irradiation times and λ_1 burn intensities as a function of the irradiated energy of λ_1 for ZnTTBP in PVHP and PVDP at 20 K.

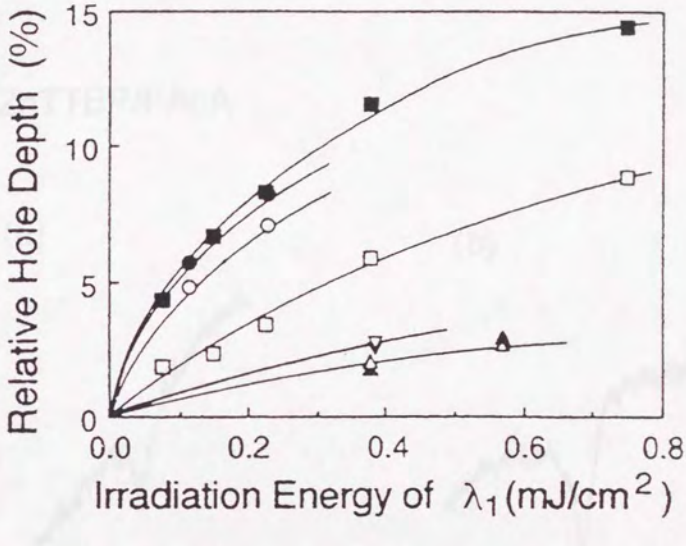

Fig.3.6. Irradiation-time dependences of hole depth for PVHP (■,□), P(MA-MMA) (●,○), CelAc (▼,▽), and PhR (▲,△), burnt by one-color (□,○,▽,△) and two-color (■,●,▼,▲) irradiations at 20 K.

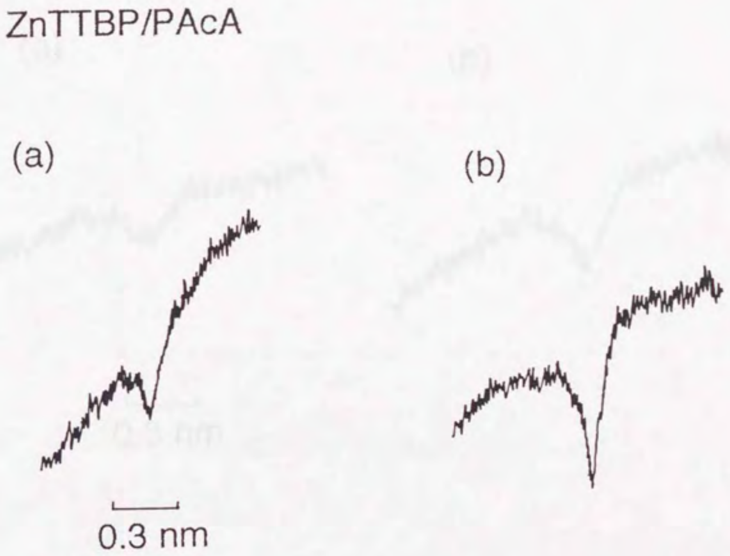

Fig.3.7. Profiles of one- (a) and two-color (b) holes for ZnTTBP in PAcA. The holes were burnt with 12 min irradiation of 0.38 mW/cm² λ_1 ((a), (b)) and 8 mW/cm² λ_2 (b).

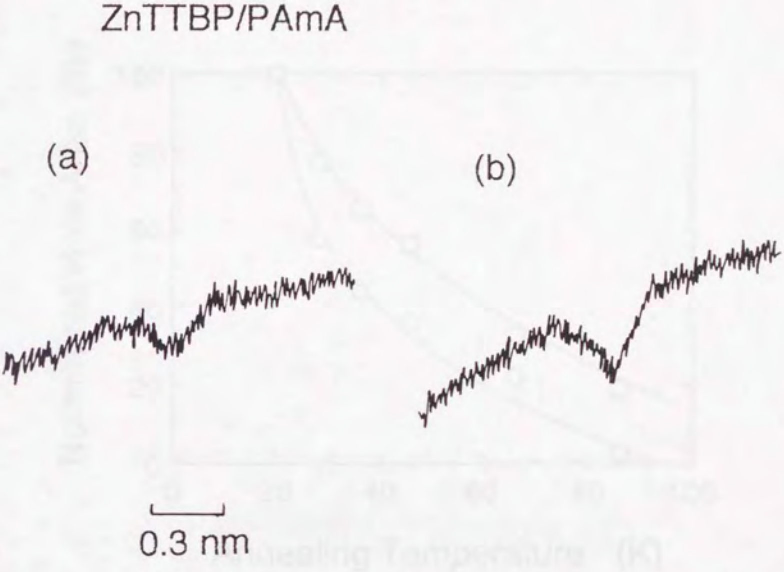

Fig.3.8. Hole profiles for ZnTTBP/PAmA. The holes were burnt by one-color ((a): λ_1 0.38 mW/cm^2, 6 min) and two-color ((b): λ_1 0.38 mW/cm^2 + λ_2 1 mW/cm^2, 6 min).

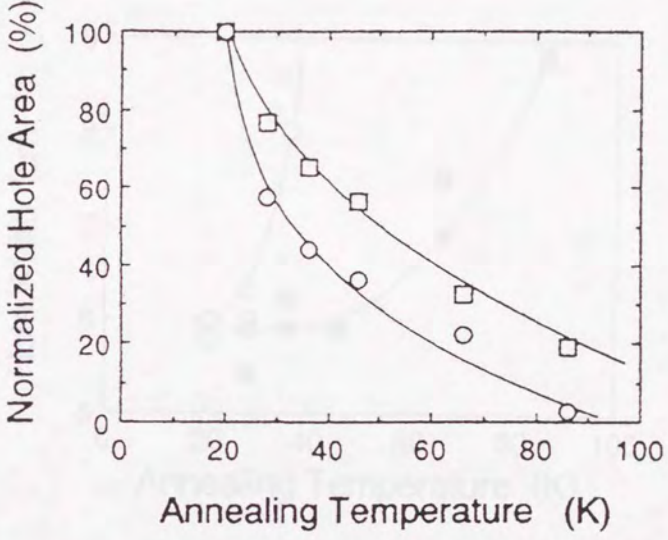

Fig.3.9. Annealing temperature dependence of normalized hole area for ZnTTBP/PVHP measured at 20 K after annealing. Two-color hole (□) was burnt at 20 K by 10 min irradiation of λ_1 (75 μW/cm^2) and λ_2 (15 mW/cm^2), and one-color hole (○) was burnt by 10 min irradiation of λ_1 (75 μW/cm^2).

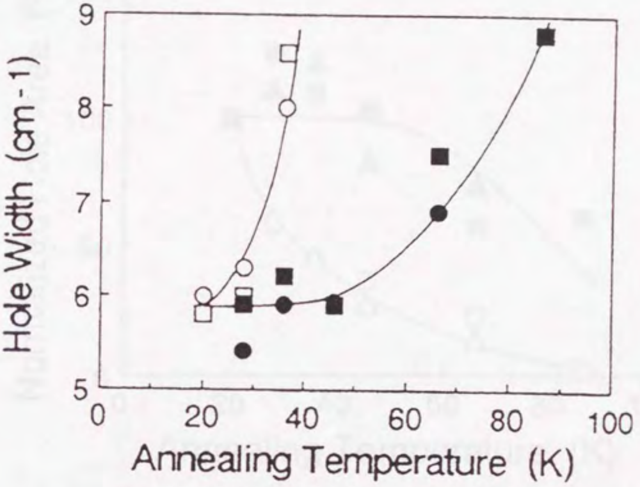

Fig.3.10. Annealing temperature dependence of hole width for ZnTTBP/PVHP. Holes were burnt with the same irradiation condition of Figure 6 at 20 K and measured at annealing temperature (1-color:○ and 2-color:□) and at 20 K after annealing (1-color:● and 2-color:■).

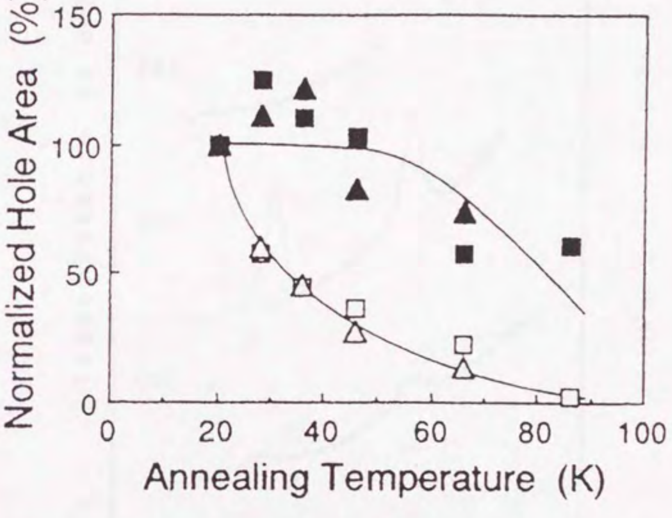

Fig.3.11. Annealing temperature dependence of normalized hole area by two-color mechanism which was estimated by subtracting the area of one-color hole from the area of two-color hole (■,▲), and normalized hole area of one-color hole (□,△), for PVHP (■,□) and PVDP (▲,△). The holes were burnt at 20 K by 10 min irradiation of λ_1 (75 μW/cm^2) and λ_2 (15 mW/cm^2) or of 75 μW/cm^2 λ_1 only.

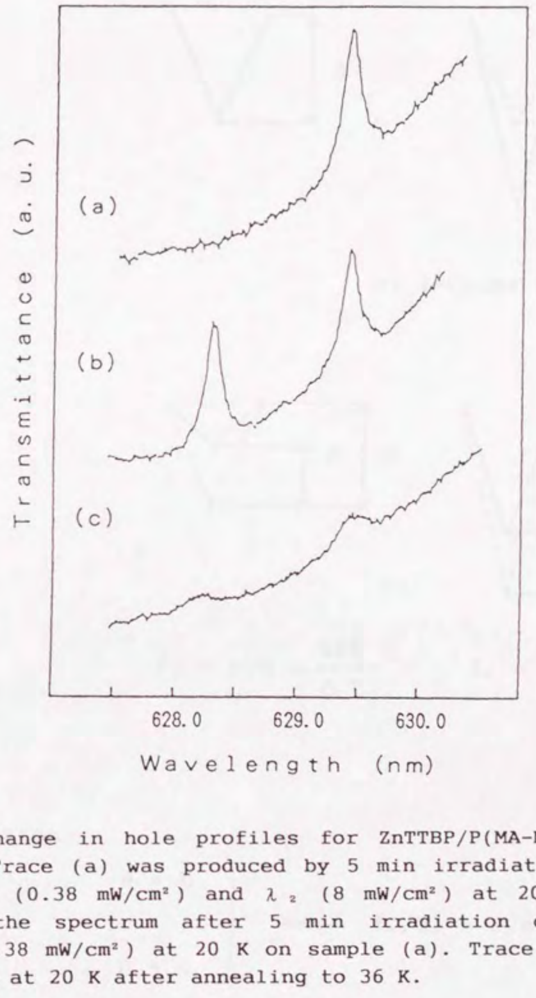

Fig.3.12. Change in hole profiles for ZnTTBP/P(MA-MMA) after annealing. Trace (a) was produced by 5 min irradiation of λ_1 at 629.4 nm (0.38 mW/cm^2) and λ_2 (8 mW/cm^2) at 20 K. Trace (b) shows the spectrum after 5 min irradiation of λ_1 at 628.3 nm (0.38 mW/cm^2) at 20 K on sample (a). Trace (c) shows the spectrum at 20 K after annealing to 36 K.

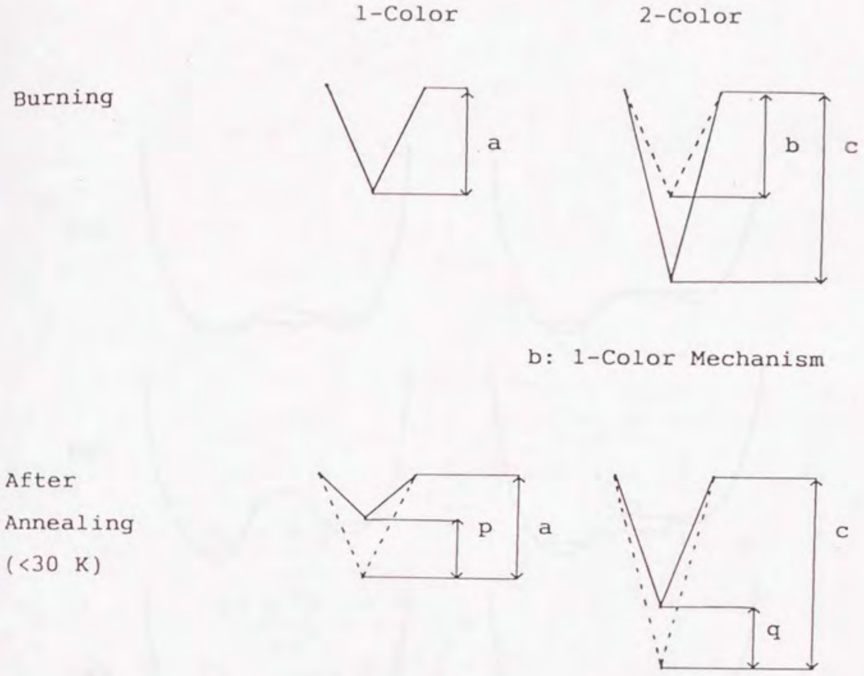

$$f_1 = p/a \times \frac{100}{\Delta T} \qquad f_2 = q/c \times \frac{100}{\Delta T}$$

Presumption:

$$\left.\begin{array}{l} a = b \\ \\ p = q \end{array}\right\} \Longrightarrow \quad f_1/f_2 = c/a = D_r$$

Fig.3.13. Schematic illustration of hole depth (or area) of the one- and two-color holes before (upper holes) and after (lower holes) annealing (<30 K). If we presume a=b and p=q, f_1/f_2 should equal to D_r for each system (see text).

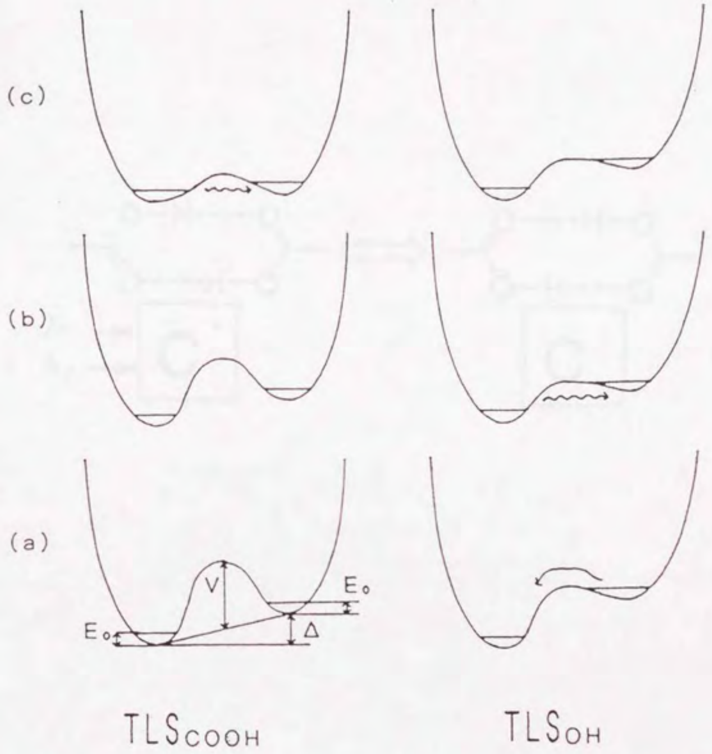

Fig.3.14. Schematic models of TLS_{COOH} and TLS_{OH}. Symbols (a), (b), and (c) show the TLSs which interact with ZnTTBP in its ground state, lowest excited state, and higher excited state, respectively.

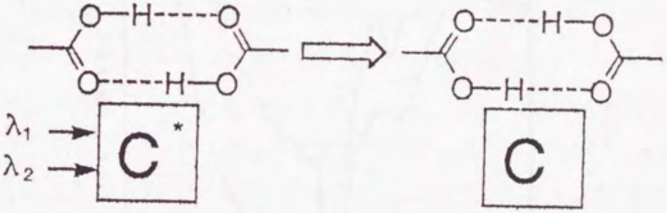

Fig.3.15. Schematic model of the proposed mechanism of two-color hole burning in carboxylic acid-containing polymers. C stands for the guest chromophore.

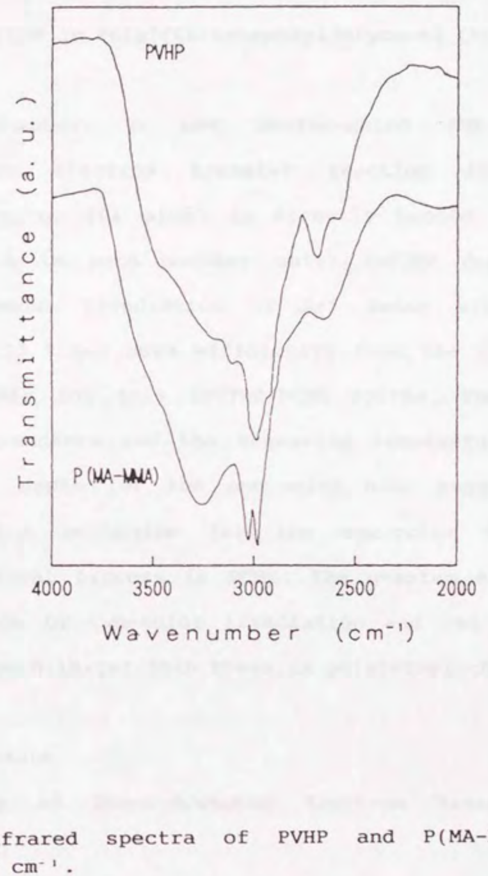

Fig.3.16. Infrared spectra of PVHP and P(MA-MMA) between 4000 and 2000 cm^{-1}.

CHAPTER 4

Photon-Gated PHB by Donor-Acceptor Electron Transfer: ZnTTBP in Poly[(Chloromethyl)styrene] (PCMS)

In this chapter, a new photon-gated PHB system by donor-acceptor electron transfer reaction in which the electron acceptor (Cl atom) is directly bonded to the matix polymer chain in each monomer unit: ZnTTBP doped in PCMS. The simultaneous irradiation of Ar^+ laser with dye laser forms holes 70 times more efficiently than the irradiation of dye laser only for this ZnTTBP/PCMS system. The irradiation intensity dependence and the annealing temperature dependence of the hole depth for the one-color hole suggest that the hole formation mechanism for the one-color hole is the non-photochemical process in PCMS. The quantum efficiency for hole formation by two-color irradiation and the gating ratio in PCMS are much larger than those in poly(vinyl chloride).

4.1. Introduction

4.1.1 Theory of Donor-Acceptor Electron Transfer (DA-ET) Processes

DA-ET is one of the most popular mechanism for the investigation of new photon-gated PHB materials. It seems because the DA-ET is one of the most popular reaction types of photochemistry and many combinations of donors and acceptors can be considered. From the scientific aspects, most attention has been paid to the energy gap dependence of reaction rate in DA-ET processes. Marcus predicted the existence of inverted region, in which the reaction rate decreases as the DA-ET process becomes exothermic, at first in 1956[1,2]. In 1979, Miller et. al. proved the existence of the inverted region experimentally[3]. Kakitani and Mataga proposed a theory which explains the numerous experimental results of DA-ET in 1985[4,5]. According to this theory, the rate constant of DA-ET has no inverted region in the case of charge separation (CS) reaction and has the inverted region in the case of charge recombination (CR) reaction (Fig.4.1). This is due to the contribution of the solvent molecules which coordinate strongly to the reactant molecules in charge separated state. As is shown in Fig.4.2, the reorientation energy of the solvent becomes large in the final state of CS reaction and the initial state of CR reaction. So the inverted region appears only in the case of CR reaction.

4.1.2. Photon-Gated PHB systems via DA-ET

Almost all of the reported PHB systems via DA-ET reaction are utilized porphyrin derivatives as a donor chromophore and halogenated compounds as an acceptor[6,7]. The advantage of using halogenated compounds as an acceptor is that the rapid detachment of halogen anion takes place after electron transfer and that the stability of the detached halogen anion prevents the backward electron transfer reaction. In the case of tetraphenylporphine (TPP) with p-benzoquinone doped in PMMA system, the hole filling due to the backward electron transfer reaction from p-benzoquinone to TPP was observed in the cycle annealing experiment to 20 K[8]. Recently, suppression of the back reaction by using sacrificially consumable molecules in the PHB systems via DA-ET is reported[9].

In addition to the suppression of the back reaction, it is important for the PHB systems via DA-ET that the acceptor must exist in the proximity to the donor porphyrin and so the matrix should contain the acceptor with high concentration without phase separation. To achieve this electron acceptors such as chloroform which can be a good solvent of the porphyrin and matrix polymers have been used in some systems[6]. The other approach to put the high concentration of electron acceptor into the matrix is to use the polymer which have the electron acceptor directly bonded to the polymer chain[10,11].

In this chapter we report a new efficient system of photon-gated PHB via DA-ET in which the matrix polymer has the chlorine acceptor in its every monomer unit. The system consists of a zinc porphyrine derivative, zinc 9, 18, 27, 36-tetra(4-tolyl)tetrabenzoporphine (ZnTTBP) as a donor chromophore, and poly(chloromethylstyrene) (PCMS) as a matrix polymer containing acceptor groups. The quantum efficiency of hole formation for ZnTTBP for the one- and two-color excitations and the gating ratio have been measured in PCMS and compared to those in poly(vinyl chloride) (PVC)[10] and PMMA with chloroform[6,7].

4.1.2. Energy Digram for DA-ET of ZnTTBP/PCMS System

Fig.4.3 illustrates the schematic diagram and the relevant parameters for photon-gated PHB via DA-ET for the ZnTTBP/PCMS and its related systems. The relevant parameters are the oxidation potentials, E_{ox}, of ZnTTBP in S_0, S_1, T_1, and T_n state, $E_{ox}(S_0)$, $E_{ox}(S_1)$, $E_{ox}(T_1)$, and $E_{ox}(T_n)$, respectively, which are estimated from $E_{ox}(S_0)$ of zinc tetrabenzoporphine[12], and the reduction potentials, E_{red}, of electron acceptors containing chlorine, namely, 3-chloropentane [$(Et)_2CHCl$], benzylchloride ($PhCH_2Cl$), and chloroform ($CHCl_3$)[13]. The $(Et)_2CHCl$ and $PhCH_2Cl$ are considered to have the similar E_{red} to PVC and PCMS, respectively. The E_{red} of $PhCH_2Cl$ is close to E_{red} of $CHCl_3$ and $E_{ox}(S_1)$ of ZnTTBP, and is lower than the E_{red} of $(Et)_2CHCl$.

In PCMS the quantum efficiency of hole formation for the two-color excitation is 70 times larger than that for the one-color excitation. The irradiation intensity dependence of hole depth of the one-color hole and the annealing experiment has suggested that the one-color hole is created by the non-photochemical process in PCMS. The hole formation efficiency for the two-color excitation and the gating ratio in PCMS are a little smaller than those in PMMA with chloroform and are much larger than those in PVC. The effects of the concentration and the reduction potential of the acceptor on the hole formation efficiency and on the gating ratio are also discussed.

4.2. Sample Preparation

The PCMS was polymerized from distilled (chloromethyl) styrene (p- and m- mixture, Tokyo Kasei) by radical polymerization using 2,2'-azobis-(isobutyronitrile) (Tokyo Kasei) as an initiator. The PMMA was obtained from distilled methyl methacrylate (Wako Pure Chemical). The PCMS, PMMA, and PVC (Wako Pure Chemical) were used after reprecipitation. Sample films containing about 1×10^{-4} mol/kg of ZnTTBP were prepared with sovent casting using tetrahydrofuran as a solvent.

4.3. Results and Discussion

4.3.1. Photon-Gated PHB for ZnTTBP/PCMS

Fig.4.4 shows the absorption spectrum of ZnTTBP/PCMS at room temperature. Because the absorption profile of the sample is the same as that of ZnTTBP solution and because the shift of the peak wavelength is not observed, ZnTTBP in PCMS does not form a chage-transfer complex at the ground state.

Typical hole profiles for ZnTTBP/PCMS are shown in Fig.4.5. Traces (a), (b), and (c) show the growth of a two-color hole at 627.8 nm burnt by 1 min, 2 min, and 4 min irradiations, respectively, of 10 μW/cm^2 dye laser and 1 mW/cm^2 Ar$^+$ laser. Trace (d) is the transmission spectrum after 4 min irradiation of 10 μW/cm^2 of λ_1 at 629.8 nm. Further irradiations with one-color at 629.8 nm on the sample (d) produced traces (e) and (f) [(e): 40 μW/cm^2, 2 min, (f): 400 μW/cm^2, 1 min]. It is apparent that the λ_2 enhances the hole formation because the total irradiated energy of λ_1 for the trace (f), for example, is 52 times larger than that for the trace (a) in which the similar depth of hole to that in trace (f) is burnt. The two-color hole burning for ZnTTBP/PCMS is attributed to the DA-ET reaction from the T_n of ZnTTBP to the chlorine atom in PCMS, because the strong irradiation of the two-color reduces the area of the absorption band of ZnTTBP.

The quantum efficiency for hole formation based on λ_1, Φ, was measured at the peak of the inhomogeneous line and was calculated by the following equation (1)[14,15]:

$$\Phi = -\{d\underline{A}/d\underline{t}\}_{\underline{t}=0}/\{10^3\,\underline{I}_0\,(1-10^{-A_0})\ \varepsilon\ \underline{R}\}$$

where $\underline{A}$ is a time-varing absorbance at the laser frequency, $\underline{A_0}$ is the absorbance before irradiation, $\underline{I_0}$ is the incident laser intensity given in einstein $cm^{-2}s^{-1}$, ε is the molar extinction coefficient for the peak absorption at room temperature, and $\underline{R}=\Gamma_i/\Gamma_h$ is the reciprocal initial ratio of a hole width, Γ_h, to an inhomogeneous width, Γ_i. In PCMS the Φ in the presence of λ_2, Φ_2, and the Φ for the case without λ_2, Φ_1, are 6.1×10^{-4} and 8.7×10^{-6}, respectively. So the initial gating ratio, $G_i=\Phi_2/\Phi_1$, becomes 70 for this ZnTTBP/PCMS system.

4.3.2. Hole Burning Mechanism of One-Color Holes for ZnTTBP/PCMS

For the high gating ratio, it is necessary not only for Φ_2 to be high but also for Φ_1 to be low. So it is significant to clarify the hole formation mechanism of the one-color holes in photon-gated PHB systems. Fig.4.6 shows the irradiation intensity dependence of the relative hole depth of the one-color hole in PCMS. The one-color holes were burnt with the various intensities of λ_1 for the fixed irradiation time of 4 min. In Fig.4.6 the hole depth is almost linear to the intensity at the low intensity region, but becomes saturated when the intensity is more than 0.2 mW/cm^2. This fact indicates that the absorption of ZnTTBP becomes saturated due to the bottleneck of T_1 state when the excitation intensity of λ_1 is more than 0.2 mW/cm^2 and that the hole formation under one-color irradiation is the one-photon process. This is reasonable because the critical intensity of λ_1, $\underline{I}_{1c}$, which induces absorption saturation, is estimated to be ~ 0.2 mW/cm^2 according to the following equations (2), (3)[16]:

$$\underline{I}_{1c}=\underline{hc}/(\sigma\,\Phi_{ISC}\,\tau_{T1}\,\lambda_1) \qquad (2)$$

$$\sigma = 10^3\ \varepsilon\,\Gamma_i/(\underline{N}_A \log \underline{e}\,\Gamma_h) \qquad (3)$$

where σ is absorption cross section of a ZnTTBP molecule, Φ_{ISC} is quantum yield of intersystem crossing, τ_{T1} is lifetime of T_1, $\underline{h}$ is Planck constant, $\underline{c}$ is velocity of light, and $\underline{N}_A$ is Avogadro's number. The values of $\Phi_{ISC}=0.9$, $\tau_{T1}=20$ ms, $\varepsilon=10^5$ $\underline{l}$ mol^{-1} cm^{-1}, and $(\Gamma_i/\Gamma_h)=300$ were used for the estimation of $\underline{I}_{1c}$. The one-photon hole formation process under the one-color irradiation in PCMS is in contrast to the the one-color process for ZnTTBP/GAP system[14] in which the one-color hole is burnt via the one-color two-photon sensitization mechanism.

Fig.4.7 shows the change in hole spectra of the one- and two-color holes for ZnTTBP/PCMS during the cyclic annealing to 35 K. Trace (a) shows the spectrum at 20 K before annealing. In trace (a) the left hole at 631.1 nm is burnt by the two-color irradiation (λ_1: 40 μW/cm^2, λ_2: 1 mW/cm^2) for 3 min, and the right hole at 632.6 nm is burnt by the one-color irradiation (400 μW/cm^2, 10 min). Trace (b) shows the spectrum of the sample (a) during the annealing at 35 K, and trace (c) shows the spectrum of the sample cooled to 20 K after the annealing. In traces (b) and (c) the degree of the thermally induced hole filling for the two-color hole is smaller than that for the one-color hole. Thus the two-color hole and the one-color hole should be produced by the different mechanisms in PCMS. The better thermal stability of the two-color hole is also observed for ZnTBP in phenoxy resin with crotonic acid$^{17)}$ and for ZnTTBP in poly(vinyl hydrogenphthalate)$^{18)}$. Usually the photochemical hole is hardly filled by the annealing below 40 K$^{19)}$. whereas the hole area by non-photochemical origin is much reduced by the annealing below 40 K$^{20)}$. So we conclude that the one-color hole for ZnTTBP/PCMS is created by a nonphotochemical mechanism. The one-color hole burning for ZnTTBP-CHCl$_3$/PMMA is also attributed to the nonphotochemical mechanism from the difference in the temperature dependence of Φ_1 and $\Phi_2$$^{7)}$.

4.3.3. PHB for ZnTTBP in Poly(vinyl chloride) (PVC)

In Fig.4.8 the results of the one- and two-color hole burnings and of the cyclic annealing for ZnTTBP/PVC are shown. Trace (a) shows the two-color hole at 630.4 nm (λ_1:

40 μW/cm^2, λ_2: 1 mW/cm^2, 8 min) at 20 K. In trace (b) the hole profile of the sample (a) at 20 K after the annealing to 35 K is shown. Traces (c) and (d) are the spectra of the one-color hole at 631.4 nm burnt and measured by the same conditions as for the traces (a) and (b), respectively, but without λ_2. In contrast to ZnTTBP/PCMS, the λ_2 hardly enhances the hole formation in PVC as is shown in traces (a) and (c). Traces (b) and (d) shows that almost all the one- and two-color holes are filled by the annealing to 35 K, suggesting that both holes are formed mainly by the nonphotochemical process. In trace (b), however, a bit of the two-color hole remains. This part is probably burnt by DA-ET reaction.

4.3.4. Gating Ratio of PHB Systems via DA-ET

The Φ_1, Φ_2, and G for ZnTTBP in PCMS, PVC, and PMMA with $CHCl_3$ measured by our experimental apparatus are shown in Table 4.1. The results for the ZnTTBP/GAP[16] in which the hole is formed by two-photon sensitized photoreaction are also shown in Table 1 for comparison. The Φ_2 in PCMS is about 4 times smaller than that in PMMA with $CHCl_3$, and is about 30 times larger than that in PVC. This indicates that the rate constant of DA-ET reaction from the T_n of ZnTTBP in PCMS is a little smaller than that in PMMA with $CHCl_3$ and much larger than that in PVC. Moerner et al., who report the photon-gated PHB for ZnTTBP-$CHCl_3$/PMMA[6,7] and ZnTTBP/PVC[10], have attributed the low Φ_2 in PVC to the low concentration of the acceptor site or chlorine in PVC[10]. But in spite of the fact that the concentration of the chlorine atom in PCMS is about 2.5 times lower than that in PVC, the Φ_2 in PCMS is about 30 times larger than that in PVC as is shown in Table 4.1. No dependence of the acceptor concentration on Φ_2 in the case where the acceptor is directly bonded to the matrix polymer is also reported in ref. 9. So we conclude that the main parameter for the photon-gated PHB system via DA-ET which determines the Φ_2 is not the concentration of the acceptor as far as the acceptor concentration is high enough. Takahashi et. al.[21] report the dependence of ΔG, the free energy release of the DA-ET reaction, on Φ_1 and Φ_2 for several photon-gated PHB systems. According to their results and discussion the Φ_2 becomes higher as ΔG increases, which is consistent with our result for ZnTTBP/PCMS and ZnTTBP/PVC. So we attribute the difference in Φ_2 for PCMS and PVC to the difference in ΔG or E_{red} of the two matrices. The difference in Φ_2 between the ZnTTBP/PCMS and ZnTTBP-$CHCl_3$/PMMA may be due to the difference in E_{red} of the two matrices or in the acceptor concentration. (We used the ZnTTBP-$CHCl_3$ sample containing more than 10 mol/kg of $CHCl_3$.)

In Table 4.1 the Φ_1 values do not differ so much from each other as Φ_2 values do, except for ZnTTBP/GAP which shows the low Φ_1 resulting in the high gating ratio. The hole formation mechanism for the one-color hole in PCMS, PVC, and PMMA with $CHCl_3$ is the nonphotochemical process. On the other hand, the one-color hole in GAP is burnt by the two-photon photochemical reaction[21]. So the suppression of the nonphotochemical hole burning process should be a good way to discover the PHB systems with high gating ratio.

4.4. Conclustion

In conclusion, we has presented a new photon-gated PHB system via DA-ET, ZnTTBP/PCMS, in which the electron acceptor is directly bonded to the matrix polymer chain in each monomer unit. The one-color hole burning for ZnTTBP/PCMS is attributed to the non-photochemical process. The Φ_2 and G for ZnTTBP/PCMS are much larger than those for ZnTTBP/PVC. It has been suggested that it is not only important to choose the acceptor with a proper reduction potential but also important the suppression of the nonphotochemical hole buring process for the reserch of the photon-gated PHB systems with high gating-ratio.

References

1) R. A. Marcus; J. Chem. Phys., 24, 966 (1956).

2) R. A. Marcus; J. Chem. Phys., 24, 979 (1956).

3) J. V. Beitz and J. R. Miller; J. Chem. Phys., 71, 4579 (1979).

4) T. Kakitani and N. Mataga; J. Phys. Chem., 87, 4572 (1985).

5) T. Kakitani and N. Mataga; J. Phys. Chem., 89, 8 (1985).

6) T. P. Carter, C. Bräuchle, V. Y. Lee, M. Manavi, and W. E. Moerner; J. Phys. Chem., 91, 3998 (1987).

7) W. P. Ambrose and W. E. Moerner; Chem. Phys., 144, 71 (1990)

8) H. Suzuki and T. Shimada; Appl. Phys. Lett., 59, 1814 (1991).

9) T. Suga, A. Furusawa, and K. Uchikawa; Chem. Phys. Lett., 210, 411 (1993).

10) W. E. Moerner; Jpn. J. Appl. Phys. Suppl., 28-3, 221 (1989).

11) H. Suzuki, T. Nishi, T. Shimada, and H. Hiratsuka; J. Lumin., 53, 271 (1992).

12) A. Vogler, B. Rethwisch, H. Kunkley, J. Hüttermann, and J. O. Besenhard; Angew. Chem. Int. Ed. Engl., 17, 951 (1978).

13) A. J. Bard; ed. "Encyclopedia of Electrochemistry of the Elements". Vol. ⅩⅥ, Marcel Dekker, New York, 1978.

14) T. Suzuki, K. Horie, and T. Yamashita; Chem. Mater., 5, 366 (1993).

15) W. E. Moerner, M. Gehrtz, and A. L. Huston; J. Phys. Chem., 88, 6459 (1984).

16) S. Machida, K. Horie, O. Kyono, and T. Yamashita; J. Lumin., 56, 85 (1993).

17) K. Horie, Z.-L. Zhang, L.-Q. Shi, S. Machida, T. Suzuki, S.-M. Yao, M.-H. Zhang; Poly. J., 24, 715 (1992).

18) S. Machida, K. Horie, T. Yamashita, and A. Furusawa; J. Phys. Chem., 97, 8234 (1993).

19) A. Furusawa and K. Horie; J. Chem. Phys., 94, 80 (1991).

20) W. Köhler and J. Friedrich; Phys. Rev. Lett., 59, 2199 (1987).

21) J. Takahashi, J. Tsuchiya, and K. Kawasaki; Chem. Phys. Lett., 209, 479 (1993).

Table 4.1. Experimental values of Φ_1, Φ_2, and G at 20 K for ZnTTBP in PCMS, PVC, PMMA with $CHCl_3$, and GAP[8]).

	PCMS	PVC	$CHCl_3$/PMMA	GAP
Φ_1	8.7×10^{-6}	1.4×10^{-5}	3.7×10^{-5}	4.0×10^{-7}
Φ_2	6.1×10^{-4}	2.2×10^{-5}	2.3×10^{-3}	9.8×10^{-4}
G	70	1.6	62	2450

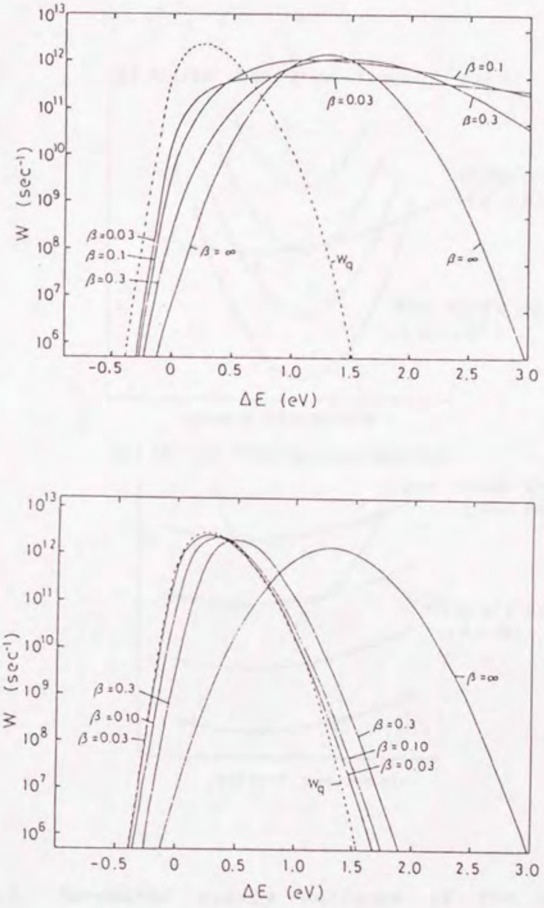

Fig.4.1. Calculated values of electron transfer rate as a function of energy gap in the case of charge separation reaction (a) and charge recombination reaction[4)].

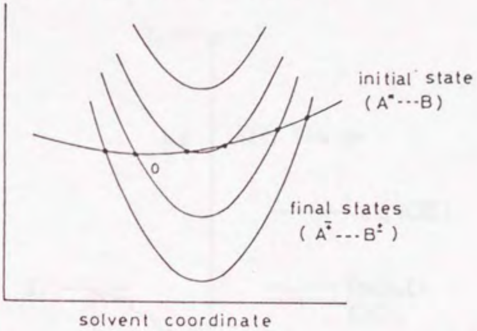

(a) charge separation reaction

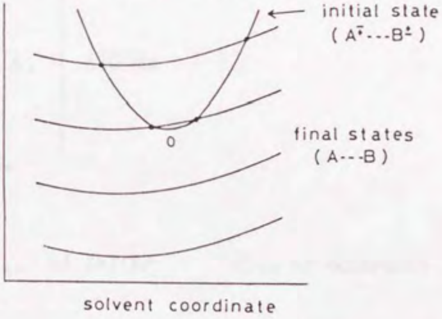

(b) charge recombination reaction

Fig.4.2. Schematic energy surfaces of the solvent mode in charge separation reaction (a) and charge recombination reaction (b)[4].

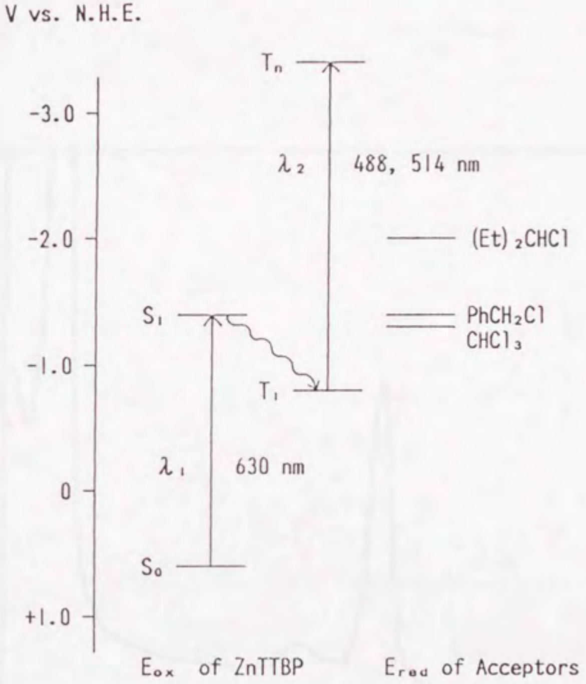

Fig.4.3. Schematic diagram of DA-ET, E_{ox} of ZnTTBP in its S_0, S_1, T_1, and T_n state, and E_{red} of $(Et)_2CHCl$, $PhCH_2Cl$, and $CHCl_3$.

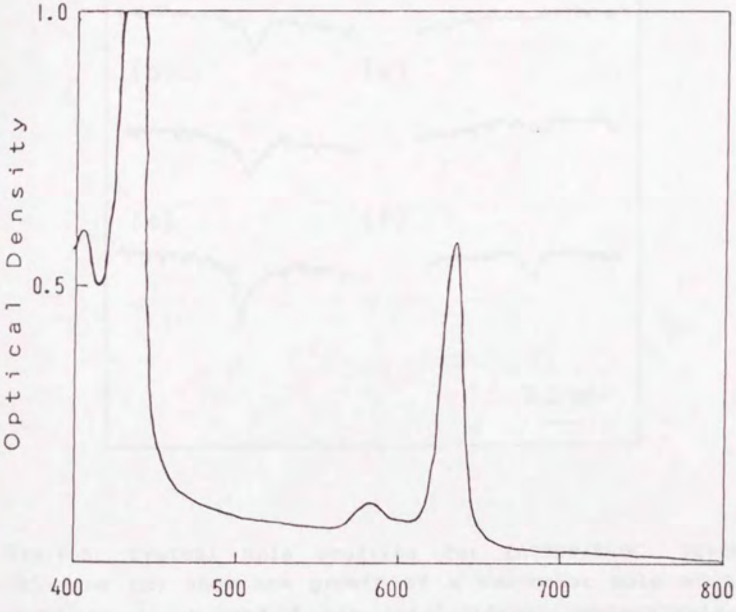

Fig.4.4. Absorption spectrum of ZnTTBP/PCMS.

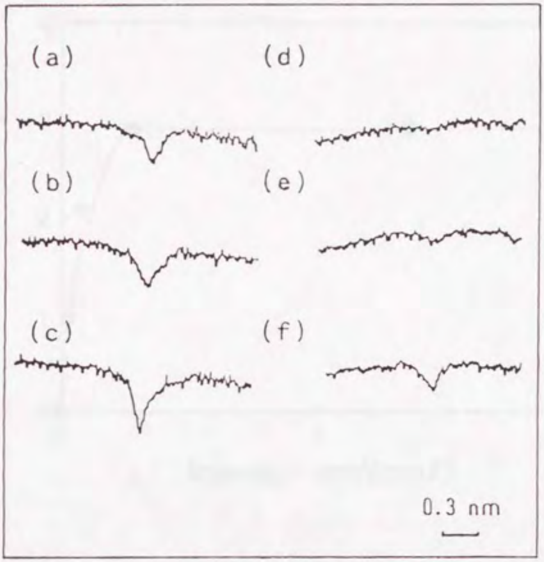

Fig.4.5. Typical hole profiles for ZnTTBP/PVBC. Traces (a), (b), and (c) show the growth of a two-color hole at 627.8 nm burnt by 1, 2, and 4 min irradiations, respectively, of 10 μW/cm^2 of λ_1 and 1 mW/cm^2 of λ_2. Traces (d), (e), and (f) show the growth of a one-color hole at 629.8 nm. Trace (d) is produced by 4 min irradiation of 10 μW/cm^2 of λ_1, and traces (e) and (f) are the hole spectra after the additional irradiations of λ_1 on the sample (d) [(e): 40 μW/cm^2, 2 min, (f): 400 μW/cm^2, 1 min].

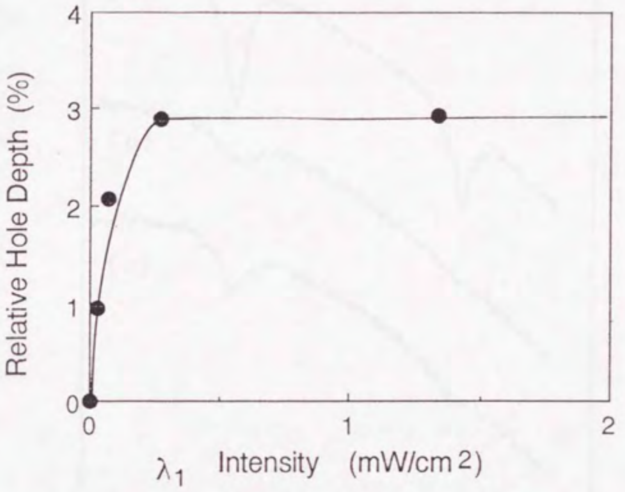

Fig.4.6. Irradiation intensity dependence of relative hole depth of the one-color holes for ZnTTBP/PCMS. The one-color hole is burnt by the various intensities of λ_1 for 4 min.

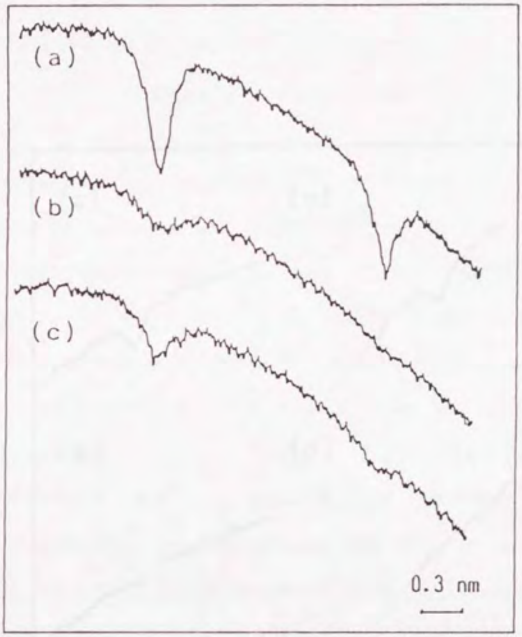

Fig.4.7. Hole profiles of the one- (left) and two-color (right) holes for ZnTTBP/PCMS before [20 K, (a)], during [(b)], and after [20 K, (c)] the annealing to 35 K. The two-color hole at 631.1 nm is burnt by 3 min irradiation : (λ_1: 40 μ W/cm^2, λ_2: 1 mW/cm^2), and the one-color hole at 632.6 nm is formed by 10 min irradiation (400 μ W/cm^2).

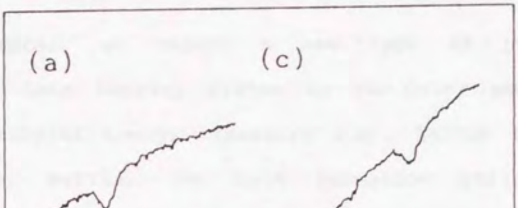

Fig.4.8. Hole profiles of the one- [(c) and (d)] and two-color [(a) and (b)] holes for ZnTTBP/PVC at 20 K before [(a) and (c)] and after [(b) and (d)] the annealing to 35 K. The holes are burnt by 8 min irradiation of λ_1 (630.4 nm, 40 μW/cm^2) and λ_2 (1 mW/cm^2) [(a)], or 8 min irradiation of 40 μW/cm^2 λ_1 (631.4 nm) [(c)].

CHAPTER 5

Photon-Gated PHB via Two-Color Sensitization of Photoreactive Matrix Polymer: ZnTTBP in Glicydil Azide Polymer (GAP)

In this chapter, we report a new type of photon-gated photochemical hole burning system by two-color sensitization via triplet-triplet energy transfer: i.e., ZnTTBP in glicydil azide polymer matrix. The hole formation efficiency for two-color excitation is 2500 times larger than that for one-color excitation in this system. The irradiation intensity dependence of hole depth indicates that the hole formation mechanism in the case of one-color excitation is also the two-photon sensitization of the decomposition of azide groups as is for the case of two-color excitation. The thermal stability of burnt holes and the temperature dependence of hole formation efficiency are also measured and discussed on the basis of the proposed hole formation mechanism. The temperature depencence of the quantum efficiency of hole formation is smaller than that for sulfonated tetraphenylporphine in poly(vinyl alcohol).

5.1. Introduction

5.1.1. Reported Mechanisms for Photon-Gated PHB Materials

There are four types of hole formation mechanisms in the photon-gated PHB systems reported sofar: ionization[1,2], decomposition[3-5], donor-acceptor electron transfer[6,7], and hydrogen-bond rearrangement of carboxylic acid[8] via two-photon excitaion. As for the decomposition, the reaction needs a high-energy source such as UV light to break the chemical bond, and the number of the reaction species is small because they are required to have a zero-phonon line. The nonphotochemical mechanism is essentially not so suitable for the photon-gated materials because it seems difficult to make threshold for the reaction. In the case of ionization and electron transfer reactions, the suppression of the recombination reactions seems to be the most important problem and thus the variation of the materials is not so large. (In the case of ionization, only HBO_2 is the reported matrix, and as for the electron transfer, almost all of the acceptors are halogenated or cyanide compounds.) The small variation of the photon-gated PHB materials should be due to the lack of the mechanism for the photon-gating.

5.1.2. Sensitization Mechanism of Photon-Gated PHB

In this chapter, a new type mechanism for photon-gated PHB: two-color sensitization reaction via triplet-triplet energy transfer is reported. Fig.5.1 illustrates the scheme of the sensitization mechanism of PHB. In this sensitization mechanism, the excited chromophore does not react itself but undergoes triplet-triplet energy transfer to a nearby photoreactive group in the matrix. The excited photoreactive group undergoes sensitized photoreaction, which induces a drastic change in the microscopic environment of the chromophore. The change in the microscopic environment leads to a change in the resonant frequency of the chromophore and a hole creation.

The newly found material consists of ZnTTBP as a sensitizer chromophore and GAP as a photoreactive matrix polymer. The chemical structures of GAP is shown in Fig.5.2. The schematic diagram of hole formation for ZnTBP/GAP is shown in Fig.5.3. ZnTTBP in its higher excited triplet state, T_n, undergoes triplet-triplet energy transfer to the nearby azide group in GAP. In solution, the triplet-triplet energy transfer occurs at a diffusion-controlled rate when the triplet energy of the donor (sensitizer) is greater than that of the acceptor9). The energy of T_n of ZnTTBP (4.0 eV) is larger than the T_1 energy of the alkyl azide group (3.4 eV for hexyl azide10)). In contrast to singlet-singlet energy transfer, the triplet-triplet energy transfer occurs only when the two electronic wave function of the donor and acceptor overlap11). The GAP contains azide group in each monomer unit, so there must exist several azide groups in the proximity to each ZnTTBP molecule. The excited azide group to T_1, decomposes and generates a nitrogen molecule and nitrene.

The decomposition of the azide group by triplet sensitization occurs with high efficiency (>0.5) when the triplet energy of the sensitizer is higher than the T_1 energy of azide[10]. The nitrene has high reactivity and undergoes hydrogen extraction, addition, or insertion reaction[12]. The decomposition of the azide group and the subsequent reaction of the generated nitrene induces the drastic change in the local environment of the sensitizer ZnTTBP molecule, which leads to the shift of resonant frequency and to the creation the hole. The gated holes are not created by the chemical reaction of the excited guest chromophore itself but created by the reaction of the photoreactive group around the chromophore in this ZnTTBP/GAP system.

In this chapter, we present the results of photon-gated PHB and temperature-cycling annealing experiments for ZnTTBP/GAP system and discuss the one-color and the two-color hole burning mechanisms for this system. The gated hole is also observed in poly(methyl methacrylate) (PMMA) containing 4,4'-diazidodiphenylsulfone (DAPS) together with ZnTTBP, and was not observed in PMMA containing ZnTTBP and diphenylsulfone (DPS) without azide group. This suggests that the azide group is indispensable for photon-gating. We interpret this as indirect evidence for the sensitization mechanism. The thermal stability and the irradiation energy dependence of one-color holes in ZnTTBP/GAP suggest that the hole formation mechanism for one-color holes is two-photon sensitization similar to that for two-color holes.

5.2. Sample Preparation

The GAP oligomer (Nippon Oil and Fats; MW=2250) was given by Iwama laboratory and was cured with trimethylol propane (TMP) (Tokyo Kasei) or ethylene glycol (Tokyo Kasei) and isophorone diisoccyanate (IPDI) (3-isocyanatomethyl, 3-methyl, 5,5-dimethylcyclohexyl- 1-isocyanate) (Daicel Hüls) using di-n-butylytin dilaurate (Tokyo Kasei) as a catalyst. The cross-linked sample was obtained by mixing the solution of ZnTTBP in tetrahydrofuran with the GAP oligomer with IPDI and TMP before the curing reaction on a 2 cm× 3 cm glass plate. The linear GAP polymer with ethylene glycol and IPDI was purified by reprecipitation and cast on a 2 cm× 3 cm glass plate after mixing with ZnTTBP solution. The thickness of the transparent samples obtained in this way were about 0.5 mm and the concentration of ZnTTBP in the samples were about 1×10^{-4} mol/kg.

The DAPS given by Hitachi Ltd. and its derivative, DPS (Wako Pure Chemical Industries) were used for ascertaining the contribution of azide group to the photon-gating. The samples of ZnTTBP-DAPS in poly(methyl methacrylate) (PMMA) and ZnTTBP-DPS/PMMA were obtained by solvent casting to contain about 0.2 mol/l of DAPS or DPS and about 1×10^{-4}

mol/l of ZnTTBP. The PMMA was obtained from methyl methacrylate (Tokyo Kasei) by radical polymerization and used after reprecipitation.

5.3. Results and Discussion

5.3.1. Gating Enhancement Effect for ZnTTBP/GAP

Fig.5.4 shows the gating enhancement effect in ZnTTBP/GAP at 20 K. Traces (a) and (b) show the two-color holes burnt by 1 min irradiation with the intensitiy of 19 μW/cm^2 of dye laser for both holes and 8 mW/cm^2 and 40 mW/cm^2 of Ar$^+$ laser, respectively. Trace (c) shows the transmission spectra after 60 min irradiation of 66 μW/cm^2 dye laser only. Apparently, the gating light enhances hole formation because in trace (c) no observable hole is created in spite of the fact that the irradiation energy of λ_1 is 200 times as large as that in the case of trace (b). Trace (d) shows a one-color hole formed by 10 min irradiation of 380 μW/cm^2 dye laser. In trace (d), an observable one-color hole is created whereas the irradiation energy in trace (d) is less than that in the case of trace (c). It suggests that the hole formation mechanism of the one-color hole is the one-color two-photon process and the hole formation efficiency has a irradiation intensity dependence. This is ascertained by the following results in this paper. Trace (e) shows that the addition of λ_2 (8 mW/cm^2) to λ_1 of the same condition as trace (d) formed a deep hole (relative hole depth: 34%). The quantum efficiency for hole formation by two-color excitation based on λ_1 absorption[13], Φ_2, was about 1.0×10^{-3} from trace (b), while Φ_1 by one-color excitation was measured to be 4.0×10^{-7} from trace (d). The ratio of Φ_2 to Φ_1 has become to 2500.

The relative hole depth as a function of irradiation intensity of λ_2 at 20 K is shown in Fig.5.5. The irradiation intensity of λ_1 and the irradiation time was fixed to 19 μW/cm^2 and 1 min, respectively. The relative hole depth increases as the λ_2 intensity increases when the λ_2 intensity is lower than 20 mW/cm^2, but becomes saturated (or decreases) when the λ_2 intensity is more than 20 mW/cm^2. This should be due to the spontaneous hole filling induced by the strong laser irradiation of λ_2.

5.3.2. Change in Absorption Spectra of ZnTTBP during Two-Color Irradiation

The low Φ_2 in GAP (1.0×10^{-3}) would be attributed to the fact that the triplet-triplet energy transfer from ZnTTBP to azide groups has to compete with an internal T_n-T_1 conversion process which is extremely fast ($10^{14} \sim 10^{15}$ s^{-1}). The mechanism of triplet-triplet energy transfer is known to be of electron-exchange type[11]. The occurence of electron transfer from T_n of ZnTTBP to acceptor molecules in PHB conditions has also been reported[5,6]. The changes in absorption spectra of the lowest Q band of ZnTTBP in GAP after strong two-color irradiations at 20 K are shown in Fig.5.6. Traces (a) show the spectra before (dashed line) and after (solid line) the irradiation of 0.38 mW/cm^2 dye laser at 627 nm and 4.7 mW/cm^2 Ar^+ laser for 2 min. Traces (b) show the spectra of another fresh sample before (dashed line) and after (solid line) 30 min irradiation of 26 mW/cm^2 He-Ne laser and 60 mW/cm^2 Ar^+ laser. The irradiation (a) does not only produce a hole at 627 nm but also reduces the area of the absorption band to about 85% of its value before irradiation. This would be explained by the occurrence of strong absorption saturation in this λ_1 irradiation condition (cf. Fig.5.10), which provides non-siteselective excitation at the foot of homogeneous absorption profiles including photon side bands. The existence of several vibronic transition with different molar extinction coefficients and Debye-Waller factors in the lowest Q band of porphyrin[14] would also influence this decrease in baseline of the whole absorption band. In the case of traces (b), the band area is also reduced by irradiation, because the absorbance of the homogeneous spectrum at room temperature after irradiation is about 85% of its value at room temperature before irradiation. Although the irradiated energy of λ_1 in Fig.5.6 (b) is 1000 times larger than that in Fig.5.6 (a), the decrease in the area of the absorption band is the same in the two cases. In Fig.5.6 (b), two antiholes are produced on both side of the deep hole at 633 nm. Such antiholes appeared only when the burning light was very intense. Of course in usual irradiation conditions as shown in Fig.5.4 ((a), (b), and (e)), the decrease in baseline of the absorption band stops at about 15% and no antiholes were observed. This means that most of ZnTTBP are regenerated after sensitization and their resonant frequencies shift far from the original frequencies due to the chemical change in azide groups as mentioned for Fig.5.3.

The results of Fig.5.6 (a) and (b) can be explained by the sensitization mechanism and by considering a distribution of distances between ZnTTBP and the azide group, $\underline{d}$, as follows. The rate constant of triplet-triplet energy transfer, $\underline{k_{T-T}}$, is proportional to exp(-$\underline{d}$) according to the electron exchange mechanism11). The $\underline{d}$ values should have a distribution due to the inhomogeneity of amorphous systems and are held fixed in a frozen matrix. Hence in the early stage of hole burning, the sensitization should proceed at those sites where $\underline{d}$ is very small. In these sites, the decomposed azide groups are so close to the sensitizer ZnTTBP molecules that the generated nitrene can react directly with ZnTTBP to form another chemical species. This may be about 15% of the initial ZnTTTBP. But most ZnTTBP molecules are not that close to the azide groups as to react with the generated nitrene and thus, the area of the absorption band is not any more changed by further irradiation. When the sample is exposed to strong and prolonged irradiation with wavelength of λ_1, the number of azide groups in the proximity to the ZnTTBP which is resonant to λ_1 becomes small and the azide groups not adjacent to the ZnTTBP are gradually sensitized. The spectral shift of the ZnTTBP caused by the sensitized reaction of non-adjacent azide groups is supposed to be small because the influence of the reaction on the interaction between ZnTTBP and its surroundings becomes small. Consequently, antiholes appear on both side of the hole only when the hole burning has proceeded enough.

5.3.3. Contribution of Azide Groups to Photon-Gating

Although the above results can be explained qualitatively by the sensitization mechanism, the direct evidence for this mechanism is not yet obtained: It is quite difficult to detect the decrease in quantity of azide groups in GAP because the concentration of ZnTTBP is 10^5 times smaller than that of azide groups in GAP. In order to get the direct evidence for the sensitization mechanism, the fact that the azide is indispensable to photon-gating is indicated in Fig.5.7. Traces (a) and (b) show the transmission spectra of the one- and the two-color holes, respectively, for ZnTTBP with 4,4'-diazidodiphenylsulfone (DAPS) in PMMA. Traces (c) and (d) show the spectra after one- and two-color irradiations, respectively, for ZnTTBP with diphenylsulfone (DPS) without azide group in PMMA. The irradiation conditions are as follows: 6 min irradiations for traces (a), (c), and (d), and 3 min irradiation for trace (b), with the intensities of 38 μW/cm^2 dye laser for the four cases together with the 4.7 mW/cm^2 Ar$^+$ laser irradiation only for traces (b) and (d). In trace (b), a hole is readily formed by 3 min irradiation (relative hole depth: 9.5%), but in traces (a), (c), and (d), only very shallow holes are formed by 6 min irradiation with the same λ_1 power as in trace (b). This fact suggests that the existence of azide groups is indispensable for the photon-gating because there is no difference between ZnTTBP-DAPS/PMMA and ZnTTBP-DPS/PMMA except that azide groups exist or not.

5.3.4. Cycle Annealing and Burning Mechanism of One-Color Holes

Fig.5.8 shows the hole width as a function of cycle-annealing temperature. The hole was burnt with two-color (0.66 mW/cm^2 He-Ne laser and 4.7 mW/cm^2 Ar$^+$ laser, 1 min) and measured at annealing temperatures and at 20 K during the annealing. The reversible part of the increase in hole width on heating with the recovery on cooling (region A) is due to the increase in homogeneous width of the chromophore. The irreversible part of the increase in hole width (region B) is attributed to the thermally induced spectral diffusion[15]. The temperature dependence of homogeneous width depends on whether the meaterial is amorphous or crystalline[16]. The result in Fig.5.8 indicates that the ZnTTBP/GAP system shows a typical temperature dependence of homogeneous width in an amorphous system. The irreversible part or thermally induced spectral diffusion is usually caused by structural relaxation of the matrix. In the GAP matrix the irreversible increase in hole width is similar to that for free-base porphin doped in various polymer systems[15].

In Fig.5.9, the dependences of the normalized hole area of one- and two-color holes burnt at 20 K in ZnTTBP/GAP on annealing temperature during cyclic annealing experiments are shown. The one-color hole was burnt by 10 min irradiation of 0.38 mW/cm^2 dye laser at 630.4 nm and the two-color hole was burnt by 1 min irradiation of 0.66 mW/cm^2 He-Ne laser and 4.7 mW/cm^2 Ar^+ laser. The two-color hole can be observed at 80 K, which is probably due to the hydrogen bonds of urethane structure in the cured GAP, because a hole is hardly been observed above the liquid nitrogen temperature in free-base porphyrin doped polymer systems except in hydrogen-bonding polymers such as poly(vinyl alcohol) (PVA) and phenoxy resin[15]. The reversible part of the decrease in hole area on heating with the recovery on cooling (region A) can be explained by the temperature dependence of Debye-Waller factor[15]. The irreversible part of the decrease in hole area by cycle annealing (region B) is attributed to the structural relaxation of host matrix which causes the change in local environments of the guest molecules and redistributes their resonant frequencies. In Fig.5.9 one-color and two-color holes have a similar temperature dependence of reversible and irreversible decreases in hole area. This suggests that the hole formation mechanism of the one-color hole is a photochemical process similar to the mechanism of the two-color hole formation, because as a rule holes burnt by non-photochemical processes are almost filled by annealing up to 80 K[17,18] because of the low barrier height of the backward reaction.

To ascertain the hole formation mechanism of the one-color hole in ZnTTBP/GAP, the depths of one-color holes as a function of irradiation energy under various irradiation intensities for ZnTTBP/GAP are measured and shown in Fig.5.10. The one-color holes were burnt with the intensities varing from 0.38 mW/cm^2 to 7.5 mW/cm^2. At a certain irradiation energy, the depth of one-color holes are the same irrespective of the intensity and irradiation time. According to this result, two cases are possible about the one-color mechanism. The one is the one-photon process under unsaturated $S_0 \rightarrow S_1$ absorption, and the other is the two-photon process under saturated $S_0 \rightarrow S_1$ absorption and unsaturated $T_1 \rightarrow T_n$ absorption. If it were one-photon process via saturated absorption, the depths for higher intensities should be smaller, and if it were two-photon process via unsaturated absorption, the depths for higher intensities should be larger.

Fig.5.11 shows the dependence of the depth of two-color holes on the irradiation intensity of λ_1, $\underline{I_1}$, under the same irradiation intensity of gating light (10 mW/cm^2) and irradiation time (30 sec) in ZnTTBP/GAP. When the $\underline{I_1}$ is more than 100 μW/cm^2, the hole depth has no dependence on $\underline{I_1}$. As is shown in Fig.5.4 (e), the two-color hole in ZnTTBP/GAP can be burnt up to more than 34% of the relative absorbance and thus the hole depth in Fig.5.10 is not saturated. So we conclude that the $S_0 \rightarrow S_1$ absorption of ZnTTBP (O.D. ~0.6) is saturated due to the bottleneck of T_1 state when the $\underline{I_1}$ is more than 100 μW/cm^2 as shown in Fig.5.12. This is reasonable because the critical intensity of λ_1, $\underline{I_{1c}}$, which induces absorption saturation, is estimated to be ~100 μW/cm^2 according to the following equations:

$$\underline{I_{1c}} = \underline{hc} / (\sigma \, \Phi_{ISC} \; \tau_{T1} \, \lambda_1) \qquad (1)$$

$$\sigma = 10^3 \, \varepsilon \, \Gamma_1 / (\underline{N_A} \; \log \underline{e} \;\; \Gamma_H) \qquad (2)$$

where σ is absorption cross section of a ZnTTBP molecule, Φ_{ISC} is quantum yield of intersystem crossing, τ_{T1} is lifetime of T_1, $\underline{h}$ is Planck constant, $\underline{c}$ is velocity of light, $\underline{N_A}$ is Avogadro's number, ε is molar extinction coefficient, Γ_H is hole width, and Γ_I is inhomogeneous width. The values of $\Phi_{ISC}=0.9$, $\tau_{T1}=40$ (ms), $\varepsilon=10^5$ ($\underline{l}$ mol^{-1} cm^{-1}), and $(\Gamma_I/\Gamma_H)=300$ were used for the estimation of I_{1c}. Because the values of $\underline{I_1}$ in Fig.5.10 are more than 100 $\mu W/cm^2$ and because the one-color hole has the similar thermal stability to that of the two-color hole, we can conclude that the hole formation mechanism of the one-color hole in ZnTTBP/GAP is the one-color two-photon sensitization process as shown in Fig.5.13. These results indicates that the low efficiency of non-photochemical hole burning process is an important factor for high gating ratios.

5.3.5. Temperature Dependence of Hole Formation Efficiency and Debye-Waller Factor

The temperature dependence of the quantum efficiency for hole formation, $\Phi(T)$, for the two-color hole burning in ZnTTBP/GAP based on λ_1 absorption is shown in Fig.5.14. The $\Phi(T)$ was calculated from the initial slope of the growth of hole area at certain temperatures and was normalized by the value of $\Phi(20)$. In the case of ZnTTBP/GAP, the $\Phi(20)$ is

1.0×10^{-3}. In Fig.5.14 the values of $\Phi(T)$ for the one-color hole burning for sulfonated tetraphenylporphine (TPPS) in PVA[15] and $\Phi(T)$ for the two-color hole burning for ZnTTBP with chloroform in PMMA[7] are also plotted. The $\Phi(T)$ for ZnTTBP/GAP decreases as the temperature increases although $\Phi(T)$ for ZnTTBP-$CHCl_3$/PMMA has no temperature dependence. But ZnTTBP/GAP has a weaker temperature dependence of $\Phi(T)$ than TPPS/PVA has. This result can be interpreted by considering the hole formation mechanism in these systems as follows. In GAP, the decomposition reaction itself is irreversible and the local environment of a sensitizer molecule which has once changed the resonant frequency can not recover to the initial state before burning. But the tautomerization reaction of TPPS is reversible and so the excitation of the photoproduct can induce the backward process of hole burning to decrease the $\Phi(T)$. On the other hand, most of the burning products in GAP have their resonant frequencies in the same absorption band before burning, which decreases $\Phi(T)$ as the homogeneous width broadens. But the photoproduct for ZnTTBP-$CHCl_3$/PMMA is a cation species and has little absorption in the burning band, so the $\Phi(T)$ is not affected by the broadening of homogeneous width.

Fig.5.15 shows the temperature dependence of Debye-Waller factor (DWF) for the GAP system. The DWF is defined as the ratio of the zero-phonon component to the integrated absorption cross section of a transition of the chromophore. The DWF at certain temperature is estimated by dividing the hole area observed at that temperature by the hole area at 20 K after cooling from that temperature[15] and is normalized by the DWF at 20 K. In Fig.5.15, the temperature dependence curve for the GAP system is similar to that for TPP doped in polymer systems[15]. The difference in temperature dependence of Φ (Fig.5.14) and DWF (Fig.5.15) for the GAP system is not so large as that in free-base porphin doped in polymer systems[15]. This should be due to the difference in hole burning mechanism as is described for Fig.5.14.

Fig.5.16 shows the hole width as a function of burning temperature. The hole widths were measured for several irradiation times and estimated to the zero-irradiation time. The hole widths in the case of burning (Fig.5.16) are larger than that in the case of annealing (upper plots of Fig.5.8) at higher temperatures. This should be due to the temperature dependence of homogeneous width which leads to the broad-range excitation at higher temperatures. The chemical reactions initiated by the nitrene may affect this phenomena.

5.4. Conclusion

Photon-gated PHB for the system of ZnTTBP/GAP has been studied and discussed from the aspect of hole formation mechanism. Two-color holes formed 2500 times more efficiently than one-color holes. Photon-gating was observed only when the matrix contained azide groups, which supports the two-photon sensitization mechanism. The thermal stability and the irradiation intensity dependence of the one-color hole suggest that the hole formation mechanism of the one-color hole is also the sensitization via one-color two-photon excitation process. The temperature dependence of the hole formation efficiency for ZnTTBP/GAP was also measured and interpreted in terms of sensitization mechanism. This type of mechanism enables us to use various photochemisry for PHB systems, which should increase the variation of the PHB materials and the interests in PHB.

References

1) H. W. Lee, M. Gehrtz, E. E. Marinero, and W. E. Moerner; Chem. Phys. Lett., 118, 611 (1985).

2) R. M. Macfarlane; J. Lumin., 38, 20 (1987).

3) D. M. Burland and D. Haarer; IBM J. Res. Dev., 23 534 (1979).

4) M. Iannone, G. W. Scott, D. Brinza, and D. R. Coulter; J. Chem. Phys., 85, 4863 (1986).

5) B. Prass, C. von Borczyskowski, and D. Stehlik; J. Lumin., 38, 48 (1987).

6) T. P. Carter, C. Bräuchle, V. Y. Lee, M. Manavi, and W. E. Moerner; J. Phys. Chem., 91 3998 (1987).

7) W. P. Ambrose and W. E. Moerner; Chem. Phys., 144, 71 (1990).

8) S. Machida, K. Horie, T. Yamashita, and A. Furusawa; J. Phys. Chem., 97, 8234 (1993).

9) W. G. Herkstroeter and G. S. Hammond; J. Am. Chem. Soc., 88, 4769 (1966).

10) F. D. Lewis and W. H. Saunders, Jr.; J. Am. Chem. Soc., 90, 7033 (1968).

11) D. L. Dexter; J. Chem. Phys., 21, 836 (1953).

12) N. J. Turro; "Modern Molecular Photochemistry". Benjamin/Cummings, Menlo Park, CA, 1978.

13) A. Furusawa, K. Horie, K. Kuroki, and I. Mita; J. Appl. Phys., 66, 6041 (1989).

14) K. Horie, M. Ikemoto, T. Suzuki, S. Machida, T. Yamashita, and N. Murase; Chem. Phys. Lett., 195, 563 (1992).

15) A. Furusawa and K. Horie; J. Chem. Phys., 94, 80 (1991).

16) K. K. Rebane and L. A. Rebane; "Persistent Sectral Hole-Burning; Science and Applications". Chapt. 2, Springer, Berlin (1987).

17) W. Köhler and J. Friedlich; Phys. Rev. Lett., 59, 2199 (1987).

18) K. Horie, Z.-L. Zhang, L.-Q. Shi, S. Machida, T. Suzuki, S.-M. Yao, and M.-H. Zhang; Polym. J., 24, 715 (1992).

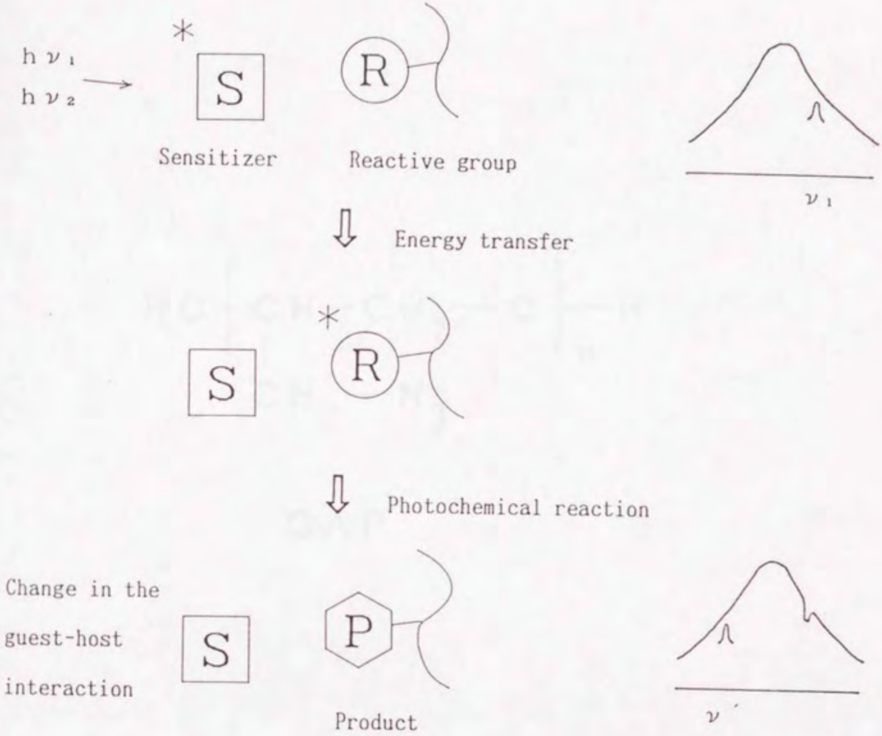

Fig.5.1. Scheme of the sensitization mechanism for PHB.

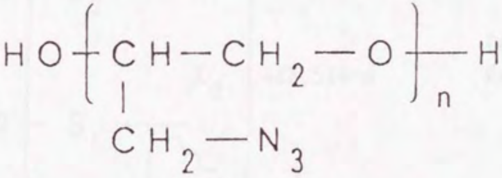

$$HO-\left(\underset{\displaystyle CH_2-N_3}{\overset{}{CH}}-CH_2-O\right)_n-H$$

GAP

Fig.5.2. Chemical structure of GAP.

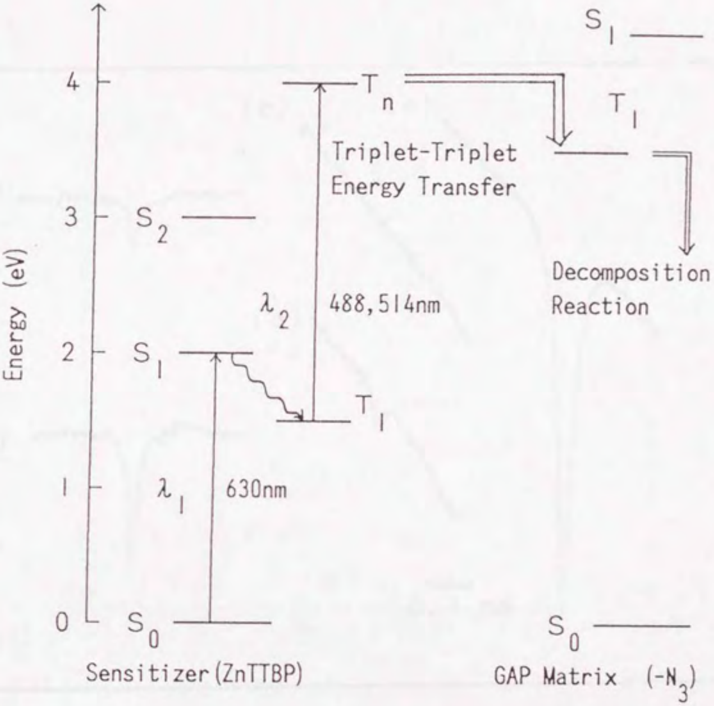

Fig.5.3. Energy levels and schematic diagram of two-color hole formation for ZnTTBP/GAP.

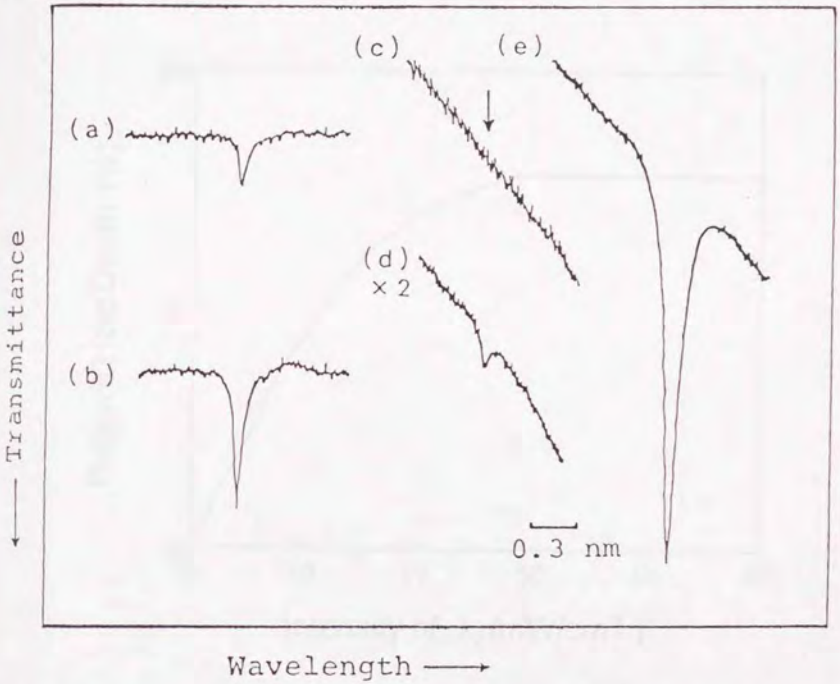

Fig.5.4. Typical hole profiles for ZnTTBP/GAP. Traces (a) and (b) show the two-color holes burnt by 1 min irradiation of 19 μW/cm^2 dye laser for both holes and of 8 mW/cm^2 and 40 mW/cm^2 Ar$^+$ laser for traces (a) and (b), respectively. Trace (c) shows the transmission spectrum after one-color irradiation (60 min, 66 μW/cm^2). Trace (d) shows the one-color hole (10 min, 380 μW/cm^2) with relative hole depth of 2.2%. The addition of 8 mW/cm^2 gating light to λ_1 of the same irradiation condition as trace (d) produced trace (e) (Relative hole depth: 34%). Sensitivity for the trace (d) is twice of those for others.

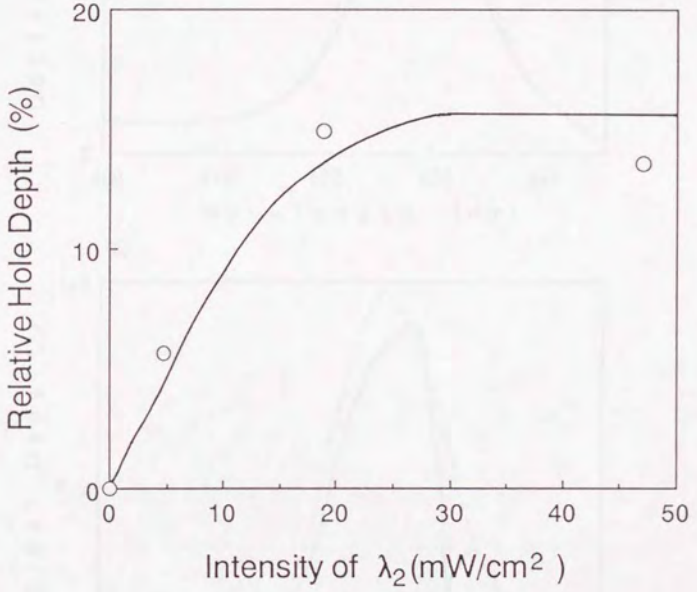

Fig.5.5. Relative hole depth of two-color holes as a function of irradiation intensity of λ_2 under the same irradiation intensity of λ_1 (19 μW/cm^2) and irradiation time (1 min).

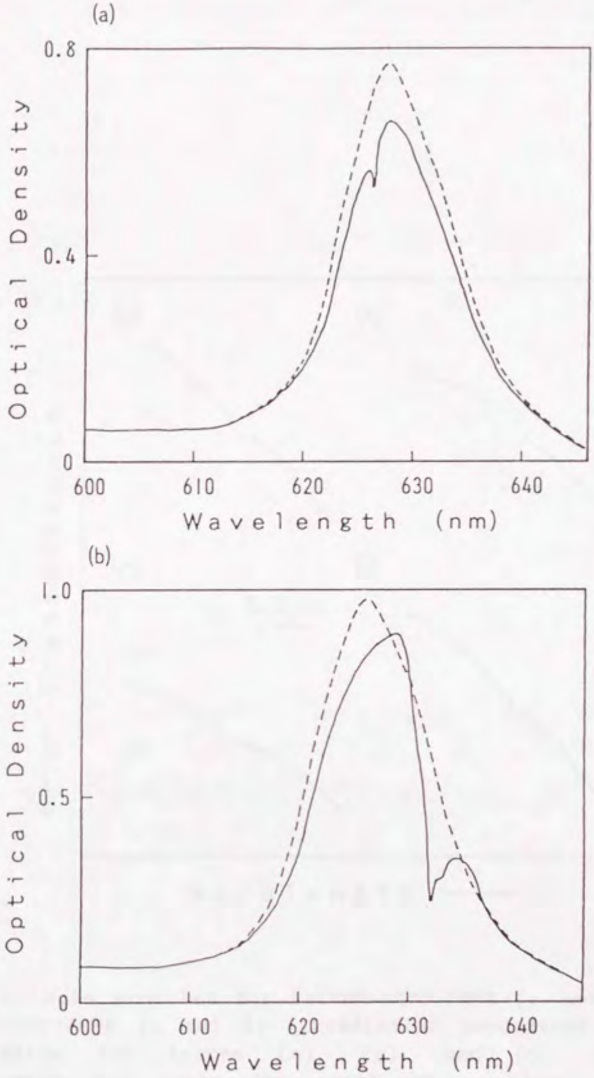

Fig.5.6. Absorption spectra of the lowest Q band of two ZnTTBP/GAP samples at 20 K before (dashed line) and after (solid line) two-color irradiations. Burning conditions are, 2 min irradiation of 0.38 mW/cm^2 dye laser at 627 nm and 5 mW/cm^2 Ar$^+$ laser for traces (a), and 30 min irradiation of 26 mW/cm^2 He-Ne laser at 633 nm and 60 mW/cm^2 Ar$^+$ laser for traces (b).

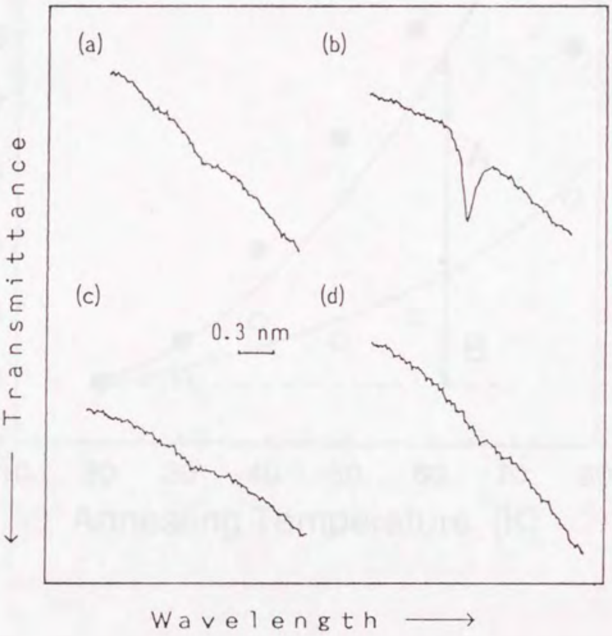

Fig.5.7. Hole profiles for ZnTTBP-DAPS/PMMA (a and b) and for ZnTTBP-DPS/PMMA (c and d). Irradiation conditions are, 6 min irradiation for traces (a), (c), and (d), and 3 min irradiation for trace (b), with 38 μW/cm² dye laser, together with 4.7 mW/cm² Ar^+ laser irradiation only for traces (b) and (d). The relative hole depth for trace (b) is 9.5%.

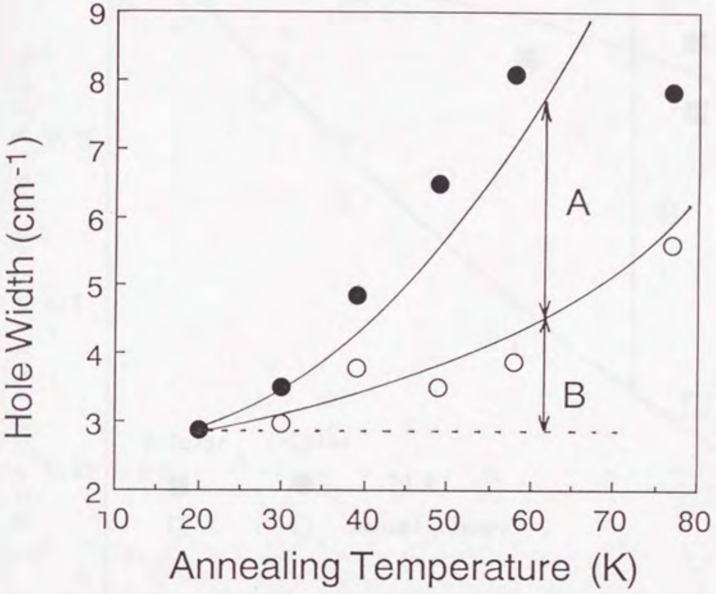

Fig.5.8. Hole widths as a function of annealing temperature. The hole was burnt with two-color at 20 K and measured at annealing temperatre (●) and at 20 K during the annealing (○).

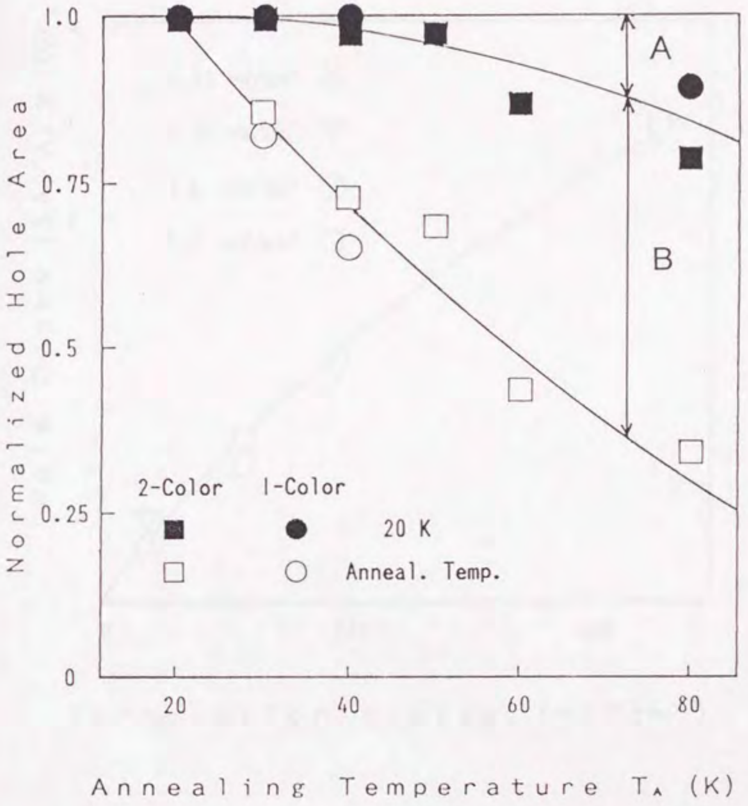

Fig.5.9. Annealing-temperature dependences of normalized hole area for ZnTTBP/GAP. The two-color (■ ,□) and one-color (● ,○) holes are measured at the annealing temperatures (□ ,○) and at 20 K after cooling from the annealing temperatures (■ ,●). Region A corresponds to reversible change due to the temperature dependence of Debye-Waller factor and region B corresponds to irreversible change due to structural relaxation of the matrix.

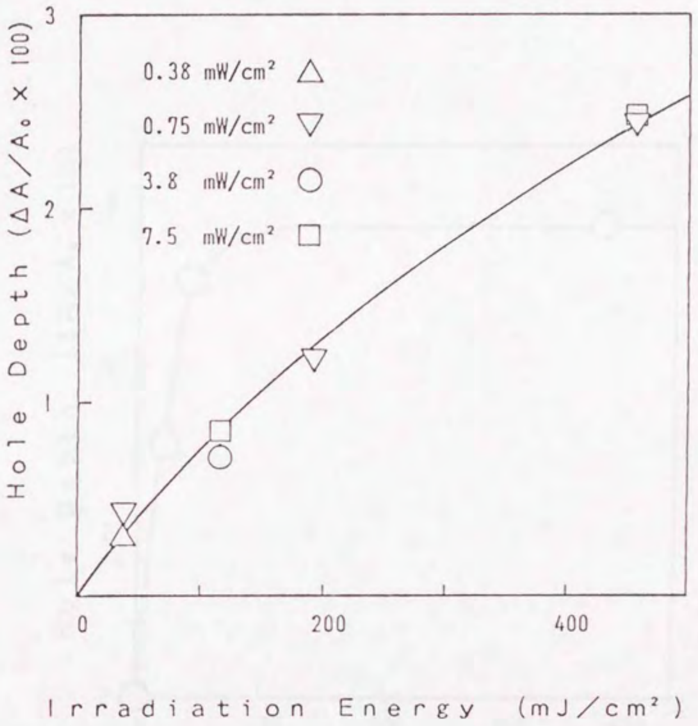

Fig.5.10. Irradiation-energy dependence of the depth of one-color holes under various irradiation intensities for ZnTTBP/GAP system.

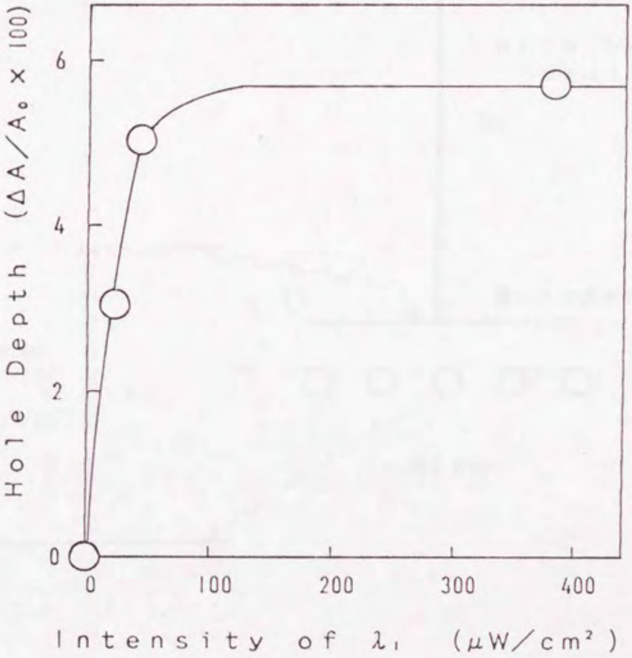

Fig.5.11. Depth of two-color holes as a function of irradiation intensity of λ_1 under the same irradiation intensity of λ_2 (10 mW/cm²) and irradiation time (30 s) for ZnTTBP/GAP system.

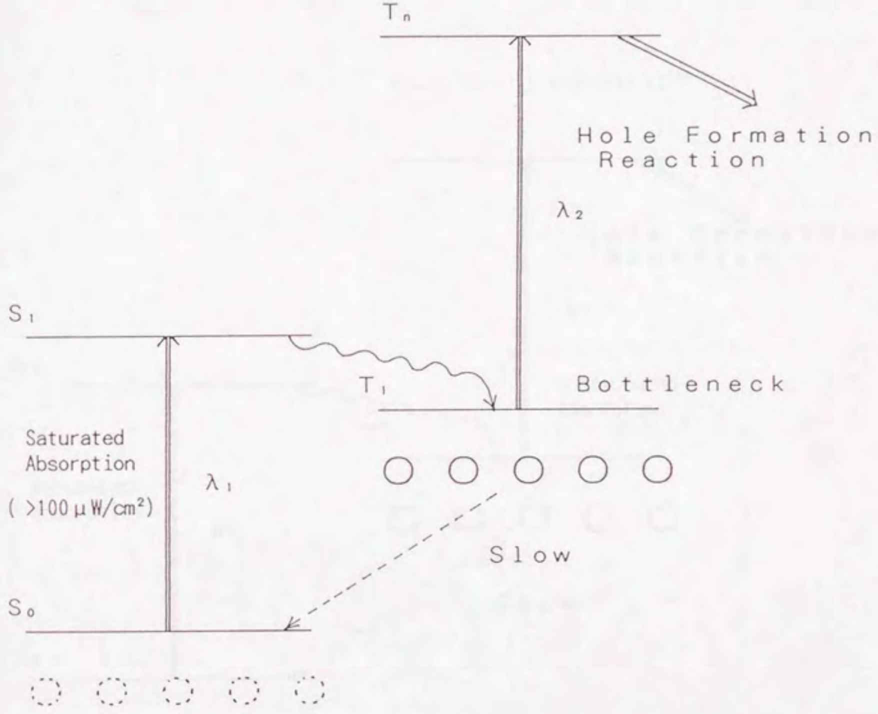

Fig.5.12. Diagram of the two-color hole burning process under strong irradiation of λ_1 (>100 μ W/cm^2).

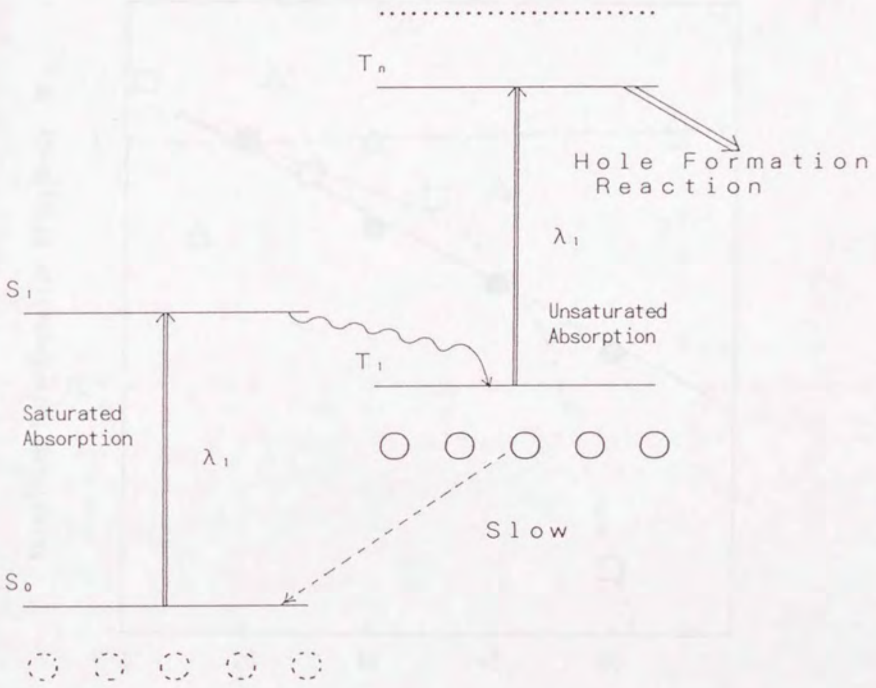

Fig.5.13. Diagram of the one-color hole burning process for the ZnTTBP/GAP system.

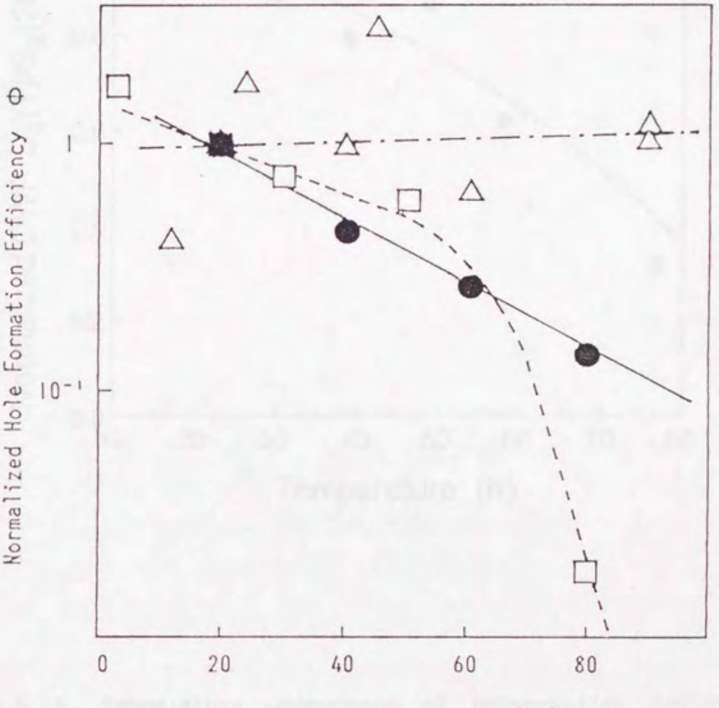

Fig.5.14. Temperature dependences of normalized hole formation efficiency, Φ, for ZnTTBP/GAP (●), TPPS/PVA (□)[15], and ZnTTBP-$CHCl_3$/PMMA (△)[7].

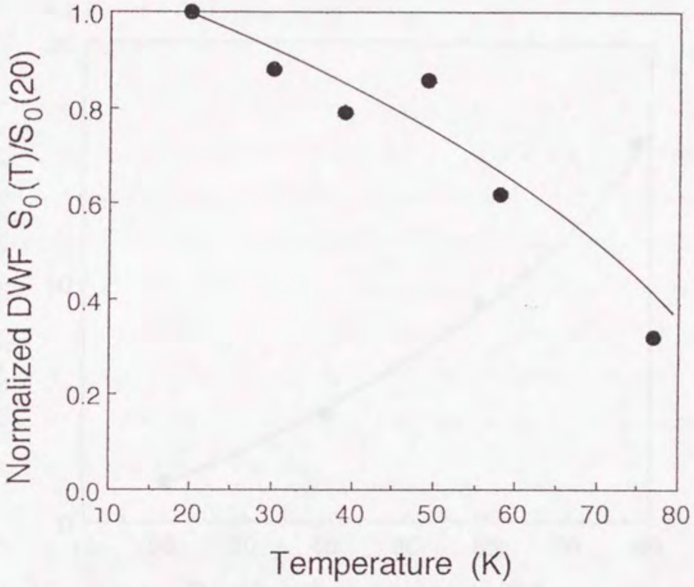

Fig.5.15. Temperature dependence of Debye-Waller factor for the ZnTTBP/GAP system. The DWFs were estimated from the results of cycle annealing experiment[15] and were normalized by the DWF at 20 K.

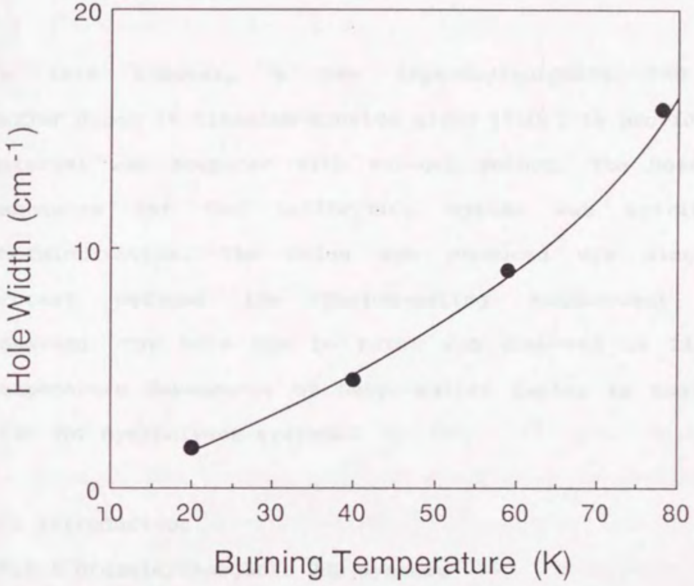

Fig.5.16. Hole width as a function of burning temperature.

CHAPTER 6

PHB for Organic Dye Doped in Semiconductor System: ZnTTBP in Titanium Dioxide

In this chapter, a new organic/inorganic PHB system: ZnTTBP doped in titanium dioxide glass (TiO_2) is provided. The material was prepared with sol-gel method. The hole burning mechanism for the ZnTTBP/TiO_2 system was attributed to photoionization. The holes are produced via single-photon process because the photon-gating enhancement is not observed. The hole can be burnt and observed at 140 K. The temperature dependence of Debye-Waller factor is smaller than that for dye/polymer systems.

6.1 Introduction

6.1.1 Organic/Inorganic PHB systems

For the realization of the PHB memory, the highly efficient hole production and the good thermal properties are required for the PHB materials as well as the high gating ratio. As for the high-efficient hole production, organic dye doped in polymer systems show relatively high quantum efficiency for hole formation[1-3]. This should be due to the high reactivity of the organic dye molecules. On the other hand, high-temperature hole burning and hole reservation are achieved mainly by inorganic materials[4-7]. In the inorganic host matrices, the dense and three-dimensional chemical bond of the matrix restricts the local motion of the color center and results in the excellent thermal properties. So the organic/inorganic PHB systems have a possibility to realize both high burning efficiency and high working temperature.

However, the number of the organic/inorganic PHB materials reported so far is quite small. This would be due to the difficulties in the sample preparation. The matrix must be prepared without destroying the guest dye molecule. The matrices of the reported organic/inorganic PHB systems are silica[8,9], almina[10], and boric acid glass[11].

6.1.2 Sol-Gel Method for Preparation of Inorganic Materials

One of the recently developed methods for the preparation of ceramics is sol-gel method[12]. In the sol-gel method, the gelation of the sol obtained by the hydrolysis of metal alcohoxide proceeds, and then the gel is heated, condensated, and dried to the ceramics. By using the sol-gel method we can easily dope an organic compound molecularly into an inorganic glass because the sample is prepared from homogeneous solution and because the gelation and condensation does not require so high temperatures. So one of the recent topics of sol-gel method science is the research of new organic/ inorganic functional materials.

6.1.3 PHB systems by Photoionization.

Photoionization is one of the most popular mechanism for PHB. Especially, photoionization is utilized for almost all of the inorganic PHB systems[4-7]. On the other hand, there are no PHB systems in which the hole burning mechanism is the ionization of organic dyes except carbazole (Cz)/boric acid (BA)[11] and perylene/BA[13]. This should be because the ionization potential of the organic dye molecule is so large that the ionization cannot be induced by the irradiation of a conventional visible laser light. In fact, both Cz/BA and perylene/BA systems need ultraviolet light and bi-photonic excitation for the ionization. BA is known as a matrix to decrease the ionization potentials of the impurities, but it still requires large energy for the organic dyes to be ionized in BA.

6.1.4 Energy Levels of ZnTTBP and TiO_2

The n-type semiconductors are known to have the low conduction band (C.B.). There are many studies about photoinduced electron transfer from the organic dye adsorbed on the surface of the n-type semiconductor to the C.B. of the semiconductor[14]. In this chapter, we present the first observation to our knowledge of the PHB for the organic dye (ZnTTBP) doped in semiconductor (titanium dioxide) system.

Fig.6.1 illustrates the oxidation potentials, E_{ox}, of

ZnTTBP in its S_0, S_1, and T_1 states, which are estimated from the E_{ox} of zinc-tetrabenzoporphine (ZnTBP), the valence band and the C.B. of the TiO_2. The E_{ox} of S_1 and T_1 of ZnTTBP are both higher than the C.B. of the TiO_2. Thus, the photoionization reaction of ZnTTBP can be energetically possible both from S_1 and T_1 states. So the hole burning by the ionization would proceed via single-photon excitation in the ZnTTBP/TiO_2 system. This may not be desirable for the application of the PHB materials to a memory system. But the dye/semiconductor system provides a new variation of PHB materials in which the holes are produced by the ionization of the conventional organic dye molecule such as porphyrin. This should increase the scientific interests in PHB and provide a possibility of gating the hole formation by the electric field instead of the gating light. In addition, this is the first report to our knowledge of the preparation of organic dye doped in semiconductor system. This type of material can be used not only for PHB but also for various photooptical applications and for scientific study of photochemistry, electrochemistry, and solid-state physics.

6.2 Sample Preparation

6.2.1 Preparation and Gelation of Precursor Sol

The precursor sol solution was obtained by a procedure similar to that in ref.16. Fig.6.2 shows the scheme of the sample preparation. The mixture of HCl, H_2O, C_2H_5OH, and ZnTTBP dissolved in dimethylformamide (DMF) was added dropwise to titanium tetraisopropoxide (TIPT) (Wako Pure Industrial Inc.) diluted with C_2H_5OH at 0℃ under stirring. We made experiments with several conditions of the molar ratio of the TIPT, C_2H_5OH, HCl, H_2O, and DMF. Table 6.1 shows the molar ratio of the components of the starting solutions and the gelation times. In most cases, clear viscous sol solution was obtained. The samples were wrapped with aluminium foil and paraffin film, and left still at room temperature. The gelation times differed with the molar ratio of the starting solution as is shown in Table 6.1.

6.2.2 Drying and Condensation Processes

The samples were heated to 40-50℃ after the gelation. The drying of the gel was started after that by making several pinholes on the wrap. The drying temperature was raised to 100 ℃ over 7-14 days. It is reported that the TiO_2 obtained by the sol-gel method needs more than 500 ℃ to complete the condensation[17]. However, the heating to above 100 ℃ induced the change in the color of the ZnTTBP and so we were obliged to finish the drying and condensation at 100 ℃. The heating conditions and the conditions of the obtained samples are also shown in Table 6.1. In almost all cases a few or several cracks were observed in each sample, and in many cases the samples were broken to a few or several peaces. However, we could get a few samples with sufficient area (~2 cm^2) for the PHB measurement by raising the temperature of the samples slowly from 40 ℃ to 60℃ over several days as is shown in the table.

6.2.3 Characterization of TiO_2 gel

The obtained TiO_2 samples were characterized by UV absorption, IR, and thermogravimetry (TG) or weight loss measurements. Fig.6.3 shows the UV spectra of TIPT/EtOH solution (a) and a TiO_2 sample prepared without ZnTTBP (b). The numbers of the Ti atom per absorption area are similar between the two cases. The wavelength of the absorption edge shifts from ~360 nm (a) to ~370 nm (b) as the condensation proceeds. This should be due to the formation of a band structure caused by Ti-O-Ti bond network. The band gap of TiO_2 is known as 380 nm and so the formation of the bond network is supposed to be incomplete.

Fig.6.4 shows the IR spectra of a TiO_2 sample without ZnTTBP during the gelation process. In Fig.6.4 (c), a few peaks of organic species are observed, which suggests that some organic compounds still remains in the sample even after the heating to 100℃. Fig.6.4 also indicates that hydroxyl groups exist in the sample, and this is probably bonded to the Ti atoms.

The changes in weight of a sample during the heating process are shown in Table 6.2. At the beginning of the condensation, the sample includes C_2H_5OH, DMF, isopropyl alcohol (i-PrOH), and H_2O as residual solvents. Table 6.2 suggests that most of them are removed at 40-70 ℃. If the sample had come to be TiO_2 completely, the weight should have been 76% of that in Table 6.2 at 100℃. The residual weight (24%) should be due to uncondensated hydroxyl and isopropoxyl groups, or unremoved i-PrOH, H_2O, and DMF. The amount of the uncondensated Ti bonds was roughly estimated as follows. Because in Fig.6.4 the absorption band of C-H bonds around 3000 cm^{-1} is hardly observed and because the hydrolysis of TIPT is known to be very fast, the OH band around 3500 cm^{-1} would consist of almost all Ti-OH bond. The relative absorbance of OH band (3500 cm^{-1}) to the absorbance of Ti-O band around 500 cm^{-1} which can be regarded to be unchanged during the condensation were estimated by the charts of Fig.6.4. According to this estimation, the amount of Ti-OH bond at 100 ℃ (Fig.6.4 (c)) is half of its initial value (Fig.6.4 (a)). Then, the amount of the residual Ti-OH bond was estimated to be about half of the amount of Ti atoms.

As for the further heating of the sample, Fig.6.5 shows the TG curve of the TiO_2 sample without ZnTTBP which was dried at 100℃ before the measurement. The total weight decreased to 68% of its initial value in Fig.6.5. This result agrees well with that in Table 6.2 which lists the weight of the sample dried at 100 ℃ to be 148% (100/68) of the weight of ideal TiO_2. In Fig.6.5, the decrease in weight stops at 500℃ and thus the residual organic species and OH group are removed below 500 ℃.

6.3. Results and Discussion

6.3.1. PHB for ZnTTBP/TiO_2 system and Hole Burning Mechanism

Fig.6.6 shows the growth of a hole at 627.8 nm burnt by one-color and two-color irradiations at 20 K. Trace (a) is the transmission spectrum before the irradiation. Trace (b) is the spectrum after 10 min irradiation of 75μ W/cm^2 of λ_1, and trace (c) is the spectrum after 10 min irradiation of λ_1 (75 μ W/cm^2) and λ_2 (5 mW/cm^2) on the sample (b). Further 10 min irradiation of λ_1 (7.5 mW/cm^2) and 10 min irradiation of λ_1 (7.5 mW/cm^2) and λ_2 (5 mW/cm^2) produced traces (d) and (e), respectively. Trace (f) was produced by further 30 min irradiation of λ_1 (7.5 mW/cm^2) and λ_2 (5 mW/cm^2). The hole widths at 20 K are relatively large (4.4 cm^{-1} for trace (d)) compared to that for ZnTTBP in polymer systems (see chapt.3-5). In Fig.6.6, the gating light does not enhance the hole formation and thus the hole burning proceeds via S_1 or T_1 state. The quantum efficiency for hole formation, Φ, was esitmated to be 2×10^{-6}.

The changes in absorption spectra of the lowest <u>Q</u> band of

ZnTTBP in TiO_2 induced by laser irradiations at 20 K are shown in Fig.6.7. Trace (a) is the spectrum before the irradiations, and trace (b) is that after the irradiation of total 14 J/cm^2 of λ_1 and 27 J/cm^2 of λ_2 to several wavelengths. In trace (b), several small holes (<5%) are burnt, but the hole profiles are not observed in this measurement. Further 1 hour irradiation of 75 mW/cm^2 of λ_1 (628 nm) produced trace (c). Trace (d) is the spectrum of the sample (c) after 2 hours irradiation of 75 mW/cm^2 of λ_1 at 628 nm. Apparently, the whole band area is decreased by the irradiations. This means that the hole burning mechanism for the ZnTTBP/TiO_2 system is a photochemical process. The mechanism should be photoionization because no other reaction of ZnTTBP except ionization seems to proceed in TiO_2. Because trace (d) is not so much changed from trace (c) for the high irradiation energy, the burning reaction should become saturated and not all the ZnTTBP molecules can be in the reactive site. The absorption of the sample irradiated for Fig.6.7 recovered to that before the irradiation after it was left for 1 day at room temperature. This fact also suggests the ionization mechanism of the PHB for the ZnTTBP/TiO_2 system.

In Fig.6.8, the irradiation intensity dependence of relative hole depth for the ZnTTBP/TiO_2 at 20 K is shown. The holes were burnt by one-color and by the same irradiation time (10 min). The saturation intensity is more than 1 mW/cm^2, and this is quite different from the case for ZnTTBP/GAP for two-color irradiation (chapt.5, Fig.5.11) and for ZnTTBP/PCMS for one-color irradiation (chapt.4, Fig.4.4). In the case of GAP and PCMS, the saturation intensities of ZnTTBP (100-200 μW/cm^2) agree to those values estimated from the reported values of τ_{T1} (20-40 ms), ε (10^5), and Φ_{isc} (0.9) of ZnTTBP. However, Fig.6.8 indicates that the mean excited lifetime ($\Phi_{isc} \times \tau_{T1}$) of ZnTTBP becomes less than 5 ms in TiO_2. This should be because the rapid electron ejection to the C.B. of TiO_2 occurs from the S_1 or T_1 of ZnTTBP leading to the decrease in Φ_{isc} and τ_{T1}. The low hole burning efficiency suggests that most of the ionized ZnTTBP molecules undergo rapid backward reaction and does not contribute to the hole production.

6.3.2. Cycle Annealing and High-Temperature PHB

Fig.6.9 shows the profiles of a hole burnt at 20 K during cycle annealing. The initial hole is the same one with Fig.6.6 (f). Fig.6.10 shows the annealing temperature dependence of relative hole area for the experiment of Fig.6.9. In Fig.6.10, the irreversible decrease in hole area (solid plots) shows a similar profile with dye/polymer systems by photochemical mechanisms (see chapt.5, Fig.5.9). After the annealing to 132 K, the hole area at 20 K decreases to about 1/3. The whole band area at 20 K after cooled from 132 K was the same with that before the annealing and was smaller than that before the hole production. This fact indicates that the irreversible decrease in hole area is not caused by the backward reaction of hole burning but by the structural ralaxation of the TiO_2 matrix.

The hole width as a function of annealing temperature is shown in Fig.6.11. The hole is the same one burnt and measured for Fig.6.9 and Fig.6.10. The reversible and irreversible increase in hole width are similar to that for ZnTTBP/GAP system (see chapt.5, Fig.5.8). This fact suggests that the temperature dependence of homogeneous width and the degree of thermally induced spectral duffusion are not so different in TiO_2 from those in polymer matrices.

The temperature dependedce of Debye-Waller factor (DWF) for the ZnTTBP/TiO_2 system is shown in Fig.6.12. The Debye-Waller factor at certain temperature was estimated by deviding the hole area at 20 K after the annealing at that temperature by the hole area measured at the annealing temperature(1). The DWF at 100 K is more than 70% of that at 20 K and the temperature dependence of DWF for this ZnTTBP/TiO_2 system is similar to that for OEP/Al_2O_3 system(10). In the case of free-base porphyrin doped in polymer systems(1) and ZnTTBP/GAP system (see chapt.5, Fig.5.15), the DWF values at 80 K are lower than 50% of that at 20 K. These facts indicates that the inorganic matrices such as TiO_2 and Al_2O_3 suppress the electron-phonon interaction, which leads to small decrease in DWF at higher temperatures.

Fig.6.13 and Fig. 6.14 demonstrantes the PHB at 140 K for ZnTTBP/TiO_2 system. The changes in the absorption band profile caused by the laser irradiation with the intensity of 3.8 mW/cm^2 at 631 nm for 20 and 60 min are shown in Fig.6.13. The decrease in absorbance is observed around 631 nm but not at the foots of the band. So we conclude that a hole is formed and detected at 140 K for the ZnTTTBP/GAP system. This is the highest PHB temperature of organic chromophore. The difference in optical density as a function of wavelength for Fig.6.13 is shown in Fig.6.14. The decrease in optical density does not become to zero at the foot of long-wavelength side. This should be due to the non-siteselective excitation via phonon-side band of vibronic transition of the chromophore[18]. The hole width was estimated to be 200 cm^{-1} for the hole burnt by 20 min irradiation and 230 cm^{-1} for the hole after 60 min irradiation. The inhomogeneous width at 140 K was estimated to be 390 cm^{-1} from Fig.6.13 and thus the ratio of the inhomogeneous width to the hole width is about 2. This value would become greater if the condition of the sample preparation is improved so that the condensation of the TiO_2 is completed.

6.3.3. Photoionization at Room Temperature

Fig.6.15 shows the change in absorption spectra of the ZnTTBP/TiO_2 at room temperature induced by the excitation of the Q band of ZnTTBP. The excitation is carried out by irradiating a Xe lamp with KL63 and VY48 filters, which transmit the light around 630 nm, or with VY48 filter only, which transmit the light of the wavelengths longer than 480 nm. The irradiation decreases the absorption of the Q band and Soret band (~430 nm), and slightly increases the absorption between 470 and 570 nm and at the wavelengths shorter than 425 nm. Because the isosbestic points are observed at 425, 465, and 580 nm, the photoreaction proceeds without subreactions. The photoproduct spectrum in Fig.6.15 is not so clear but is similar to the spectrum of ZnTBP cation[15]. Thus, the photoreaction of the ZnTTBP/TiO_2 system must be the ionization reaction both at low temperatures and at room temperature.

In Fig.6.16, the time-dependent absorption recovery of the ZnTTBP/TiO_2 sample at 634 nm in the dark after the irradiation is shown. The sample is the same one as is used for the experiment of Fig.6.15 and was irradiated with VY48 filter for 30 min after the irradiation for Fig.6.15. The absorption recovers slowly with a time scale of minutes or hours in Fig.6.16. The absorbance of this sample left for 1 day in the dark after the measurement becomes almost the same with that before the irradiation for Fig.6.15. So the recombination of the ejected electron and the ZnTTBP cation proceeds for hours and completes in 1 day. This behaviour should be useful for the phase conjugation caused by a light-induced transient hologram.

6.4. Conclusion

A PHB material with a new type guest-host combination; organic dye doped in semiconductor system is provided. The material consists of ZnTTBP as a guest chromophore and TiO_2 as a host matrix and was prepared by the sol-gel method. The PHB in the ZnTTBP/TiO_2 system is attributed to ionization reaction because the absorption band area of ZnTTBP is decreased by the irradiation. The gating enhancement by the λ_2 is not observed and thus the ionization undergoes by the single-photon process. The hole can be burnt and observed at 140 K, which is the higest PHB temperature of organic chromophore. The temperature dependence of DWF is smaller than that for dye/polymer systems, suggesting the low electron-phonon coupling at higher temperatures in the TiO_2 matrix. The irradiation at room temperature also induced the reversible photoionization reaction to the ZnTTBP/TiO_2 system.

These results would provide a new type of photo-functional materials which can be used for PHB, phase conjugation, and other photooptical applications. This type of materials should be useful also for the purely scientific study on photochemistry, electrochemistry, solid-state physics, and other fields.

Referances

1) A. Furusawa and K. Horie; J. Chem. Phys., 94, 80 (1991).

2) T. P. Carter, C. Bräuchle, V. Y. Lee, M. Manavi, and W. E. Moerner; J. Phys. Chem., 91, 3998 (1987).

3) W. P. Ambrose and W. E. Moerner; Chem. Phys., 144, 71 (1990).

4) A. Winnacker, R. M. Shelby, and R. M. Macfarlane; J. de Phys., C 7, 543 (1985).

5) R. Jaaniso, H. Bill; Europhys. Lett., 16, 569 (1991).

6) J. Zhang, S. Huang, J. Yu; 発光学報, 12, 181 (1991).

7) K. Hirao, S. Todoroki, and N. Soga; J. Lumin., 55, 217 (1993).

8) A. Makishima and T. Tani; J. Am. Chem. Soc., 69, C-72 (1986).

9) H. Inoue, T. Iwamoto, A. Makishima, M. Ikemoto, and K. Horie; J. Opt. Soc. Am. B., 9, 816 (1992).

10) B. Sauter and C. Bräuchle; Chem. Phys. Lett., 192, 321 (1993).

11) H. W. Lee, M. Gehrtz, E. E. Marinero, and W. E. Moerner; Chem. Phys. Lett., 118, 611 (1985).

12) S. Sakka; 化学, 44, 598 (1989).

13) E. I. Alshits, B. M. Kharlamov, and R. I. Personov; Opt. Spectrosk., 65, 548 (1988).

14) J. Moser and M. Grätzel; J. Am. Chem. Soc., 106, 6557 (1984).

15) A. Vogler, B. Rethwisch, H. Kunkely, J. Hüttermann, and

J. O. Besenhard; Angew. Chem. Int. Ed. Engl. 17, 951 (1978).

16) T. Yoko, K. Kamiya, and S. Sakka; Yogyo-Kyokai-Shi, 95, 12 (1987).

17) G. Gusmano, G. Montesperelli, P. Nunziante, E. Traversa, A. Montenero, M. Braghini, G. Mattogno, and A. Bearzotti; J. Ceram. Soc. Jap., 101, 1095 (1993).

18) N. Murase and K. Horie; Chem. Phys. Lett., 209, 42 (1993).

Table 6.1. Sample preparation conditions and results.

Sample Number	molar ratio						Gelation time	Heating Condition	Results
	TIPT	EtOH	H_2O	HCl	EtOH	ZnTTBP/DMF			
a	1	4	1	0.08	4	2.5	4-5 days	Slow	○
b	1	4	1	0.08	4	2.5	1-2 min	Slow	△
c	1	4	3	0.08	4	2	1-2 min	Slow	△
d	1	4	1	0.08	4	2.5	No Gel		—
e	1	2	1.3	0.08	2	2	3-4 days	Fast	×
f	1	4	1.5	0.08	2	2	3-4 days	Fast	×
g	1	2	1.5	0.08	2	2	3-4 days	Slow	△
h	1	2	1.5	0.08	2	2	3-4 days	Slow	○
i	1	2	1	0.08	2	2	No Gel		—

No Gel: Gelation did not occured but precipitation was observed.

Slow: The sample was heated from 40 ℃ to 60 ℃ over more than 5 days.

Fast: The sample was heated from 40 ℃ to 60 ℃ over less than 2 days.

○: The sample was condensated without breaking.

△: The sample was broken into a few peaces but had a sufficient area for PHB measurement (~2 cm^2).

×: The sample was broken into more than several peaces.

Table 6.2. Change in weight of a ZnTTBP/TiO_2 sample during the condensation process.

	Initial Solution	After Gelation at Room. Temp.	40 ℃ Before Drying	70 ℃	100 ℃ After Drying
Weight (g)	9.12 (TIPT 4.00)	8.51	7.29	2.77	1.48
Relative weight* (%)	809	755	647	245	131

* Relative weight is based on the ideal weight which would be shown if the sample has become completely to TiO_2.

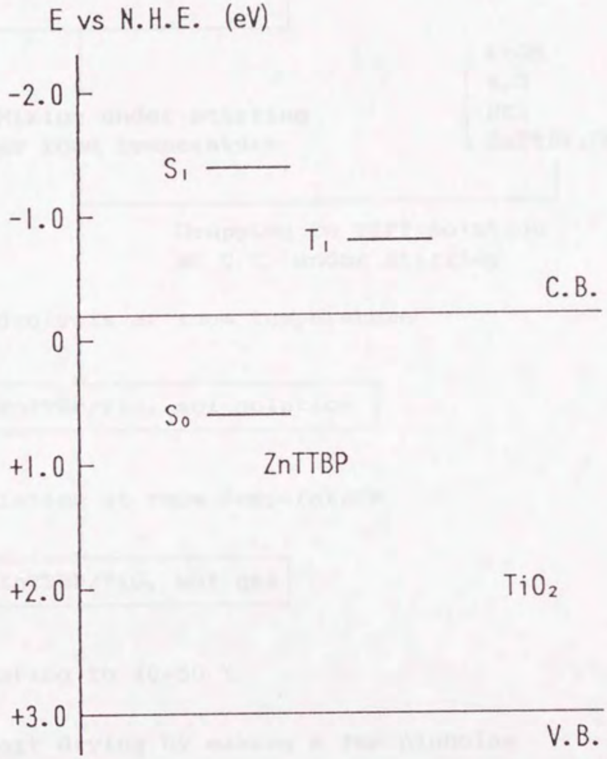

Fig.6.1. Energy diagram of ZnTTBP/TiO_2 system.

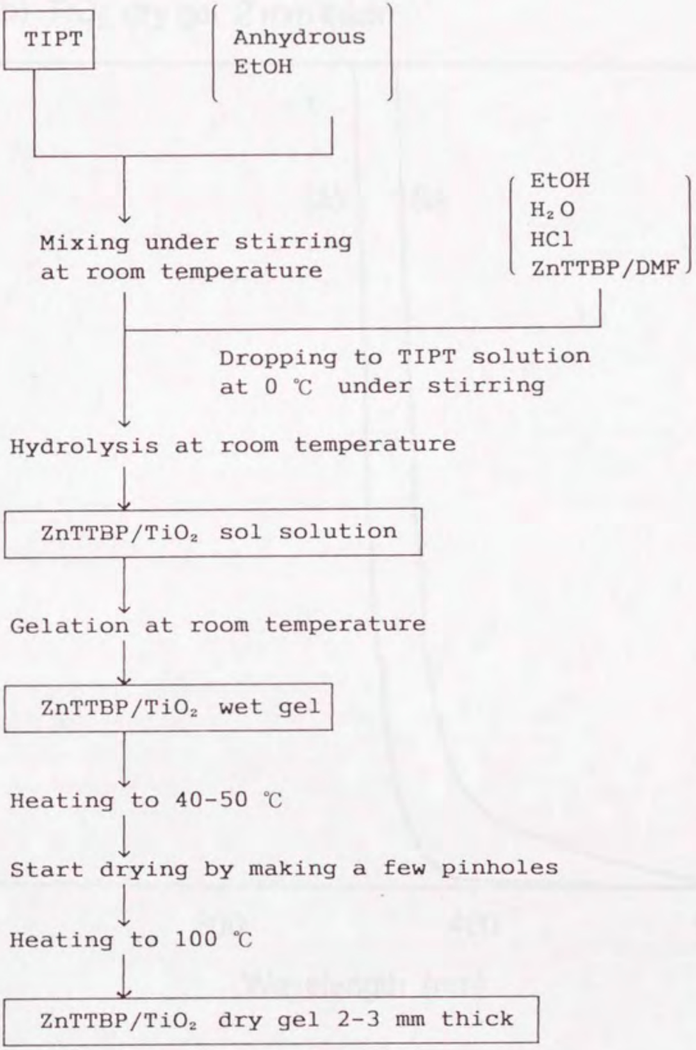

Fig.6.2. Scheme of sample preparation.

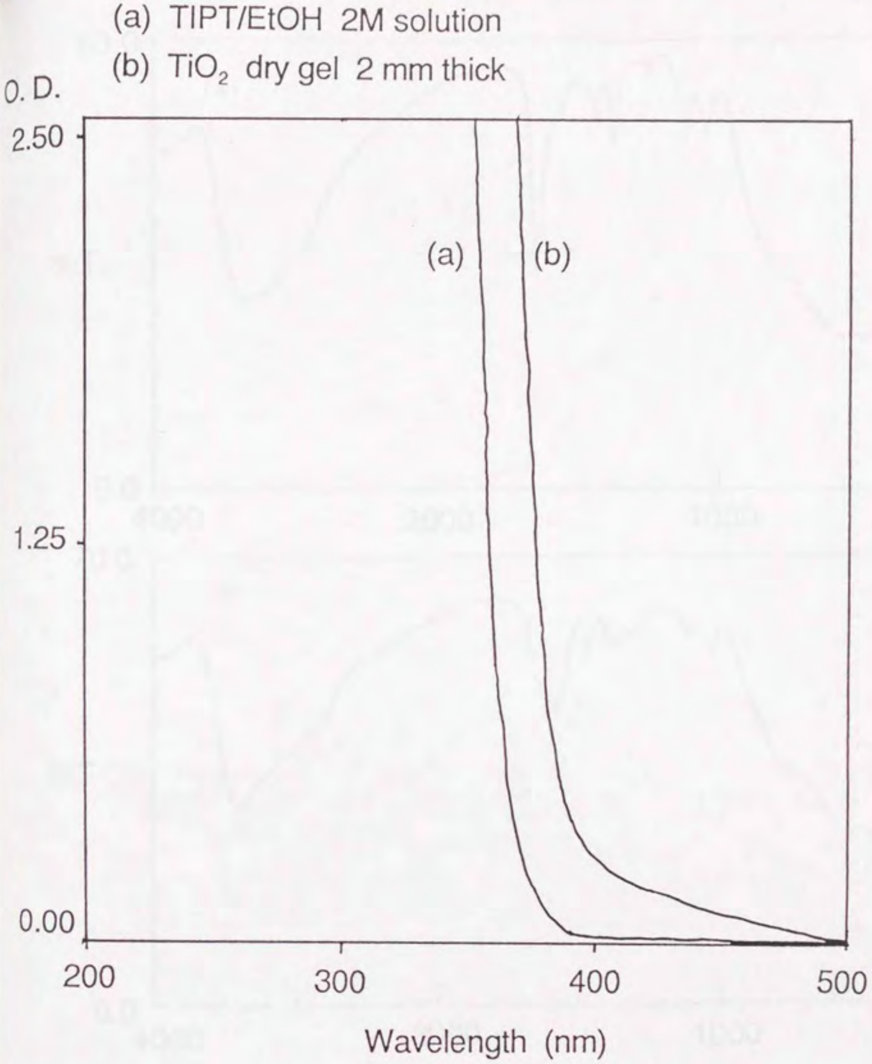

Fig.6.3. UV absorption spectra of TIPT/ethanol solution (~ 2 mol/l) (a) and TiO_2 without ZnTTBP (2-3 mm thick) (b) obtained by the same procedure as ZnTTBP/TiO_2 samples.

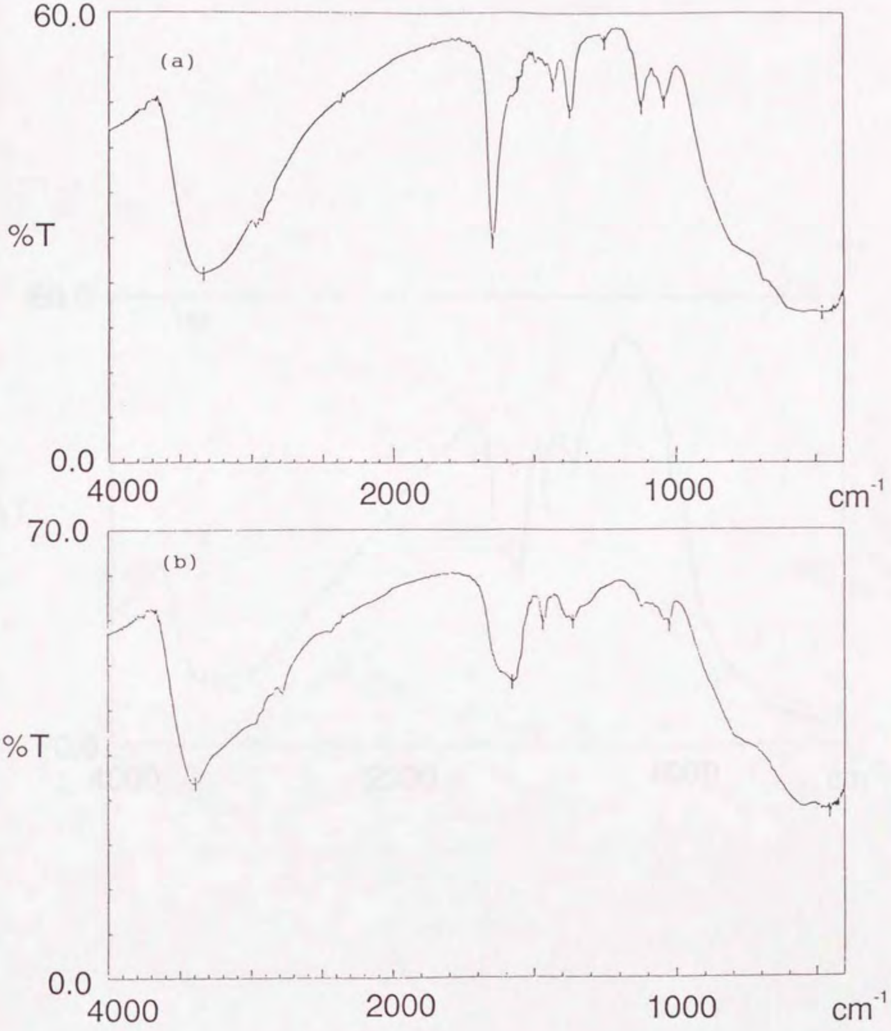

Fig.6.4. IR spectra of TiO_2 gel just after the gelation (a), heated at 40 ℃ (b), and heated at 100 ℃ (c).

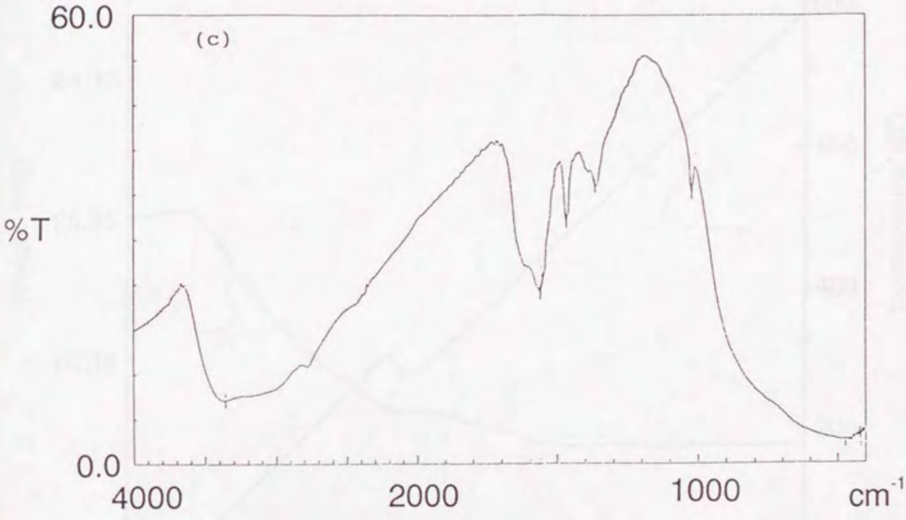

Fig.6.4. IR spectra of TiO_2 gel just after the gelation (a), heated at 40 ℃ (b), and heated at 100 ℃ (c).

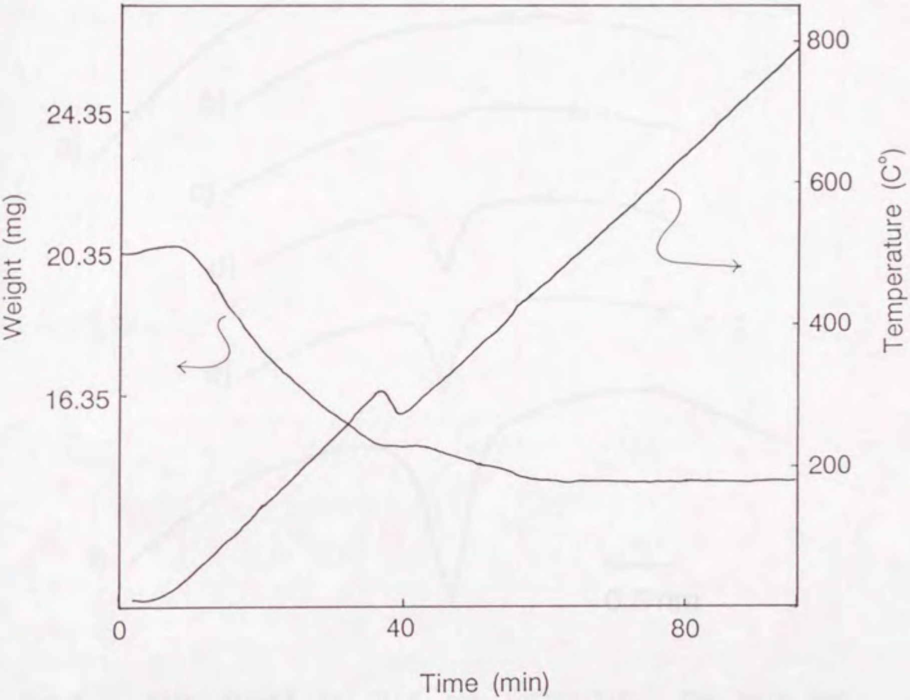

Fig.6.5. Thermogravimetry curve of TiO_2 sample without ZnTTBP which was dried at 100℃ before the measurement. Temperature was raised at the rate of 10℃ /min.

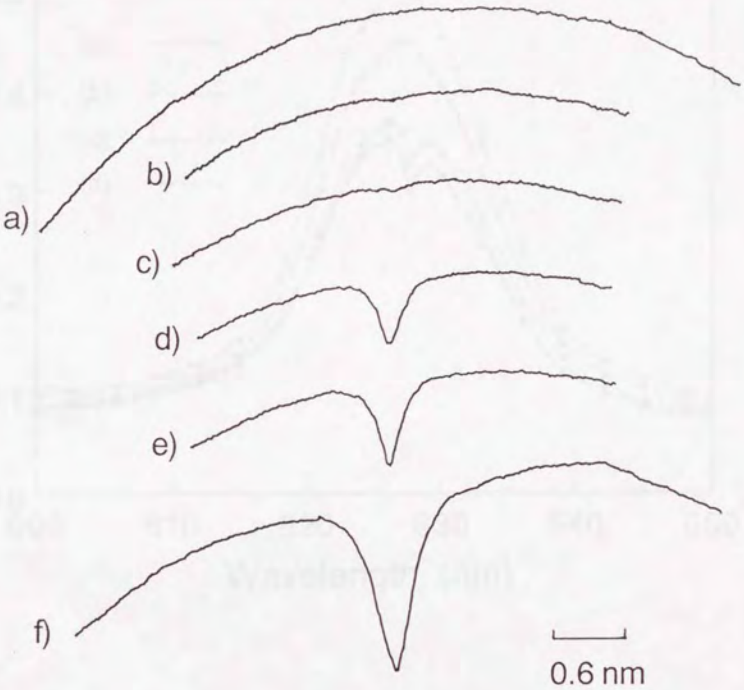

Fig.6.6. Hole growth at 20 K for ZnTTBP/TiO_2. The hole was burnt at 627.8 nm. The irradiations were carried out from traces (a) to (f) as follows. (a): Before irradiation. (b): λ_1 75 μW/cm^2, 10 min. (c): λ_1 75 μW/cm^2 + λ_2 5 mW/cm^2, 10 min. (d): λ_1 7.5 mW/cm^2, 10 min. (e): λ_1 7.5 mW/cm^2 + λ_2 5 mW/cm^2, 10 min. (f): λ_1 75 mW/cm^2 + λ_2 5 mW/cm^2, 30 min.

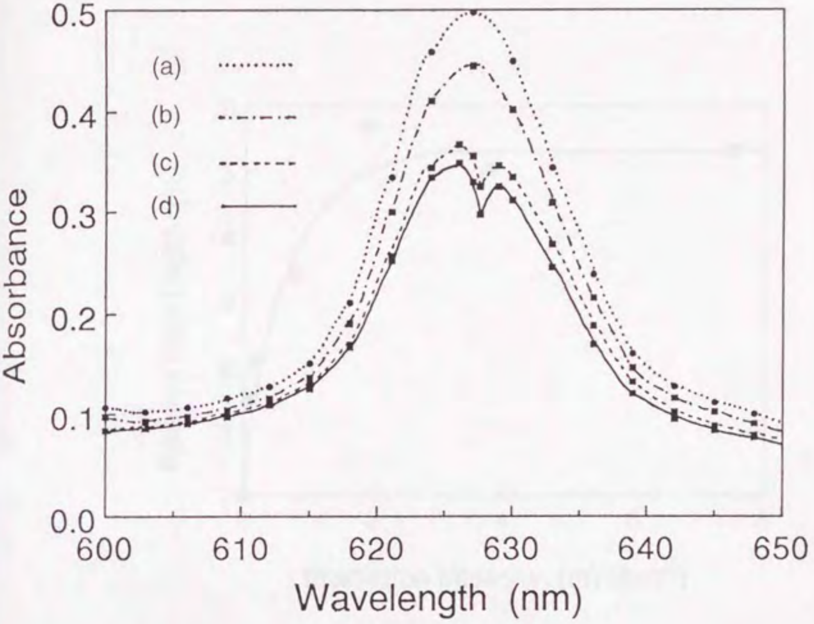

Fig.6.7. Change in absorption spectra of ZnTTBP/TiO$_2$ caused by laser irradiations at 20 K. Trace (a) is the spectrum before the irradiations. Trace (b) is the spectrum after the irradiation of total 14 J/cm^2 of λ_1 and 27 J/cm^2 of λ_2 to several wavelengths. Traces (c) and (d) were produced by 1 hour and 3 hours irradiations, respectively, of 75 mW/cm^2 λ_1 at 627.5 nm on the sample (b).

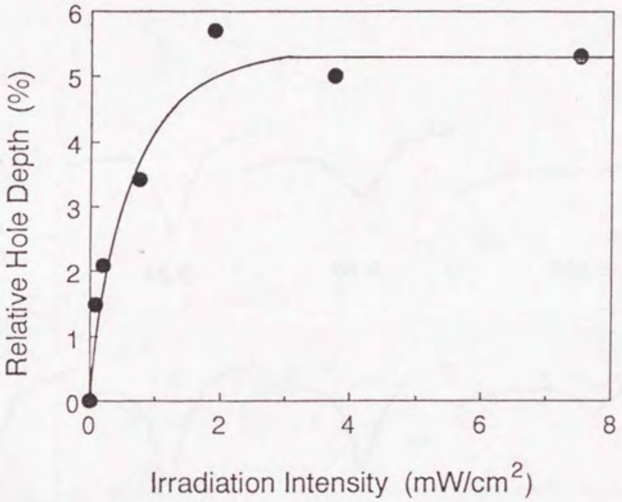

Fig.6.8. Irradiation intensity dependence of hole depth for one-color irradiation to ZnTTBP/TiO_2 system.

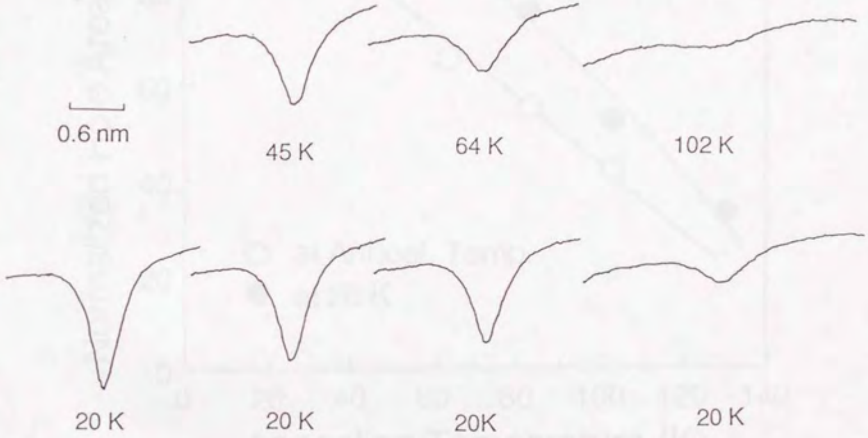

Fig.6.9. Hole profiles during cycle annealing for ZnTTBP/TiO_2. The initial hole is the same one with Fig.6.5 (f).

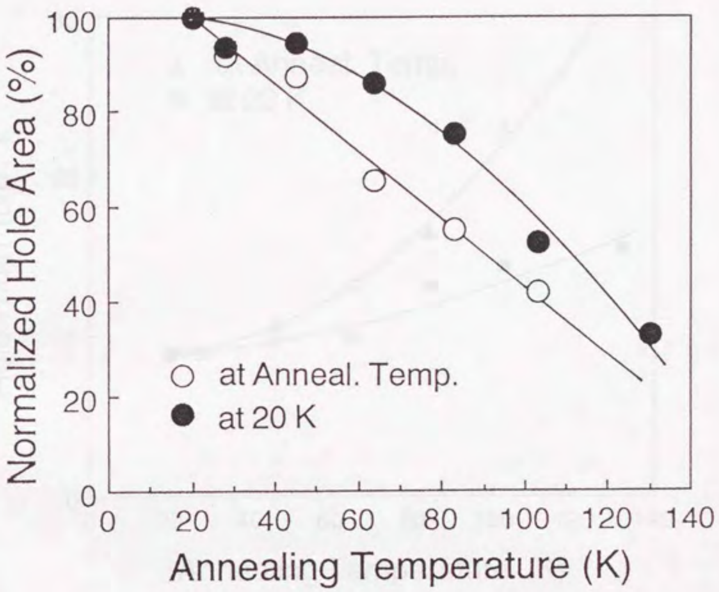

Fig.6.10. Normalized hole area as a function of annealing temperature for ZnTTBP/TiO_2.

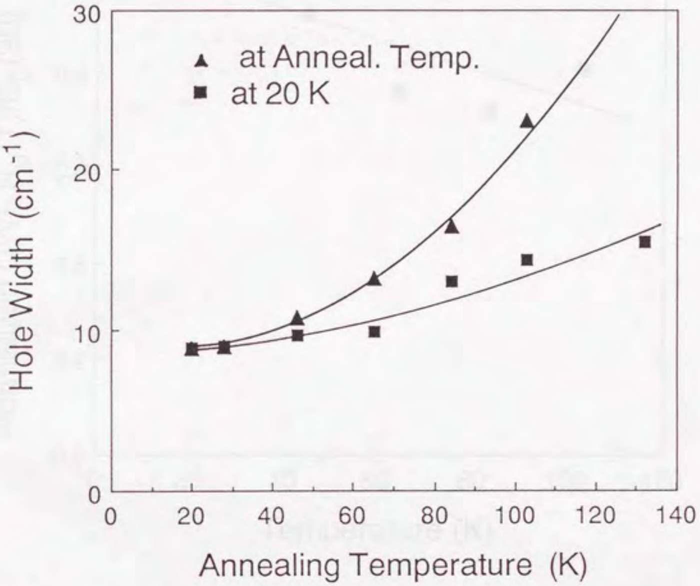

Fig.6.11. Hole width as a function of annealing temperature for ZnTTBP/TiO$_2$. The hole was the same one burnt and measured for Fig.6.9 and 10.

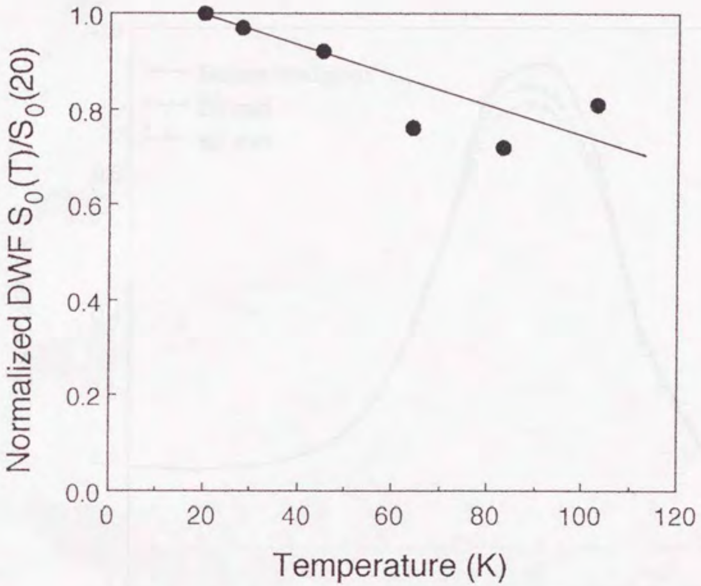

Fig.6.12. Temperature dependence of Debye-Waller factor for ZnTTBP/TiO_2 system.

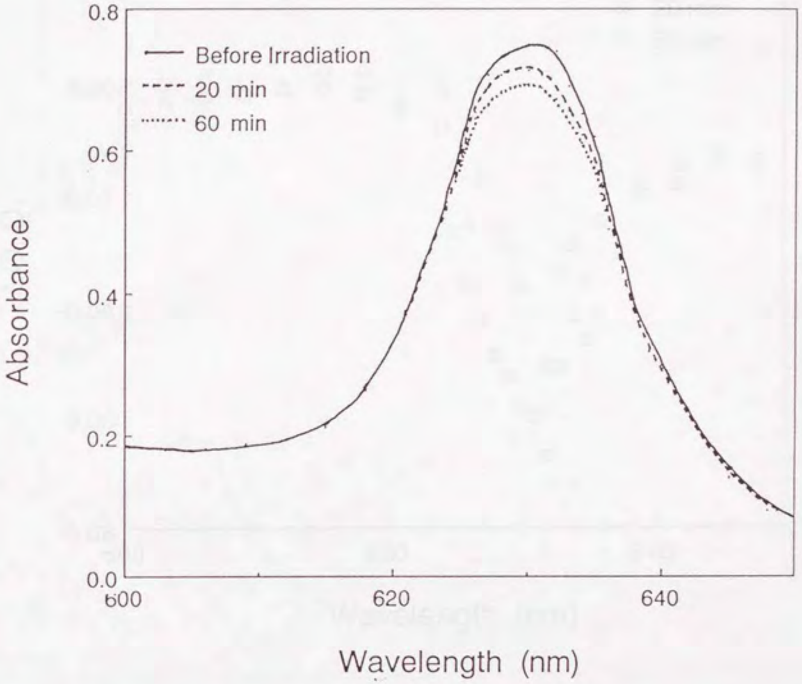

Fig.6.13. Change in absorption spectra of ZnTTBP/TiO$_2$ at 140 K caused by the irradiation of 3.8 mW/cm^2 λ_1 at 631 nm for 20 min and 60 min.

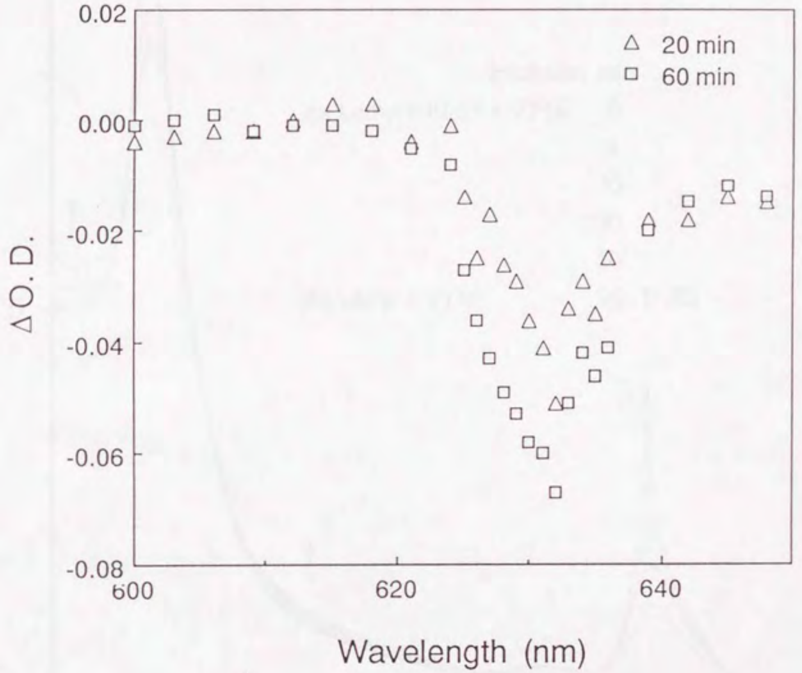

Fig.6.14. Difference in optical density as a function of wavelength after 20 (△) and 60 min (□) irradiation of 3.8 mW/cm² λ_1 at 140 K.

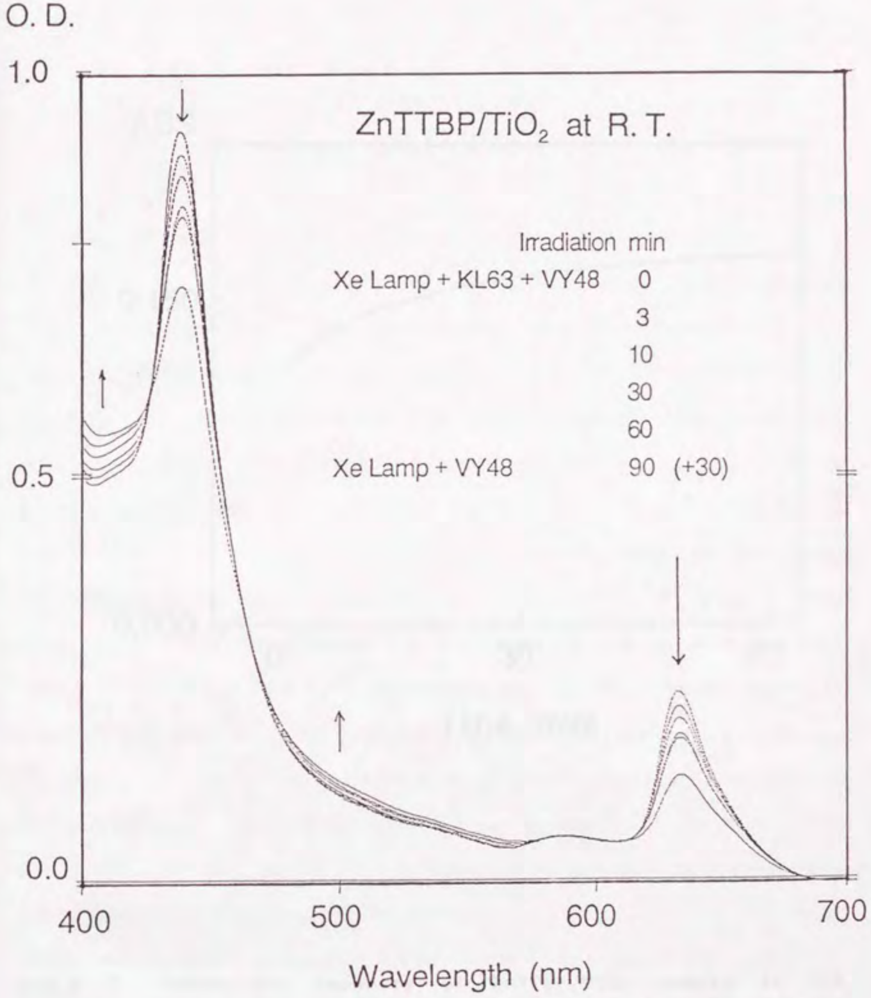

Fig.6.15. Photoinduced change in absorption spectra of ZnTTBP/TiO$_2$ at room temperature. The sample was irradiated with 70 μW/cm^2 of Xe lamp (+ KL63 + VY48 filters) from 0 to 60 min, and with 2.5 mW/cm^2 of Xe lamp (+ VY48 filter) from 60 to 90 min.

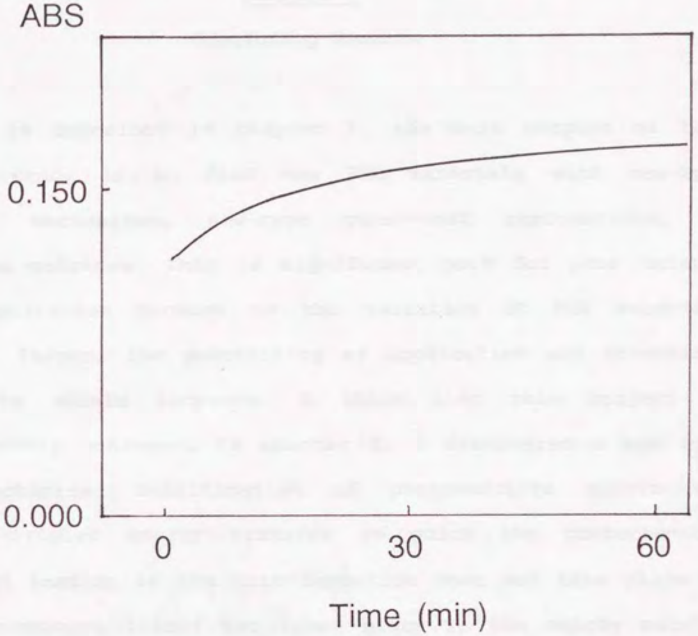

Fig.6.16. Absorption recovery of ZnTTBP/TiO_2 sample at 634 nm after further 30 min irradiation of 2.5 mW/cm^2 Xe lamp (+ VY48) on the sample for Fig.6.11.

CHAPTER 7

Concluding Remarks

As is described in chapter 1, the main purpose of this thesis study is to find new PHB materials with new-type burning mechanisms, new-type guest-host combinations, or new-type matrices. This is significant both for pure science and application because as the variation of PHB materials becomes larger, the possibility of application and scientific interests should increase. I think that this subject is considerably achieved. In chapter 5, I discovered a new type PHB mechanism: sensitization of photoreactive matrix via triplet-triplet energy transfer in which the photochemical reaction leading to the hole formation does not take place in the chromophore itself but takes place in the nearby matrix. In chapter 3, I found a new type photon-gated PHB mechanism: hydrogen-bond rearrangement of carboxylic acid. The photon-gated mechanism was supposed to be hydrogen-bond tautomerizm of carboxylic acid dimer. In addition, a new-type guest-host combination for PHB: organic dye (ZnTTBP) doped in inorganic semiconductor (TiO_2) was demonstrated in chapter 6. The PHB mechanism of this material was concluded to be ionization via single-photon process. In chapter 4, I demonstrated a new-type PHB matrix: polymer bearing electron acceptor in its every monomer unit. The system undergoes electron transfer via two-color excitation.

This thesis also aims to clarify the various aspects of low-temperature photoinduced processes, especially photoreactions from highly excited states. In chapter 3, photophysical processes or hydrogen-bond rearrangements around the highly excited guest chromophore (ZnTTBP) were detected. The donor-acceptor electron transfer reactions from the ZnTTBP in its highly excited triplet states, T_n, to the nearby chlorine acceptor in the matrices were measured and discussed in chapter 4. The quantum efficiency for hole formation in the matrix with low reduction potential was relatively high, and the concentration of the acceptor did not influence so much on the electron transfer rate. In chapter 5, tiplet-triplet energy transfer from the T_n of the ZnTTBP to the nearby azide groups and the subsequent reactions were observed. The frequency shift of the sensitizer (ZnTTBP) was discussed based on the distribution of the distance from the sensitizer to the azide group. In this ZnTTBP/GAP system (chapt.5), the photon-gated PHB proceeded efficiently although the triplet-triplet energy transfer was not so exothermic as the electron transfer in the systems in chapter 4 in which the PHB efficency became much lower in the matrix with higher reduction potential (compare Fig.4.1 and Fig.5.3.). I think this is because the energy transfer does not need the reorientation of the polar solvent as the electron transfer. These results should prove that the photon-gated PHB is a very good way to observe the photoreactions from highly excited states.

The thermally induced relaxation processes of the matrices and the electron-phonon interactions at low temperatures are important subjects for this thesis study. As far as I know, there were no series of PHB study on this point both with photochemical and nonphotochemical systems, and both with organic and inorganic materials. In chapter 3 and 4, the thermally induced backreaction of NPHB was observed by cycle annealing experiment. In these systems the low-temperature annealing did not change the hole width at 20 K but changed the hole area. This should be characteristic of dye/polymer NPHB systems. In chapters 4 and 5, the thermally induced structural relaxation of the matrix polymer was obsereved by cycle annealing. In these systems the PHB reaction is photochemical mechanism and is irreversible. The temperature dependence of PHB efficiency was also measured and discussed for ZnTTBP/GAP system in chapter 5. This system showed relatively weaker temperature dependence of PHB efficiency than the system of free-base porphyrin, which was attributed to the fact that the tautomerization is photochemically reversible. In chapter 6, the structural relaxation and the electron-phonon interaction of the organic dye (ZnTTBP) doped in inorganic matrix (TiO_2) was probed. The weak temperature dependence of Debye-Waller factor of this material indicated that this system has a weak electron-phonon coupling at higher temperatures. This must be due to the existence of the dense chemical bond specific to the inorganic matrices. These results indicate that the thermal stability of persistent holes is specific to the PHB mechanism and the kind of matrix. This is quite important because the kind of phenomena which can be detected by the PHB method depends on what material we choose for the experiment.

As for the application of PHB materials to an optical devices, this thesis study would indicate some important factors for high quantum efficiency, Φ, high gating ratio, G, and high-temperature hole burning. In chapters 3, 4 and 5, the ways to increase Φ and G were suggested. In chapter 4, it was proved that the electron acceptors with low reduction potentials are better for high Φ_2 and G, and that the suppression of NPHB is important for high G. As for the NPHB, it was suggested in chapter 3 that the hydroxyl and phenyl groups in the matrix enhance the NPHB process. In chapter 5, the matrix without NPHB active groups achieved low Φ_1 and high G. I clarified in chapter 5 that the one-color two-photon process is responsible for the one-color hole burning and that the suppression of the one-color two-photon mechanism is important for the high gating ratio. In chapters

5 and 6, the important factors affecting high-temperature hole burning was suggested. In chapter 5, photochemically irreversible reactions were proved to be better for the high-temperature PHB because ZnTTBP/GAP system showed smaller decrease in Φ at higher temperatures than the systems of free-base porphyrin. It was also proved in chapter 6 that the PHB is possible at 140 K in the TiO_2 matrix, which should be due to the weak electron-phonon coupling at high temperatures. This is the highest PHB temperature of organic chromophore. Therefore, this thesis study would be helpful for the research of new PHB materials for the optical applications.

Of course, it is true that further study is needed to find new PHB materials with other type of mechanisms and matrices, and with more preferable properties for the optical applications. It is also true that this thesis work is not enough to clarify various photoinduced processes, structural relaxation of matrices, electron-phonon interactions, and other aspects of solids at low temperatures. However, I believe that this thesis study performs some parts of these fields. I am very glad if the thesis study becomes to be a guide to the study on PHB both for pure science and application.

List of Publications

Original Papers

1) Photon-Gated Photochemical Hole Burning by Two-Color Sensitization of a Photoreactive Polymer via Triplet-Triplet Energy Transfer.
   S. Machida, K. Horie, and T. Yamashita; Appl. Phys. Lett., 20, 286 (1992).

2) Enhancement of Nonphotochemical Hole Burning by Two-Color Excitation in Polymers Containing Carboxylic Acid.
   S. Machida, K. Horie, T. Yamashita, and A. Furusawa; J. Phys. Chem., 97, 8234 (1993).

3) Photon-Gated Photochemical Hole Burning by Two-Color Sensitization in an Azide Polymr Matrix.
   S. Machida, K. Horie, O. Kyono, and T. Yamashita; J. Lumin., 56, 85 (1993).

4) Photon-Gated Photochemical Hole Burning by Electron Transfer Reaction: Zinc Tetratolyltetrabenzoporphine in Poly(chloromethylstyrene).
   S. Machida, O. Kyono, K. Horie, R. Matsuno, and T. Yamashita; Polymer, in press.

5) Photochemical Hole Burning of Organic Dye Doped in Inorganic Semiconductor.

S. Machida, K. Horie, and T. Yamashita; Submitted to Appl. Phys. Lett.

Related Papers

1) Photochemical Hole Burning of Tetraphenylporphin in Epoxy Resin: Effects of Crosslinked Structure.

A. Furusawa, K. Horie, T. Suzuki, S. Machida, and I. Mita; Appl. Phys. Lett., 57, 141 (1990).

2) Photon-Gated Persistent Spectral Hole Burning of Zinc-Tetrabenzoporphin with Crotonic Acid in Phenoxy Resin.

K. Horie, Z.-L. Zhang, L.-Q. Shi, S. Machida, T. Suzuki, S.-M. Yao, and M.-H. Zhang; Polym. J., 24, 715 (1992).

3) Frequency Dependence of Quantum Efficiency for Hole Formation in Photochemical Hole-Burning for Dye-Doped Polymer Systems.

K. Horie, M. Ikemoto, T. Suzuki, S. Machida, T. Yamashita, and N. Murase; Chem. Phys. Lett., 195, 563 (1992).

Reviews

1) PHB、フォトンエコー材料　（堀江一之、町田真二郎 分担執筆）
堀江一之、谷口彬雄　編　”光・電子機能有機材料ハンドブック”
第Ⅲ編「材料」　第1章第3節　朝倉書店　（1994年発行予定）

2) 光記録　（堀江一之、町田真二郎　分担執筆）
松永　孜　編　”分子機能材料と素子開発”　第3章第13節
（株）エヌ・ティー・エス　（1994年発行予定）

3) ホールバーニング効果と分子凝縮系　（町田真二郎、堀江一之 分担執筆）
高分子学会　高分子錯体研究会　編　”高分子錯体アニュアルレビュー1993”　（1994年発行予定）

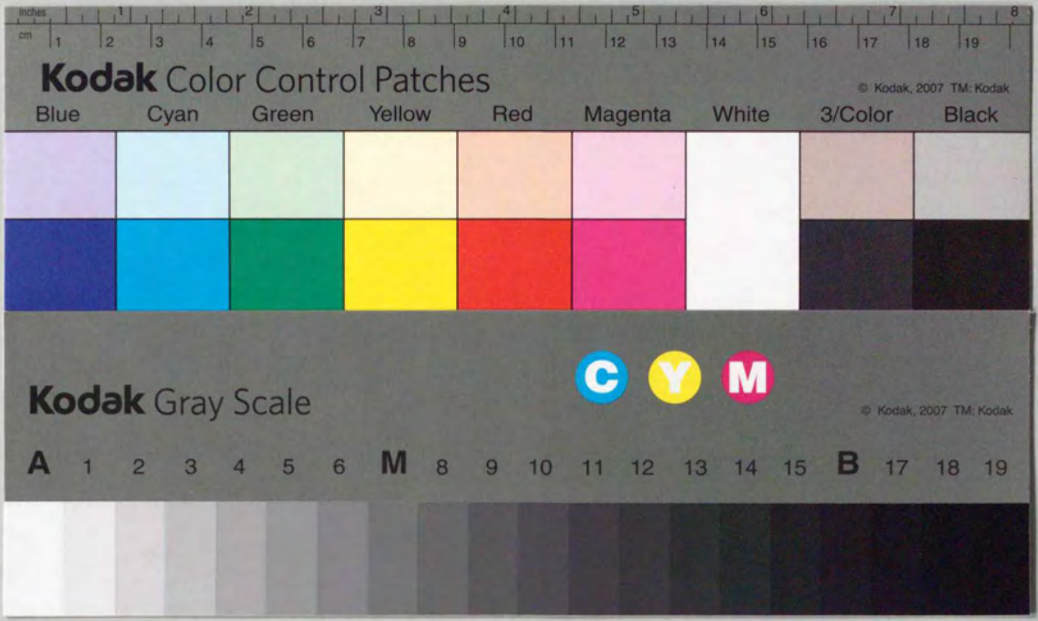
Inches
cm
Kodak Color Control Patches
© Kodak, 2007 TM: Kodak
Blue
Cyan
Green
Yellow
Red
Magenta
White
3/Color
Black
C
Y
M
Kodak Gray Scale
© Kodak, 2007 TM: Kodak
A 1 2 3 4 5 6 M 8 9 10 11 12 13 14 15 B 17 18 19